

Supplemental Data

Structural Chromosomal Rearrangements Require Nucleotide-Level Resolution: Lessons from Next-Generation Sequencing in Prenatal Diagnosis

Zehra Ordulu, Tammy Kammin, Harrison Brand, Vamsee Pillalamarri, Claire E. Redin, Ryan L. Collins, Ian Blumenthal, Carrie Hanscom, Shahrin Pereira, India Bradley, Barbara F. Crandall, Pamela Gerrol, Mark A. Hayden, Naveed Hussain, Bibi Kanengisser-Pines, Sibel Kantarci, Brynn Levy, Michael J. Macera, Fabiola Quintero-Rivera, Erica Spiegel, Blair Stevens, Janet E. Ulm, Dorothy Warburton, Louise E. Wilkins-Haug, Naomi Yachelevich, James F. Gusella, Michael E. Talkowski, and Cynthia C. Morton

Supplemental Note

Case Reports

DGAP239¹

46,XY,t(6;8)(q13;q13)dn.arr(1-22)x2,(XY)x1.seq[GRCh37/hg19] t(6;8)(q13;q12.2)dn

Prenatal History: A 37 year-old G2P0SAB1 female conceived after *in vitro* fertilization (IVF) and had normal first trimester screening. Starting in the second trimester, the following abnormal findings were detected: hypoplastic right ventricle and tricuspid atresia (18.8 weeks), polyhydramnios with a small, intermittently undetected stomach and suspicion of esophageal atresia (27.3 and 30.4 weeks), flexed extremities, protruding upper lip, and micrognathia with initiation of multiple periodic therapeutic amnioreductions (33.3 weeks), and undescended right testicle (35.3 weeks). The differential diagnosis during the prenatal period included arthrogryposis, Stickler syndrome, and trisomy 18. A sample of the initial therapeutic amniocentesis fluid at 33.3 weeks was collected for cytogenetic analysis and DNA extraction.

Postnatal History: At 36.2 weeks, during a therapeutic amnioreduction for polyhydramnios, poor fetal movements were noted and an emergent C-section was performed. The birth weight was 2985 grams (68th percentile), length was 45 cm (21st percentile), and head circumference was 33.5 cm (78th percentile). General examination showed a dusky, lethargic male on the ventilator with generalized edema. The chin was slightly retrognathic and there was a high arched palate. Ears were slightly retroverted with 'snipped off' helix, prominent antihelix and patent canals. Neck was short and edematous. Genitalia appeared male, with an underdeveloped male phallus and impalpable testes. Extremities had low tone with weak grasp and clenched fists with cortical thumb. Skin showed scattered ecchymoses and duskeness. After initial stabilization of respiratory and cardiac status, the newborn was transported to the Neonatal Intensive Care Unit (NICU) for further care. Choanal atresia was confirmed by maxillofacial CT scan. Esophageal atresia and tracheoesophageal fistula were confirmed by chest radiography and CT scan. Bilateral optic nerve hypoplasia was noted on ophthalmic examination, absence of the semicircular canals was detected in the ear complex after CT, and mild bilateral hydronephrosis was noted by ultrasound. Cardiovascular system evaluation with echocardiogram revealed tricuspid atresia, hypoplastic right ventricle, atrial and ventricular septal defects with mostly left to right flow, patent ductus arteriosus, small pulmonic valve annulus and normal branch pulmonary arteries. Neurologically, the newborn initially presented with poor tone and showed signs of encephalopathy (detected by EEG) with intermittent decorticate posturing. Clinical seizure activity was not observed. Cranial MRI suggested malformation of the brain including simplicity of the gyri in the frontal and prefrontal areas and also migrational defects. The infant's cardiopulmonary status started to deteriorate by day 8, and on day 10, the infant was removed from the ventilator to allow a natural death.

The spectrum of the infant's clinical findings detected in the postnatal period was consistent with a diagnosis of CHARGE syndrome.²⁻⁴ Of note, optic nerve hypoplasia can be considered in the spectrum of ocular coloboma, a major characteristic finding in CHARGE syndrome.⁵⁻⁷ On the basis of the newborn screening and metabolic tests, the presence of any metabolic disease was excluded.

Sequencing Results and Interpretation of Convergent Genomic Evidence: Sequencing of the prenatal DNA sample identified the translocation breakpoints directly disrupting *CHD7* at 8q12.2 and *LMBRD1* at 6q13. While biallelic losses of *LMBRD1* are associated with methylmalonic aciduria and homocystinuria, cbf1 type (a metabolic syndrome without any phenotypic overlap with DGAP239), haploinsufficiency of *CHD7* is well known to be associated with CHARGE syndrome (mutated in more than 90% of the cases), correlating with the postnatal diagnosis of CHARGE syndrome in DGAP239. An analysis of the protein-coding genes localized in

the same TAD as the breakpoints did not reveal any additional monoallelic or imprinted genes associated with an abnormal phenotype (Figure 2A, Table 4).

BLA(S)T Outputs of Sequencing Results:

Rearrangement_A (on der(6))

1	GTTGTTGTAT	TGCTTTTGT	GTTCCTTTTA	AATTGTTTCT	TTGTTATCTT	TTATTTTCC
61	CAAATTATTT	CTGACCCAAA	GTTGGCTGAA	TCCATGGATC	TGGAACCCAT	TAATATGGAG
121	GGCTAACTGT	ATACCCAACT	GCTTATGAGA	CCTCCACCTG	AACATTTTG	AGACATCTCA
181	AGTCAACTAA	TCATTTTTT	TTACAATTTC	TCTAACCTTA	GTACTTTTT	TTTTTTTTT
241	CCCTGAGACA	GAGTCCTGCC	CTGTCGCCTG	GGTCAGAGTG	CAGTGGCACG	ATCTCAGCTC
301	ACTGCAACTT	CCACCTCCC	GGTTCAAGTG	ATTCTCCTGC	CTCAGCCTCC	CAAGTAG{CT}T
361	TAAAGTATAT	GCAGAGTCTG	ATACCTTTTC	TCTCCACTTC	TACCACCCGG	GTCCAAGTGG
421	CCTTTTTCC	TTGCCGGTGT	TACTGCAGTA	GCTCCCCAAC	TGCTCTCCCT	GCTGTTGCCT
481	GTGTTGCCTG	CAGTCCTTCC	AATGTTAGCA	GTCAAAGTCA	TCTCTCAGAG	CCAGAGCTGG

Score	Start	End	qSize	Identity	Chro	Strand	Start	End	Span
357	1	359	540	99.8%	6	(+)	70405510	70405868	359
183	358	540	549	100%	8	(+)	61628671	61628853	183

BLA(S)T Output: 6q13(+)(70,405,86{7-8})::8q12.2(+)(61,628,67{1-2})

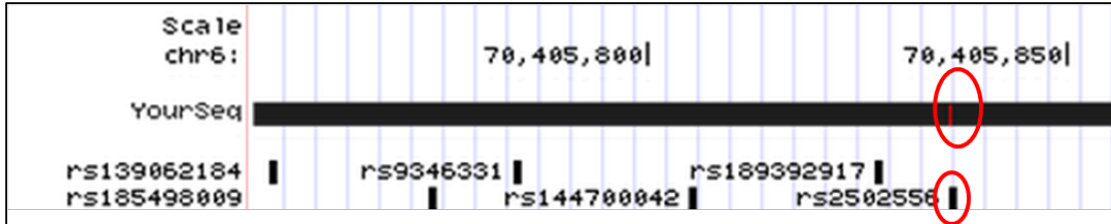


Figure S-DGAP239. BLA(S)T Output, Rearrangement_A on der(6): Circled mismatch represents a SNP (dbSNP build 141, rs2502556).

Rearrangement_B (on der(8))

1	GGGATCCGCC	TGCCTTGGCC	TCCTAAAATG	CTGGGATTAC	AGGC GTGAGC	CACCGCGCCC
61	AGCCCCTTCC	TCTTTTGGC	TTCCACTTGG	CCAAAGGGAGC	TTCCCTTGG	GGCCCGCTCT
121	GAGTCATGTT	AGCCGCTGGT	TCAAGGGAGC	CATCTGAAAC	TCCTGGAGC	AGGGTTTCTC
181	CTGTATATGG	CAATACTCTA	CCTTAGAAAA	ACAAAACAAA	ACAAAACAAA	ACGTCAAGTT
241	ACATGGTATA	ATGGAAAAAA	ACCCTAAACT	TGGGCTAGAA	AATATAGGCC	ACTATTTGT
301	TTCTAATACC	ACTATGTATA	TGGACAGAAC	AGTTAACGTG	CCACGCCCTG	TGTCTCCTT
361	CGTGAAGAGT	GGTGACACTG	TACCTTCACA	GCCTACTTCA	TAGGACTTTG	GTGTAAAATG
421	AGACAGCAGA	TGTTAAAGTA	CCTTCCGAGA	CCATTGTTTC	CAGAACCTTC	ATCACATTGT
481	GGTATTAGAA	ACCTTGGAGT	CCTCCTTGAC	TCTTCACAA	GCTACATTTGA	ATTGTTCTC
541	AAAGCCTCTG	GCT{CTG}GGAT	TACAGGGTG	CCCCACCAAC	CTCAACTAGT	TTTTGTATT
601	TTAGTAGAGA	CAAAGTTTCG	CCATGTTGGC	CAGGCTGGTC	TCAAACCTCT	GACCTAAGGT
661	GATCCGCCTG	CCTCGGCCTC	CCAGTGTATT	TTTTATCTCA	GCTGGTAACA	CCAAAATTAA
721	TCAAAGTACT	CAGTAACCTAG	AGTGTCTAGC	TAGAATCTTC	TGTTCTCTC	ACCATTGCTC
781	TACAACCAAT	CAGAAATTCT	TTCAATTAC	TTCTTAAATT	GCTTTATTTC	ACACCCCTCAT
841	GACCACTGTT	TAGTCAGGC	TTTCAACTCT	CTTGGATTAT	TTTAGATAGC	TCTCCCTCCC
901	CTAAG					

Score	Start	End	qSize	Identity	Chro	Strand	Start	End	Span
556	1	556	905	100%	8	(+)	61628114	61628669	556
352	554	905	905	100%	6	(+)	70405867	70406218	352

BLA(S)T Output: 8q12.2(+)(61,628,66{7-9})::6q13(+)(70,405,86{7-9})

Next-Gen Cytogenetic Nomenclature:

Short System

46,XY,t(6;8)(q13;q13)dn.seq[GRCh37/hg19] t(6;8)(q13;q12.2)dn

Detailed System

46,XY,t(6;8)(q13;q13)dn.seq[GRCh37/hg19] t(6;8)(6pter->6q13(70,405,86{7-8})::8q12.2(61,628,67{1-2})-8qter;8pter->8q12.2(61,628,66{7-9})::6q13(70,405,86{7-9})->6qter)dn

DGAP247

46,XY,inv(8)(q13q24.1)dn.arr(1-22)x2,(XY)x1.seq[GRCh37/hg19] inv(8)(q11.21q24.23)dn

Prenatal History: A 41 year-old G3P1TAB1 female had normal first trimester screening (low risk for trisomies 13, 18, and 21, normal nuchal translucency results with normal appearing nasal bone at 12.5 weeks ultrasound). At 16.3 weeks, amniocentesis was performed for advanced maternal age. Pregnancy continued without any complications with normal ultrasound examinations at 32 and 36 weeks.

Postnatal History: The mother presented with spontaneous labor at 38 weeks and delivery occurred without complications. The newborn examination was normal. At 31 months of age, the mother reported that her son is healthy and continues to develop normally.

Sequencing Results and Interpretation of Convergent Genomic Evidence: Sequencing of the prenatal DNA sample identified the inversion breakpoints within a non-genic region at 8q11.2, and within *KHDRBS3* at 8q24.23, disrupting this gene with consequent decreased RNA expression (Figures S1 and S2). Although *KHDRBS3* (KH domain-containing, RNA-binding, signal transduction-associated protein 3) has a borderline haploinsufficiency index of 10.52%, it is not reported to be associated with an abnormal phenotype.⁸ An analysis of the protein-coding genes localized in the same TAD as the breakpoints did not reveal any additional monoallelic or imprinted genes associated with an abnormal phenotype, correlating with the normal clinical phenotype of DGAP247 (Figure 2B, Table 4).

BLA(S)T Outputs of Sequencing Results:

Rearrangement_A (at proximal breakpoints of inv(8))

1	TTTGACAAAC	CTGACAAAAA	CAAGAAATGA	GGAAAGGATT	CCCTATTTAA	TAAATGGTGC
61	TGGGAAAACT	GGCTAGCCAT	ATGTAGAAAG	CTGAAACTGG	ATCCCTTCCT	TACACCTTAT
121	ACAAAAATTA	AATCAAGATG	GATTAAGAC	TTAAATGTAA	GACCCAAAAC	CATAAAAACC
181	CTAGGAATAA	TGCAAACACTCA	GAGTACGAAT	CTGAAGTCTA	TGCTTTATAC	TACTTAGTTC
241	CAGGGACTAA	TTAGCTTCAG	ATTCCGAAGG	GCAGAAAATT	CCCTCCATTT	TCTCCCATAG
301	CCACCATGAC	AACATCTTAC	TACACCCCAA	TCTGACGGCA	ATGACAGCCA	GCATGGGCAG
361	TTACAAACCA	CAACAAACCA	CTAATGGCAG	CAGAATGTGT	TTACTTGCCA	CAATCCATCA
421	TGCTTTGGGT	TCAGTGCTGT	ATAATGCAAC	TGTAATAATT	ACTGGTTGA	GAAGAAGATA
481	TTTCAGACA	GGTCAGACCA	CTGTGCCACA	TGTTTAATGT	AAAAGAAAAG	AGTCCATAAA
541	TATAATCAGC	AACTTTCAAA	TATCAGCCAG	TTGCAAAGAG	TATTTAATTA	ATAAAATACAA
601	TTCGATAGAG	AAAACCCTTC	AGTTTGACC	TTTCTTTTA	ATGCAAAAGA	GATACAGGGT
661	TGGGGGTGG	AGAAAGATAC	TTGATGTCTA	GAAATGCTGA	GAAACAAAAA	AAACAAATAA
721	TGATATTGTC	TCCAGGAATA	AGCATGAGAA	CAACAAAGCA	CTACCTGTTA	TTTACGTAC
781	ATCGTTCTTT	CCTAGATGTT	CTGATGGAAA			

Score	Start	End	Qsize	Identity	Chro	Strand	Start	End	Span
624	185	810	810	99.9%	8	(-)	136495195	136495820	626
184	1	184	810	100%	8	(+)	51889318	51889501	184

BLA(S)T Output: 8q11.21(+)(51,889,501)::8q24.23(-)(136,495,820)

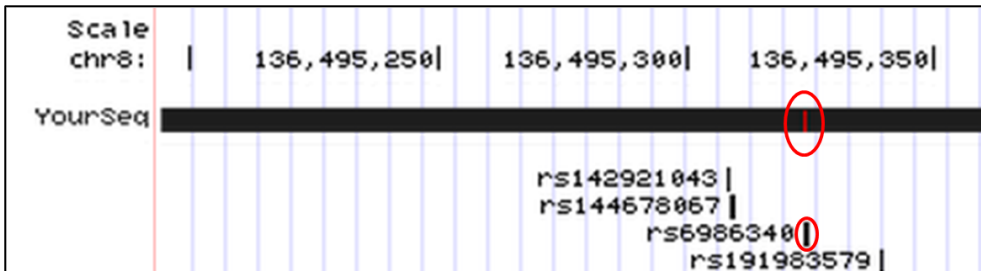


Figure S-DGAP247. BLA(S)T Output, Rearrangement_A at proximal breakpoints of inv(8): Circled mismatch represents a SNP (dbSNP build 141, rs6986340).

Rearrangement_B (at distal breakpoints of inv(8))

1	TTGGCTTCTG	TTGCCATTGC	TTTGCGTGT	TTAGACATGA	AGTCCTGCC	CATGCCTATG
61	TCCTGAATGA	TATTGCCTAG	GTTTTCTT(TA TTCTT)(TATTC TT)(TATTCTT)(T ATTCTT)TACT			
121	TTCCCTTTAT	GAACAGAGGA	GGATATTCAT	GTCATGAGGG	TATCATATCC	TTATGATAGA
181	GGATATTTGT	GTGATGAGGG	CATCAGCCTT	AGGTGCCTGG	TTCTGTCCCC	TGCATGGCTT
241	CCTCCTGTCC	ATCTGCCGTC	TCTTGCAGGG	CTGAACATTAC	TCTTCCAGAT	TTGGAGATAAC
301	TTGGAGTGT	TGATGCTTGA	ATCCTGTCA	GACCTGCTTA	TTCTCTCTCC	CTATCTAGGG
361	CTGTTGGGAC	TGTCCTGTT	TGGGCCTGGA	CAGGACATTT	TTAGATATGT	TTAGAGCATA
421	AATGAAGAAC	TCCCATTGGT	TTTGATGTAA	GATGACTT	AATGTTCACT	ATTTTTGGAA
481	GACAGGATAG	CATGGTGATG	AAGATGAGGC	CTCTGGAATT	GGACCGCTTA	GGTTTGGGTC
541	TGTCTTATCC	CTGTTGGCTTA	CTAGCTGTAT	GTCCTGGGG	AAGTAATTAA	ACCCCTCACT
601	ACCTACATT	CCTCAGTAAA	TTAGAGGTAA	AATGTGGAAT	AGGTAAAAAT	AACCACCA
661	AAGAGTTAAT	GTGAAGTAA	ATGCTAACAT	ATGTAAGCA	TTGAGAAATA	AAAATAAAAT
721	CCTAAGCCAC	CCAAGTGACT	GGGTAGACCC	CTCTTG		

Score	Start	End	Qsize	Identity	Chro	Strand	Start	End	Span
648	109	756	756	100%	8	(+)	136495815	136496462	648
88	1	88	756	100%	8	(-)	51889502	51889589	88

BLA(S)T Output: 8q11.21(-)(51,889,502)::TATTCTTATTCTTTATTCT::8q24.23(+)(136,495,815)

or

BLA(S)T Output: 8q11.21(-)(51,889,502)::8q24.23(136,495,816-136,495,822)x4::8q24.23(+)(136,495,823)

Next-Gen Cytogenetic Nomenclature:

Short System

46,XY,inv(8)(q13q24.1)dn.seq[GRCh37/hg19] inv(8)(q11.21q24.23)dn

Detailed System

46,XY,inv(8)(q13q24.1)dn.seq[GRCh37/hg19] inv(8)(pter->q11.21(51,889,501)::q24.23q11.21(136,495,820-51,889,502)::TATTCTTATTCTTTATTCT::q24.23(136,495,815)->pter)dn

or

46,XY,inv(8)(q13q24.1)dn.seq[GRCh37/hg19] inv(8)(pter->q11.21(51,889,501)::q24.23q11.21(136,495,815-51,889,502)::q24.23(136,495,816-136,495,822)x4::q24.23(136,495,823)->pter)dn

DGAP248

46,XY,t(2;13)(p13;q14)dn.arr(1-22)x2,(XY)x1.seq[GRCh37/hg19] t(2;13)(p12;q13.2)dn

Prenatal History: A 44 year-old G1P0 female had normal first trimester screening. At 10.9 weeks, CVS was performed for advanced maternal age. At 17.3 weeks, fetal ultrasound was interpreted to be normal. At 19.4 weeks, the pregnancy was terminated prior to an appointment to receive the results of sequencing. The mother stated that she decided to end the pregnancy as the couple was conflicted about continuing the pregnancy for personal and psychosocial reasons, and that it was a multi-layered decision. No fetopsy was performed.

Sequencing Results and Interpretation of Convergent Genomic Evidence: Sequencing of the prenatal DNA sample identified the translocation breakpoints within a non-genic region at 2p12, and within *RFC3* at 13q13.2, disrupting this gene with consequent decreased RNA expression. *RFC3* encodes the 38 kDa subunit of replication factor C complex,⁹ with a predicted haploinsufficiency index of 4.93% (likely to be monoallelic)⁸, however without any known abnormal phenotypic associations. In addition, 13q13.2 breakpoints are 973 kb upstream to *NBEA*, a candidate haploinsufficient gene for autism based on animal models and disruption in a patient with idiopathic autism,¹⁰⁻¹² located within the same 2.16 Mb TAD with the breakpoints. The 2p12 rearrangement is located within a TAD that includes *LRRTM4*, a gene with low haploinsufficiency index with no reported abnormal phenotypic association. However, structure and expression profiles of *LRRTM* mRNAs in mice suggest a role in development and maintenance of the vertebrate nervous system.¹³ These sequencing results remain of unknown clinical significance, as the pregnancy was terminated and an assessment of potential autism-like behavior would not have been possible in a fetopsy had it been performed (Figure 2C, Table 4).

BLA(S)T Outputs of Sequencing Results:

Rearrangement_A (on der(2))

1	AAATTTGTAC	GGTGGGTGAA	CTGTGAGCTG	GAGTGTGTTGA	GTGGTACCTG	GTAAAGTC
61	CACAATGCCG	GCATTAGTAT	TCAGATGAAA	TCTCAGCTCC	TGTGAACAAG	CTGCCATGCA
121	GTCAATTG	CAAGATAAAA	CTTCAGAGCC	TTGTTCTGTG	TCTCTTCTCT	TTAATAACCA
181	GAACCTCCAA	GACAACGTAA	GAGGCAATT	CAAGGATATT	GACGACAATC	TTCTTTCTGA
241	AAGGGTTGCA	CTGAATATAC	TGGCAAAGTG	CTTAGTCAAG	CACTTATAAA	TTTACAAAGT
301	GTCCTCTCCG	AATTTGCTG	TTTGGTCTGC	ACAATCATTT	CTTGGAGTTG	AGAACATTTT
361	TCAACAATGT	TGGATACTAA	TTATTCTACT	GATTATTAAG	TACTTCATGC	A{TG} TAATCCC
421	AGCACCTTGG	GAGGCTGAGG	CGGGCGGATC	ACAAAGTCAG	GAGATCGAGA	CCAACCTGGC
481	GAACACGGTG	AAACCCCGTC	TCTACTAAAA	ACACAAAAAA	AATTAGCTGG	CGTGGTGGC
541	GGGCGCCTGT	AGTCCCAGCT	ACTCGGGAGG	CTGAGGCAGG	AGAATGGTCT	GAACCCGGGA
601	GGCGGAGCTT	TCAGTGAGCC	GAGATCGC	CACTGCAGTC	CAGCCTGGC	GACAGAGATG
661	GACTCTGTCT	CAAAAAAATA	AAATAAAATA	AAATAAATAA	AGGGATATTA	CAGAAATAAC
721	AGGCCTAGAG	TTCT				

Score	Start	End	Qsize	Identity	Chro	Strand	Start	End	Span
411	1	413	734	99.8%	13	(-)	34542731	34543143	413
317	412	734	734	99.1%	2	(+)	78301911	78302233	323

BLA(S)T Output: 13q13.2(-)(34,542,73{2-1}):2p12(+)(78,301,91{1-2})

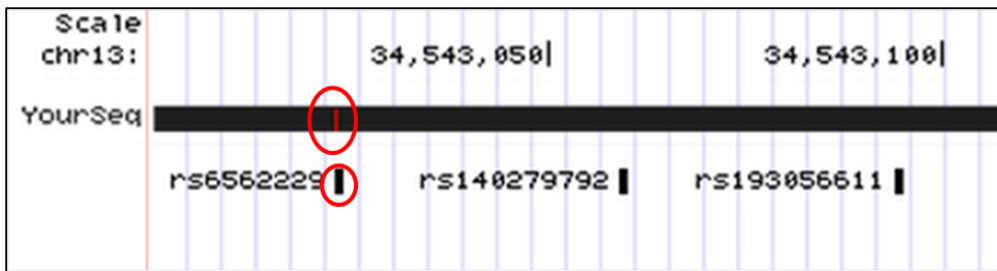


Figure S-DGAP248_1. BLA(S)T Output, Rearrangement_A on der(2): Circled mismatch represents a SNP (dbSNP build 141, rs6562229).

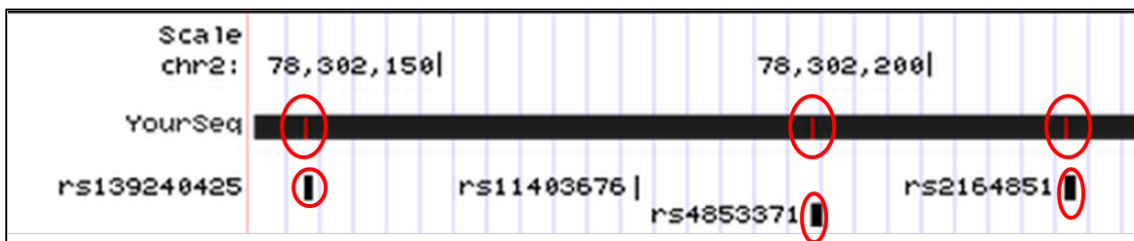


Figure S-DGAP248_2. BLA(S)T Output, Rearrangement_A on der(2): Circled mismatches represent three SNPs (dbSNP build 141, rs139240425, rs4853371, and rs2164851).

Rearrangement_B (on der(13))

1	CACCTGGCTA	ATTTTGTA	TTTCGTAGA	GACGAGGTTT	CACAATGTTG	GCCAGGCTGG
61	TCTCAAACTC	CCGACCTCAA	GTGATCCTCC	CACCTCGGCC	TCCTGCAGTG	CTGGGATTAC
121	AGGTGTGCCA	CCACGCCTGG	CCCAGCATTT	ACTCTTACA	AATGTAGCTG	AGAACATGGG
181	GATCAGATGG	TAATTTAACT	AAATGATCAA	CGAGTAGGTT	CACAGAAATGA	AGGACAACCA
241	GACTTTACCA	AAGCTTAGGT	TGCCTTGT	TTAGCCAATC	AAACAATCAA	AAGTTTT{ T
301	GTG}AGCCACC	GTGCGCCCGG	CCTGTAATAT	CTCTTGTTG	ATTAGCCTCC	TAGCCATATC
361	CCCGCTACTG	AATTATCTAT	CTTCCCCTTT	TATCTAAATT	CTCTGCTGCA	TCATTTTAAT
421	CATTCTCTTG	CCAACATCTC	AAATTCTTTT	CCTTATTG	ATGCCTATTA	CATGCTGCCA
481	GTTAAACTGT	GATTTGTAA	AAGTCTAAAT	GTTGGCTTCT	CAGCTTTCC	ATCTAGCTTT
541	CAAAGGCCAC	TGAAAAAAAG	AACAACTTA	AGTTTATTG	TATTCTTAAT	TGACAAATAA
601	TGATTGCACA	TATTTATTAA	GTAAGACTGG	TGGTATTATG	CTGCCCATGT	

Score	Start	End	Qsize	Identity	Chro	Strand	Start	End	Span
351	300	650	650	100%	2	(-)	78301558	78301908	351
301	1	303	650	99.7%	13	(+)	34542421	34542723	303

BLA(S)T Output: 13q13.2(+)(34,542,7{20-23})::2p12(-)(78,301,90{8-5})

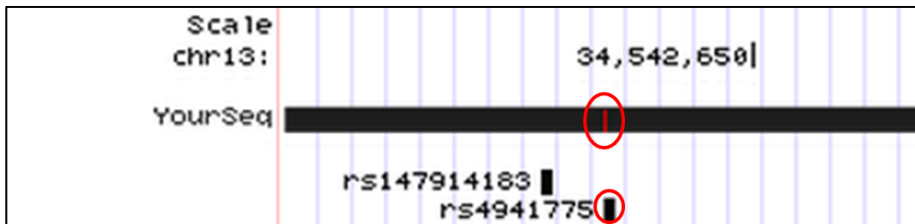


Figure S-DGAP248_3. BLA(S)T Output, Rearrangement_B on der(13): Circled mismatch represents a SNP (dbSNP build 141, rs4941775).

Next-Gen Cytogenetic Nomenclature:

Short System

46,XY,t(2;13)(p13;q14)dn.seq[GRCh37/hg19] t(2;13)(p12;q13.2)dn

Detailed System

46,XY,t(2;13)(p13;q14)dn.seq[GRCh37/hg19] t(2;13)(13qter->13q13.2(34,542,73{2-1})::2p12(78,301,91{1-2})->2qter;13pter->13q13.2(34,542,7{20-23})::2p12(78,301,90{8-5})->pter)dn

DGAP258

46,XY,inv(6)(p23q13)dn.arr(1-22)x2,(XY)x1.seq[GRCh37/hg19] inv(6)(p25.3q16.1)dn(q15q15)pat

or

46,XY,inv(6)(p23q13)dn.arr(1-22)x2,(XY)x1.seq[GRCh37/hg19] inv(6)(p25.3q16.1)dn,inv(6)(q15q15)pat

Prenatal History: A 28 year-old G1P0 female conceived after IVF and had abnormal maternal first trimester serum screening with an increased risk of chromosomal abnormality. Amniocentesis was performed at 15.9 weeks and the twins were determined to be monozygotic based upon SNP microarray results. The twin fetuses had normal ultrasound findings at 12 and 20 weeks.

Postnatal History: The twins were born prematurely at 33 weeks by C-section due to breech/breech presentation. Birth weights were 3 pounds 3 ounces and 3 pounds 4 ounces. They spent one month in the NICU for growth monitoring and did not require intubation nor have any illness or major complication during the NICU stay. At 2.5 years of age, the mother reports that the twins continue to be healthy without any hospitalization or developmental delay.

Sequencing Results and Interpretation of Convergent Genomic Evidence: Sequencing of the prenatal DNA sample identified the inversion breakpoints in non-genic regions at both 6p25.3 and 6q16.1. In addition, a paternally inherited cryptic rearrangement at 6q15 was identified. Due to the length of the sequencing reads, it was not possible to determine whether both of the breakpoints on 6q reside in the same paternally inherited chromosome, however, given their relative close proximity and localization within the same 2.21 Mb TAD, this is a likely possibility. An analysis of the protein-coding genes localized in the same TAD as the breakpoints did not reveal any additional monoallelic or imprinted genes associated with an abnormal phenotype, correlating with the normal clinical phenotype of DGAP258 (Figure 2D, Table 4).

BLA(S)T Outputs of Sequencing Results:

Rearrangement_A (on proximal part of inv(6))

1	TCTGCACCTCT	CATGTTGTT	GCAGCACTCT	TCACAATAGC	CAAGATTG	AAGCAACCTA
61	AGTGGCCAGG	AACAGATGAA	TGGATAAAGA	AAATGTGGTA	CTTATACACA	ATGGAGTAC {T}
121	GGAAGACCAC	AAAAAGCACC	CTCCCTGAGA	GCAGGCCTCT	CCCAGTGAAA	TGCAAGTTCC
181	AGGAAATGAC	TGAGTTGTCC	CATGTGCAGC	CGAGTCCATC	ATGAGGTGCA	GGGAGATT

Score	Start	End	Qsize	Identity	Chro	Strand	Start	End	Span
120	1	120	238	100%	6	(-)	93191547	93191666	120
117	120	238	238	99.2%	6	(+)	776786	776904	119

BLA(S)T Output: 6q16.1(-)(93,191,54{7})::6p25.3(+)(776,81{6})



Figure S-DGAP258_1. BLA(S)T Output, Rearrangement_A on proximal part of inv(6): Circled mismatch represents a SNP (dbSNP build 141, rs9406007).

Rearrangement_B (on distal part of inv(6))

1	GTTGTTGCAA	ATGACTGAAT	CTCATTATT	TTTATGTTG	AGCATGTACA	GCTAATTAAG
61	ATTCTGACTG	GGTTTAGGAT	CAAAGAAAGC	TGTCCCATTG	CATTCCCACA	TTCTTCCTTC
121	TTCTTTCAAT	GTCTTCCAAG	ATCTATTTA	AACGGGAAGT	GTTGTGTACT	TTTCAGGGGC

Score	Start	End	Qsize	Identity	Chro	Strand	Start	End	Span
138	43	180	180	100%	6	(-)	776650	776787	138
42	1	42	180	100%	6	(+)	93191504	93191545	42

BLA(S)T Output: 6q16.1(+)(93,191,545)::6p25.3(-)(776,787)

Rearrangement_C

Cryptic inversion spanning 6q15(92,254,978~92,235,543~)

Next-Gen Cytogenetic Nomenclature:

Short System

46,XY,inv(6)(p23q13)dn.seq[GRCh37/hg19] inv(6)(p25.3q16.1)dn(q15q15)pat

or

46,XY,inv(6)(p23q13)dn.seq[GRCh37/hg19] inv(6)(p25.3q16.1)dn,inv(6)(q15q15)pat

Detailed System

46,XY,inv(6)(p23q13)dn.seq[GRCh37/hg19] inv(6)(pter->q16.1(93,191,54{7})::p25.3q15(776,81{6}-92,235,543~)dn::q15(92,254,978~92,235,543~)pat::q15q16.1(92,254,978~93,191,545)dn::p25.3(776,787)->pter)

or

46,XY,inv(6)(p23q13)dn.seq[GRCh37/hg19] inv(6)(pter->q16.1(93,191,54{7})::p25.3q16.1(776,81{6}-93,191,545)::p25.3(776,787)->pter)dn,inv(6)(pter->q15(92,235,543)::q15(92,254,978-92,235,543)::q15(92,254,978)->pter)pat

DGAP259

46,XX,t(3;18;5;7)(p25;p11.2;q13.3;q32),t(9;18)(p22;q21)dn.arr(1-22,X)x2.seq[GRCh37/hg19](3,5,7,9,18)cx,der(3)t(3;7)(p24.3;q36.3)dn,der(5)t(5;7)(q14.3;q35)t(3;7)(p24.3;q36.3)t(3;18)(p26.3;p11.31)dn,der(7)t(5;7)dn,der(9)t(9;18)(p23;q21.3)dn,der(18)t(3;18)inv(18)(p11.31q21.3)t(9;18)dn

Prenatal History: A 28-year-old G1P0 female had abnormal fetal imaging findings of bilateral ventriculomegaly and colpocephaly, with partial agenesis of the corpus callosum observed by ultrasound and MRI. Amniocentesis was performed at 21 weeks. The pregnancy was terminated at 22 weeks due to the abnormal imaging findings. Fetal autopsy showed microencephaly (40 g vs normal 75 g for the gestational age), ventriculomegaly, agenesis of the corpus callosum, left renal aplasia and hypoplasia of the right kidney.

Sequencing Results and Interpretation of Convergent Genomic Evidence: Sequencing of the prenatal DNA sample identified all of the breakpoints of this complex aberration with nine rearrangement sequences located at 3p26.3, 3p24.3, 5q14.3, 7q35, 7q36.3, 9p23, 18p11.31, and 18q21.3. An analysis of the protein-coding genes localized in the same TAD as the breakpoints revealed multiple genes associated with phenotypes overlapping with DGAP259. In particular, the breakpoints at 7q36.3 disrupt the regulatory region of *SHH* that is associated with holoprosencephaly (Supplemental Table 2), which is consistent with the cerebral malformation phenotype of DGAP259.¹⁴ The breakpoints at 5q14.3 are located within the same TAD as *MEF2C*, a haploinsufficient region associated with cerebral malformation and hypoplastic corpus callosum,^{12, 15} as observed in DGAP259. Furthermore, two well-known genome organizer and chromatin regulator protein encoding regions, *SATB1*^{16, 17} and *EZH1*¹⁸ reside in the vicinity of *TBC1D5* and *CNTNAP2*, which are disrupted in the respective breakpoints at 3p24.3 and 7q35 and might be relevant to the complex chromosome aberration of DGAP259 (Figure 3, Table 5).

BLA(S)T Outputs of Sequencing Results:

Rearrangement_A (on der(3))

1	TGCTCGTCCC	ACCCCAGCGT	GGGGTGTGGA	GAGGTGGGCC	AGTAGGAGGG	GTGGCTGT
61	GGAGGCAGCT	TCCTCCAAA	TGGTTTAGTG	CAGTCTCCC	ATAGTGCCTG	AGGTCCCCCT
121	CTCTAGAGAC	GATTCAATTCT	GGCCGACTTA	CATTCAATTG	TTAAAAAGCC	AGGACACCCC
181	TTGAGTTCC	CCTCACTGAA	GGCATCTTGT	TCCCCTTGT	CCTTCCCCAC	CATGTTATGA
241	GGAAGCACAA	GAGGTCTCCC	CAGAACGCTG	GGCCATGCC	TTGAACCTCT	CAGACTGGAG
301	AACCGTGAGC	AAAATATACC	TTTTTCTTT	ATAAATTACC	CAGTCTGAGG	TATTATTTA
361	TAGCAAGGCC	CATCCAACAA	GTTTATGCTA	CTTAAATAAA	GTTCCTTCA	ATAAAAGATG
421	CCACAGTGGC	ACACAGTTAA	CTATGAGGAA	ATTTTTTAA	CTATATTAT	TTTGTGTCA
481	AAGGCTTAGG	TGTGCATTAG	ACAACCATT	ATTAATTAA	ATTTTGCTTG	GAATAAACAC
541	CCTGACAAC	AGCATTCAA	TTCAAGCTGC	TATACAACAG	AATCATTAC	TTTCAGATAC
601	AATCATGCA	TAACACCACA	AGCTCCTGCT	TCACAAATTG	CTCAATCCCC	AATCCCCAAA
661	TACTATAGAA	GATGGCTTAT	ATATAAGTTA	TACAAGACAT	GCATTCTAAT	ATTCAAGCCA

Score	Start	End	Qsize	Identity	Chro	Strand	Start	End	Span
363	1	367	720	99.5%	7	(-)	155701797	155702163	367
353	368	720	720	100%	3	(+)	17392144	17392496	353

BLA(S)T Output: 7q36.3(-)(155,701,797)::3p24.3(+)(17,392,144)

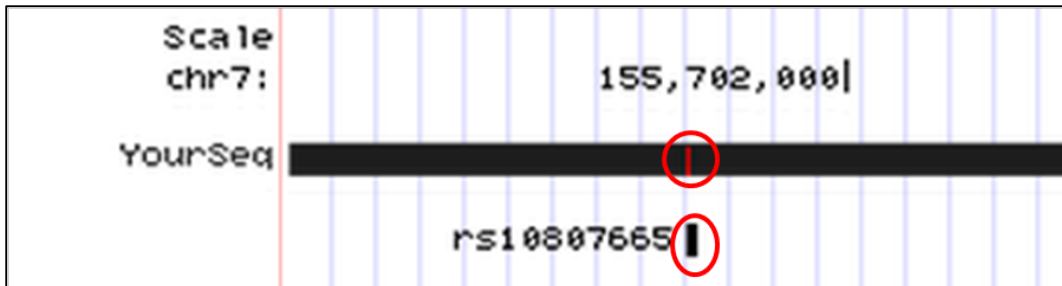


Figure S-DGAP259_1. BLA(S)T Output, Rearrangement_A on der(3): Circled mismatch represents a SNP (dbSNP build 141, rs10807665).

Rearrangement_B (on der(5))

1	AGCAGTAAAA	GGCACTAGCT	GGGTAGGTAG	TTATCAAGAA	TGACAAATAT	CCTAAAGTTG
61	TTAAATCTCC	CATTCTGAGG	AGTTGAAGTG	GGAAATGGAG	AGATTATTCA	ACTCTATCAA
121	CATCTGATAC	AGTAATTGAA	CTTACTTAAT	CATTATGTCT	CATCTTCAT	TATTAATTAA
181	AACAATTGTTG	GAATTATGTT	ATTCACGAAT	CAGACTTGTG	TGATAGTAAA	TACGCATTA
241	AAATAGTATT	TTGTGGAATA	TTTCAGAACT	TGTACTTTT	ACCATTGTT	CTTAGGCAGG
301	TAGAATCAAG	TAGTCACTA	AGGCTTGAAT	AATAGAGGGT	AAACCTCCTA	GTTCTAAGAT
361	GTCTGATATC	TGCTCTGTAA	AAAAATAAAA	TAAAATCACC	CAAATTACAC	TACAATAAAA
421	CAAGAGCCAT	TTTATTATGTC	TCAAACAATC	CATGGGTCAG	AACAAGGCAG	AGTGGATATG
481	GCTTATTCTA	TTATCATGCT	CTATGTCTGC	AGCATTAAATT	GAGGAAACTC	AAATGATGGA
541	GATTACCAGT	GTTGCTGGGG	TGTGGAATGA	GCTAGAACGCT	CGTTCATTCA	CATAATGTT
601	GCC {TGCTCCA AA} GCTGTACC	GAGTCAGTGG	CGGAGGCCGG	GTGAGCGTGG	GGAAGGGCAT	
661	CAGACACGGT	ATACCTGCTC	TTTTGTTTG	TTGTCACAAG	AGGCACTACT	
721	TCGCTGCCTC	CGTCTCCTCT	GTGGGTGGAA	AGGATGGACC	CAAAGGAACA	GAACGCTGTG
781	GCCACTCGAC	GATGGTTTG	ATAGGGACTT	ATCTTGCTCT	CTCTCCCTGG	ACACTCT

Score	Start	End	Qsize	Identity	Chro	Strand	Start	End	Span
611	1	612	837	100%	5	(+)	88755635	88756256	622
232	604	837	837	99.6%	7	(+)	147718911	147719144	234

BLA(S)T Output: 5q14.3(+) (88,756,2{48-56})::7q35(+) (147,718,91{1-9})

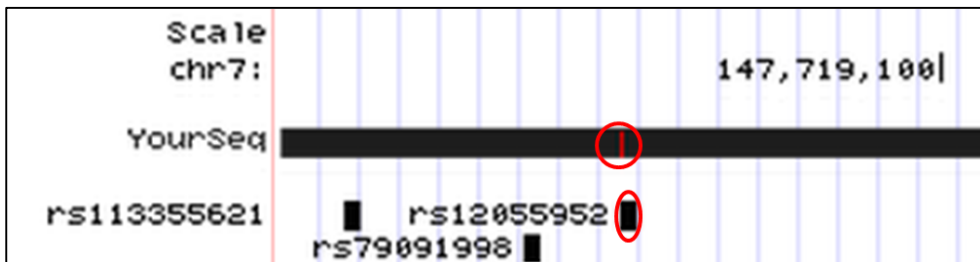


Figure S-DGAP259_2. BLA(S)T Output, Rearrangement_B on der (5): Circled mismatch represents a SNP (dbSNP build 141, rs12055952).

Rearrangement_C (on der(5))

1	GGCCTCACTC	AGTGCCTCG	GGTCTGGAGA	CATGAATCAC	GAACCCCTCCC	ACCAGCCCCA
61	GGATTTGGTC	AGTTATAAAA	ATATCCGGAT	TTGGCATGGG	GC GGATTCAG	GAACCGAAGT
121	TTGCTCTTGC	CCTGTTCTTG	CAGTATTGGA	TTGTACAATT	ATAGCTCTT	AGAAAGTTCC
181	TAATATGCCA	CAAGATGTCA	AGCAGCAGCA	CCAAGATTAA	TACTTTTTT	AATGACCATT
241	GCTGACTTTG	ACCTTGAAGT	GTGTGGTGTG	TTCTGAGAGC	ATATTTCCTC	CCCTCTGCTT
301	TGCAGCTCCT	GGATTTGAA	AAATTAACTC	CTTGCTCTCA	TCTGAACAGT	TCACCTAAGG
361	TGTTCACTTG	TTCTGTTTAC	CTTGAGCTAA	AGTGTAGGG	AGAGAGAGGG	AGAGGGAGGA
421	GGGAGGTAGA	GAAAAGGAGA	GGGGAGGTGG	AGAGGTAGGG	GGAGAGGAAG	GAAGGTGGGA
481	AGGAAGGGGA	GGGAGAGGTA	GGGAGAAGGG	GAGAACAAAT	GATGATTGTT	TAATGCAAAT
541	GTGTCGCGAA	TGACTGGTAG	TACATCTGTC	TCTTCATCCA	TAGGCCATTA	CTGAGCAACG
601	TTAGCACATG	ATTGTAAAAA	AGGAGAAATC	ATTACATGCA	GGTAGTACAC	ATTCAATCAA
661	TTCTGAGCTT	ATGTCTCTGG	TGAAATAAAA	AAGTATATAA	TGTAAATGAT	ATTTAATCTG
721	AATAACAAAA	AAGCAGCTCT	TTGACTCTGG	CTCAAGCTGT	TAGGTGAGGT	GACTGCTGTT

781	TGGGATTGAT	GTTTATTGGT	GGCCCAGTGG	GGAAAGGCTA	TCAC TTTTAT	TCTTTGTCAT
841	TCCTCCCATG	CGTTTCTCTA	ACCCACATCA	TATTTTAAGT	TCTGTTTCC	TTTTTTTCT
901	TATCTATTTT	TTTCTTTCA	TTATTTCTTT	CTTTGGGGA	GTAGTTGTG	GGATAGTGGT
961	AAAAAATGGG	TGCTGATGAC	CACCAAGTGTG	AGCAGTCAA	GCAAGCAATG	ACAATTAATA
1021	CAACAACAAC	AAAAGTTGTA	CGATTAGCTT	CAGCTCCATA	AGTGTCTAAT	GAGCCATTG
1081	TCAGTCTTT	GGTGAAATAA	ACTACTCTAT	CTTAATTCTC	CACTCTGCA	GTAAATAAAT
1141	AAAAGTTATG	AAACACCCGG	GCAACAATAA	AATATAATTT	ATTCATAGG	GCATGACAGA
1201	ACTCTTTACA	TATCTAAAAT	GAACATGTTA	TTTACAAATG	ACTTGTGATA	CTCATATAAA
1261	CCATGGATCT	GTGTGTTAAC	TGCTTTCATT	AGGGAGATAT	GCATTTTTT	CCTAATTGTT
1321	TAATCGTTA	AATGTATCAT	TACTCCTAAA	GGCATGTGAG	TTAAAGTGAC	TTCTCTGGT
1381	GCGATTAAC	CATAAGGCTA	AGAAGAACCT	CAGAAATGAG	CTCTCTGCA	GCTGAAGACA
1441	TTAAGAATT	AATGGAAAGG	ACAAAACAAT	AATTTCATT	TGGGAACCTC	TCAGCTCT
1501	GCTGATTATC	TTCCTGCCCT	TATTTATTT	TAGGAACCCC	A	

Score	Start	End	Qsize	Identity	Chro	Strand	Start	End	Span
511	1	511	1541	100%	7	(+)	155700363	155700873	511
1025	517	1541	1541	100%	3	(-)	17391112	17392136	1025

BLA(S)T Output: 7q36.3(+)(155,700,873)::AGAAC::3p24.3(-)(17,392,136)

Rearrangement_D (on der(5))

1	TTTCTATGGC	TGCTACCACC	ATTATCTCCA	TCCCTTAAG	AGGCCAGGT	TCTGATGTGC
61	CCATGCCCTC	AGGACTCCAG	GACTATGACT	ACCCAGGCAA	GCATGTGCAC	ACCTGCACAC
121	CACACCAACT	GCTGTGCACG	CATGCCGACT	GCTGGGTCTT	TAAGCCTGAA	CTTGTGTGTG
181	CAGGAGCTGC	CACATATGCA	TGTGGGTATG	GTGAAGCAGC	AGCAGCAGCA	GCTCATGCAC
241	ACACAGGTTA	CAAATAAATT	CTTAATCATT	TTACCTCTCA	ATTGTGTTT	AGTATGTACA
301	AAACACAAAT	TGAGAGGTA	AATGATTAAG	AATTCAAGA	CAGTCACAGC	AGAATATTTC
361	AAACATGGGG	ACTTCCTCAG	CACAGGGCTC	TGTGTGACTG	GATTGTATGT	CCATGAAACC
421	AGCTCTGGAT	GTCACGCTAA	GAATATATT	CTTACATAGT	AGAGAGTAGC	ATAGTAAAGA
481	GTAGCATGGT	GGTTATCAGA	GGCTGGTGGG	AG{G}CAGCCCG	AGTTTCCAA	TGCACCAAAG
541	CAGAAGCTT	TTGGAAACCT	ATATATTTT	TCATACTATT	GGGAATTCT	TCAGAATATG
601	AAGGCTTTAT	CGAATTGTGT	CTGAAATGAA	TTTCATTAA	ATACTGAATT	AATTGAAAGC
661	TTTGCTTCCTG	AATATTTTTC	CATAGATTTC	ACGGTGCTTT	AGAAATTTC	TTTGCTCTCA
721	TGTTTTAGTA	CTGGCAATAA	CTGCCAGTAA	TAGAAGTGGC	AGTGTGAGG	GAAATGGTGG
781	TGGCGAGTGT	GGGATGGTCT	CAGTGGGCAG	CTTTCTTACG	ATGAGGAGAG	GCGGGGCGTG
841	ACTGGTTCTA	TCGTGTTTC	ACTGGGACCA	GGACTCACTG	TGGAAGGGCA	GGAAGTACCA
901	CTTAGTGGTG	AGAACAGCAC	GCAGGCTCCA	GTTCACATT	CTGGTGATT	GACTIONTAATG
961	AAGCCCTTG	GAATTGGAC	TG			

Score	Start	End	Qsize	Identity	Chro	Strand	Start	End	Span
470	513	982	982	100%	18	(-)	6374582	6375051	470
513	1	513	982	100%	3	(-)	1408996	1409508	513

BLA(S)T Output: 3p26.3(-)(1,408,99{6})::18p11.31(-)(6,375,05{1})

Rearrangement_E (on der(7))

1	GTAGACTGTT	GAGTGAATT	CTAATAATAA	AGCCAAAAGG	AAAAATAATG	GCAATATGAT
61	TGGACAAGCA	GTTCAGAAT	CAAGGTAGGA	TGCCTTTTG	TTGGTGGAGG	TTTTTTGTTT
121	TTGTTTTGTT	TTTGGACTTA	TTCTCCCTCA	TATCAAATAA	ATTTATTAAA	CACACCTGAA
181	CACTTGTAT	GTGCCACTGT	CGGCCACGTA	TTAGGGACAC	GGAAGAACAA	TAAGACATAC
241	TCCCTACCAA	AAGAGGCTTA	TGGTTTAGAA	GGAAAGACACA	GTCTTGTAAA	CAGGTAAGTA
301	AAATAAAATG	TGAGCTGCAC	TATGCTGGAA	GTCAGCCCAG	GGTGGCCCAA	GTAGACCATA
361	GCCAGTCTAC	ATAAAATAGGG	AGACACGGGG	GACAGCTTTC	TAGATGTCCC	TAACGCTGAA
421	TCCTAAAAGA	TGAGAAGCAT	TTCTAGGGTG	CCAGAGTGG	GAAAACACCT	GACTTGTGGG
481	AGAACGGAAG	GCCTCGTGT	CATTCAATGG	ATCAACTATC	ATTGGCATT	TCCACCTGCG
541	AGAGACGGCG	CTAGCCCCCTG	GGGATCCAGT	CCCCGGTGAG	CTGGAAAGCT	ACTCTGTGCT
601	CTCAGAGGAC	TTGGAACAGA	GAATGCAGAC	AGGGTGGCAG	GAATGCAGGA	ATGTGCTCAC
661	AGTGCAGGAA	CCCGGTGGCT	CGCAGAGAAG	GGCACCAAAC	TTAGACCTGG	GAGATCAGGA
721	CCCTCTCCCC	CAAAACCTGG	A{GG}TTGGAAT	ACCTCCAAAT	CTGAACTCAG	CTTTGACTGT

781	CAATGGAGTG	CAGCTTGTGA	CCTCTCCATG	TAGTTGAGC	CTTTCAAAAA	ATGAAGTGTG
841	GCTACCTACA	ACCAACTGAT	TTTCAAAAG	TCAACAAAAA	TATGAAGTGG	AAAAAGGACA
901	CTCTATTAG	TAATGGTAC	TGAAACAATT	AAATAGCCAT	ATGCAGAAAA	ATGAAACTGG
961	ACCCCTATCC	TTTACCATAT	ATAAAATTAA	CTCAAGATTA	ATAAAGACTT	ATATGCAAGA
1021	CCTGAAACTA	TAAAAATCTT	ATAGGAAAAA	CTCTTCCAGA	CTCTGGCATA	AGCAAAGATT
1081	TTATGACCAA	GACCTCAAAA	GCAAATGCAA	CAAAAAGAAA	AATAGACAAA	TGGGACTTAA
1141	TTAAAGAGCT	TCTGCACAGC	AAGAAAAAAT	AATAATAATA	ATAAACAGAG	TAAACAAACA
1201	ACTTACAAA	TGGGAAAAAA	TATTTGCAAA	CTATGTGTCT	GACACAGAAC	TAACATCCGG
1261	AATCCAGAAG	CAACTCAAAA	CAACTCAAGA	AGAAAAAAAC	AATCCCATT	AGAAGTGGAC

Score	Start	End	Qsize	Identity	Chro	Strand	Start	End	Span
743	1	743	1320	100%	7	(+)	147718166	147718908	743
577	742	1320	1320	99.9%	5	(+)	88756239	88757077	579

BLA(S)T Output: 7q35(+)(147,718,90{7-8})::5q14.3(+)(88,756,2{39-40})

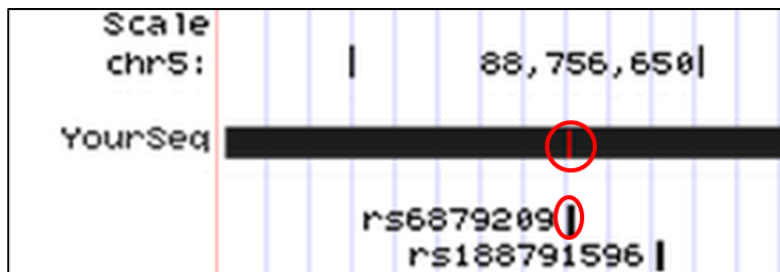


Figure S-DGAP259_3. BLA(S)T Output, Rearrangement_E on der(7): Circled mismatch represents a SNP (dbSNP build 141, rs6879209).

Rearrangement_F (on der(9))

1	AGCCTCATCT	CATTATAGCA	GATGGCATCA	TTCCAAAAGA	AAATAAAAGA	AAAAAAATTAA
61	ATTGATTACT	ATGTCAACCT	TGGCATCCAT	ATGCCAAATT	GTTTTTGAT	AAGAGCTAAG
121	TATTAGGTAG	AAACTCGAGA	AAAATTATTT	TCTCAATTCC	AAATTCTTC	TATAAGAATT
181	TCTTAAGTTC	ATAGATGCAT	ATTAAACAA	TCTGAGTATT	TCCAAAATAA	CCAGCTTTA
241	AACTTCCCTT	CTAAGGAGAC	CAATTATTC	ATCTACTAAG	TACCTTGT	CTTCCCTCAA
301	ATTACTCCAT	TTCATCTAAA	CTATTGTCA	CATATGAAA	AACAGATATA	ATATATAGTC
361	AATTACCAGC	AATAGAGCTT	TGGGTTTGAG	TTTGGGAGGT	GTAGAATTTC	AGAAAATGTT
421	AGGTTATTAC	AGCACTGAGT	CAGCTTGTAG	TTTGAATCAG	CAAGGATCAT	TATCTATCAA
481	AACATCAGTA	TGGTTTACCT	ACTGCTCTCA	TTC{A}CTATTA	AGTTTCTGT	TTATTTTCT
541	GCTGGCTCGC	TATGATGTAT	CAGAATGTAG	GTATTATTAT	CTGTTTATAC	TGAGAATCAA
601	TGTGTTTTTC	AACAATTTC	AAAGGTATCA	GCCAGCTATC	ATCTAGTTGA	ATATGCCTTC
661	TTCCTCCTCT	TTATACTATC	CTATAAAAAA	TAGTAGTCCC	TCTCTTATCC	ACAGGGCGTA
721	CATTCTAAGA	CCCTCAGTGG	ATGCCTGAAA	CTGCAGATAG	TACTGAACCC	TACGTACACT
781	GTGTTTTTC	CTATACATGC	ATATCTATAA	TAAAGTTAA	AATTAGTTA	TAAATTAGGC
841	ACAGGAAAAG	ATGAACAACA	ATAACTAAGA	ATAGAACAAAT	TATAAAAGTA	TATTGTAGTA
901	CAATAATGTG	GTCTTCTCT	CTCTCAGAAC	ACCTTGTGT	ACTATACCAC	AGGTTGGCTG
961	AAACTATGGA	AAGCAAAACT	GTGGATAAGC	TGGGGAGGTG	CAGGGGGCTC	ATATAGAGTA
1021	TATACTGTTG	TGGACATTTA	TACACTGGCC	TACATTTTT	ACCCTCTCAT	AATTTCATC
1081	TCTTGTGCCCA	TCTGTGCTTA	ATTCTAAATA	ACTTCTTCAG	GTCTGAATAA	ATTT

Score	Start	End	Qsize	Identity	Chro	Strand	Start	End	Span
514	1	514	1134	100%	18	(-)	54660138	54660651	514
621	514	1134	1134	100%	9	(+)	9646475	9647095	621

BLA(S)T Output: 18q21.31(-)(54,660,13{8})::9p23(+)(9,646,47{5})

Rearrangement_G (on der(18))

1	AATGAACCT	TTGAGAGAGC	AATCAATGGC	CTCATGGCTA	TTAGACAGCC	ATCTGCACAG
61	GATGAGGACA	GGTCTGCCTG	TGGTGGGTGG	AGAGGATACA	GCAGTTAAAA	TGTTCTTGTC

121	CAAGCACCTC	TTCACCCACA	CAGGAGGCTA	CTCCCAGGAG	GAACTATGCA	TCCCCTTTT
181	CTGGATAATA	AGCATGCTTA	TGTAGAGCTA	CTTCTTTCA	AATACAGTCT	ATTTTTCACA
241	CTGCAGATAA	TGGTATGTCA	TCATATCACT	CCTCTGCTTC	ATACTTCAA	AGTTTTAAC
301	TTTTCAGCA	AAAAATGCAT	TTCTAAAATT	TTTAATTGAT	GAATAGTAAT	TTTGTTTAT
361	GTATTTGTGG	GATATAATGT	GATATTTGA	TACATGTTA	CATTGTGAA	TGATTAAATC
421	AAGCTAGTTA	ACACAGCCAT	CACTTCACAT	CCTATCATT	TTTGTGATG	AGAATTAAAA
481	TCCTCATTGG	GTAATTTGA	AATATGTATT	ACATTAACGT	TAGTCACCCT	GCTGTGCCGT
541	AGGTCTCTAA	AACTTATTCC	TCCCCTCTGA	AACTTAGTAC	GCTGTGAACA	ACATCTCCTC
601	ATTTTGTGT	TTCTGCTTCT	GGAAATAGGA	GATAGAGATT	TTAGCTACAG	CAATCAGAAT
661	CCACCTCTGGA	GTGTGCTGTT	TTCCGTGAT	AGCAAGAAAA	TGTTCCATT	GAAAAGTGC
721	CCACAAAGAA	TCATCAGAAA	CCACAGAAAA	CAAATGATGG	TGTTGGCGGC	TT

Score	Start	End	Qsize	Identity	Chro	Strand	Start	End	Span
603	1	603	772	100%	3	(+)	1408382	1408984	603
169	604	772	772	100%	18	(-)	6559443	6559611	169

BLA(S)T Output: 3p26.3(+)(1,408,984)::18p11.31(=)(6,559,611)

Rearrangement_H (on der(18))

1	ATTGACGACC	TCCTGTGCC	CAGACGTTAT	TCCAGGTGCT	GGAGATACAG	TGACAAAGAG
61	CCCTCTCGGA	GGGCTCAAGT	AAAGGAACTA	GGATGAAAAG	TGCTGAGTGT	CATGCTAAGG
121	GAAGCGCTGG	CTGTGGAAGT	GTCCCTCACC	TAGCCTGGGA	TCGGGGTGGT	GGTTGCAGGA
181	GGCATCCAAG	GAAATGACAT	TTACACGGAG	GTCTGAGGGG	CAGCGAGGTG	GTGGGAAGGT
241	GGCTCCAGGT	AGGAGGTGAG	AAGAGAGCAG	ACAAAGTCAG	GTTGTAGCAC	AGTCTGGCTG
301	GGAAGAGAAG	TCGGCTGGTC	AGGTGGGGAG	CCAGGTCAGG	AGGTGCCTCA	GAAGCCGTGG
361	CAGCCTGGAC	TTATCCTTA	GGGCGGGAGA	GCCATGGAGG	GGCCATAAAAT	GGGGGAGAGA
421	GAGCCAAGCC	GTAGAGGCAT	TTTAGGTCCA	CATATGGACA	GTAAGTTGG	AAGGTATAAA
481	GACTGGAGTT	CCTGTATCGA	CTGGGGCAGA	TGCAGTGTAC	TAGGTGGCCG	CCAGTGBAAG
541	GCACCTGTGA	GTCAGGGTTT	GCAGTTCCCTG	TGTGGACGTC	TGAATTAATT	CTGCAGATCA
601	GACTGCGTAA	CACTGCAAG {A	GCAG} AAACAC	AAATGAGGTC	TGATGTTGA	AAACTTAATG
661	GAAGAAAAAA	ATAGAACATT	TATGCATAGA	AATAAACACA	TACACACAAA	GGAATACAGG
721	AAAAAACTGGG	AAATCTGAAT	AAGATCAGTG	GATTGTATTA	GTGTCAATT	CCTGGCTCTG
781	ATATTGTACT	ACAGTTTAC	AAGATGTTAT	CACTGGGAGA	AACTAGGTTA	AAAAGTACAT
841	GAGATACCTC	TGTATTATT	ATTATAATTG	CATGTGAATC	TAAAATTATC	TCAAAATAAA
901	AAAATAATT	TTAAAAAAATT	TGGAAAAGTA	ACAAAAGGAA	AACTAAATAG	TACCTAAAAA
961	ATAAAAAAACT	ATTAAACATT	TGTATTTGA	AAATAATTAG	AAGCATATGA	AAGAGATTGT
1021	GGCTTTTTG	TTCAATTCTT	TATAAATTAC	T		

Score	Start	End	Qsize	Identity	Chro	Strand	Start	End	Span
624	1	624	1051	100%	18	(-)	6375048	6375671	624
432	620	1051	1051	100%	18	(+)	6559598	6560029	432

BLA(S)T Output: 18p11.31(=)(6,375,0{52-48})::18p11.31(+) (6,559,{598-602})

Rearrangement_I (on der(18))

1	GTAATTATT	TGAAAATGA	TGTAATGCAA	ACCTAGTC	ATGAAGGTAT	GATGAACCAG
61	ACATTTCTG	GCGCATTGTC	TTCCCTCAGTC	TTGTCCTGTG	ACTTCTCTAA	GCCAATTCAA
121	TCAATTCCC	AATATTCAC	TGAACTAGAA	GTTCAGGGAT	ACGATAGTTA	AAAGAACCTA
181	CAGCATGCAT	TTGGTAAGTT	TCTCATGAAG	AGACATGTCC	CAGGTCTGGA	TAGTTGTTG
241	TCCTCATTG	GGGCAGAGG	AAACAGGCAG	ATTTCTTCA	AAGGACTGGT	ACTTACTCTG
301	CTAAATGGTT	TTTCAACAAAT	GGAATTAGAA	AACAGCAGAA	TAACATACCT	GTGCTGGGCA
361	AATACACACA	CACACACACA	CCCACACACA	CACACACACA	CACACACCA	CACACACACA
421	CACCCCTCCC	AAAATGGTCA	CCCTACAATT	CTATAGACTA	ACAACATCCA	AGAAAACCTT
481	CCATCAAGAG	CAGAGGCAAG	ATAACAAATC	TACAGACAAA	CAAATATTAA	GTTTACCACC
541	AACAGACCCT	CAAAAAACAA	ACTCTAAAT	ATGTAATT	GGCAGAGGGA	ATACTATCAC

Score	Start	End	Qsize	Identity	Chro	Strand	Start	End	Span
346	255	600	600	100%	9	(-)	9646126	9646471	346
252	1	254	600	99.7%	18	(+)	54659883	54660136	254

BLA(S)T Output: 18q21.31(+) (54,660,136)::9p23(=) (9,646,471)

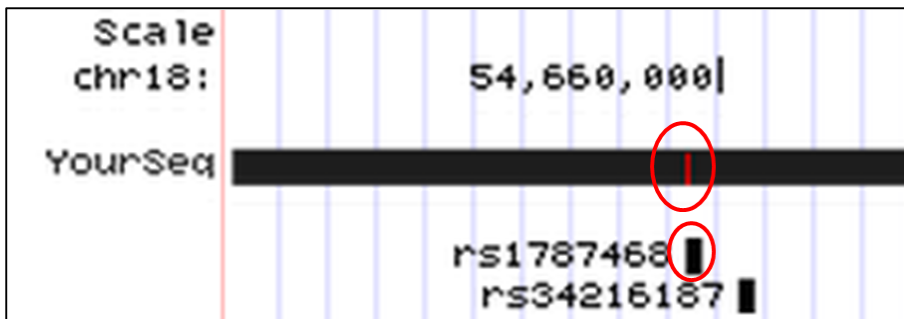


Figure S-DGAP259_4. BLA(S)T Output, Rearrangement_I on der(18): Circled mismatch represents a SNP (dbSNP build 141, rs1787468).

Next-Gen Cytogenetic Nomenclature:

Short System

46,XX,t(3;18;5;7)(p25;p11.2;q13.3;q32),t(9;18)(p22;q21)dn.seq[GRCh37/hg19](3,5,7,9,18)cx,der(3)t(3;7)(p24.3;q36.3)dn,der(5)t(5;7)(q14.3;q35)t(3;7)(p24.3;q36.3)t(3;18)(p26.3;p11.31)dn,der(7)t(5;7)dn,der(9)t(9;18)(p23;q21.3)dn,der(18)t(3;18)inv(18)(p11.31q21.3)t(9;18)dn

Detailed System

46,XX,t(3;18;5;7)(p25;p11.2;q13.3;q32),t(9;18)(p22;q21)dn.seq[GRCh37/hg19],(3,5,7,18)cx,der(3)(7qter->7q36.3(155,701,797)::3p24.3(17,392,144)->3qter)dn,der(5)(5pter->5q14.3(88,756,2{48-56})::7q35q36.3(147,718,91{1-9}-155,700,873)::AGAAC::3p24.3p26.3(17,392,136-1,408,99{6})::18p11.31(6,375,05{1})->18pter)dn,der(7)(7pter->7q35(147,718,90{7-8})::5q14.3(88,756,2{39-40})->5qter)dn,der(9)(18qter->18q21.31(54,660,13{8})::9p23(9,646,47{5})->9qter)dn,der(18)(3pter->3p26.3(1,408,984)::18p11.31(6,559,611-6,375,0{52-48})::18p11.31q21.31(6,559,{598-602}-54,660,136)::9p23(9,646,471)->9pter)dn

DGAP268

46,XY,inv(10)(p13q24)dn.arr(1-22)x2,(XY)x1.seq[GRCh37/hg19] inv(10)(p12.2p12.31)(p12.2q23.32)dn

Prenatal History: A 28 year-old G4P2TAB1 female had a previous pregnancy termination at 23 weeks due to hydrops fetalis. The father, who is of Iranian Jewish descent and the first-cousin of the mother, had two brothers who were deceased in the neonatal period. At 12 weeks of gestation, fetal ultrasound revealed abnormal nuchal translucency. Amniocentesis was performed at 17 weeks. The ultrasound findings at 15 and 22 weeks were normal. There were no complications during the pregnancy.

Postnatal History: Delivery occurred at 33 weeks at an outside facility (the reason for premature delivery is unknown). The newborn medical examination was normal. At 1 year of age, the baby was reported to be healthy and meeting all developmental milestones.

Sequencing Results and Interpretation of Convergent Genomic Evidence: Sequencing of the prenatal DNA sample identified the inversion breakpoints in non-genic regions at 10p12.31 and 10p12.2, and disruption of *CPEB3* at 10q23.32. An analysis of the protein-coding genes localized in the same TAD as the breakpoints did not reveal any monoallelic or imprinted genes associated with an abnormal phenotype, correlating with the normal clinical phenotype of DGAP268 (Figure 4A, Table 6).

BLA(S)T Outputs of Sequencing Results:

Rearrangement_A (at proximal breakpoints of the pericentric inv(10))

BLA(S)T Output: 10q23.32(-)(93,983,897~)::10p12.2(+)(23,659,495~)

Rearrangement_B (at distal breakpoints of the pericentric inv(10))

1	GATGCCCTC	TGCTCCAGAA	ATCACCAACT	CCTACTACTT	TCCCCAGCTC	TATTTTCCAC
61	TCCTTTCATT	AGGTTACAAT	AGTAGGAACA	GACCTTAGGT	CATAACACCA	CCAAATAAGT
121	GAATGCAGAG	TAGAAATGTT	CCCCTAAAGA	GAGGAGGTCA	TTTGAACAAA	CAGCAATACC
181	TGTCAAGTTA	ATATTTCTGA	GTTATAACTC	CTGTACCAGA	AATGTAACAA	CATCTCACTC
241	TTGAATCAAA	ACTTCAGGC	CAGGTGTGGT	GACTTGTGCC	TGTAATCCC	GCATTTGGG
301	AGGCCATGGC	AGGTGGATCA	CTTGAGGTCA	GGAGTTCGAG	ACCACCTGG	ACAATATGAT
361	GAAACCCAT	CTGTACTAAA	AATACAAAAAA	ATAGCTGGGC	ATGGTGGCAG	GTGCCTGTA
421	TCCCAGCTAC	TCGGGAGGCT	GAGACAGGAG	AATCTCTTG	GCCCAGAGG	CAAAGCCTGC
481	AGTGAGACGA	GATCACGCCA	GTGCACTCCA	GCCCTGGACAA	CAGAGCAAGA	CTCCATCTCA
541	AAAAAATAAA	AACTCTCAA	TTCATTTATT	TATTCAAATA	TATAATAAGC	ATCTACTACA
601	GCTGAAGCTT	TGCTGCTGTG	GTCTGAATGT	GGTATACCCC	CAAAATGCAC	ATGTTGAAAT
661	TTACTCCCCA	TTGTGATAGT	ATTAAGAGGT	GGGGCCTTCG	AGGAAGTAAT	TAAGTCATGG
721	AGGCTCTGCC	CTCATTAATG	GGGTTAGAGC	TTTATAAGA	AAGAGAGGCT	TGTAGTCCC
781	GCTACACAGA	AGGCTGAGGC	AGGAGGATAG	CTTGAGCCCA	GGAGTTCAAG	TCCAGAATGG
841	GCAGTACAAT	GAGACCCAT	CTCTAAAAG	AGGGAGAGAG	AGAGAGAGAC	ATTGATTGAA
901	GGGTGTGTGT	TTGCCCTTC	TGCCATGTGA	GGACACAGAA	AGAGGCACCA	TTCATGAAGC
961	AGAGAACGAG	CCTTATTACAG	ACAATGAATC	AGCTAGTGC	TTTATCTTGG	ACTTTCTAGC
1021	CTCTATAATT	GTGAGAAGTA	TTAAAATTTC	TATTATTTAT	AAATTACCCC	ATCGAAGACG
1081	TTCACTTACC	TGACTTTCCA	GATTAATCTC	TGTGTTTTAT	CTTCCTATA	AAAAATATCC
1141	ACAGCACATT	CAACAGCCGT	GACCAATAAG	ACCATAAATT	TCTGCCAAC	AGATGAATTG
1201	CAAGCTTACC	TAGAGATGGT	AAAGGTTGT	CTCCAAACCT	CTTTTTTTT	TTTTTTAATT
1261	TTTCATAGAG	ATGGGATCTT	CTATGTTGC	CCAGGCTGGT	CTCGAACTAC	CGAGTTCAAG
1321	CAATCCACCC	ACCTCAGCCT	CCCAAAGTGC	TGGGATTACA	GGTATGAGCC	ACTGCACTCA
1381	GTTCTAAACC	TTTTTAATGT	CAGTATTATT	GTAATTATGT	GACTTAAATA	TATGCAAACC
1441	AATGAAATGA	ATGCCAAAAAA	ATTATTTGAT	GAAAAGCAAT	TTGAATTG	TAGATTGAA
1501	TTTAGAAAAA	GCTAGATACA	ACAGCAATCA	GGTTTCATTT	ATTCAAAACG	TTATCAAAGT
1561	TCAGCAGGAA	TTCTCTCAGC	TCTGAAGAGG	GAAAAGAGA	AATTTAAGA	GATGCTATG
1621	TTTTAAAATC	TTAAAACCTT	GCATTGGGTG	CCATGTTGTT	GGGTGCCATG	TAGCAGTGCT
1681	TTTACTCTGT	ATCTGTAAGC	TCCCAGATGC	ACTGTAGCAC	CCCAGGCTAG	AGTGCAATGG

1741	TGCGATCTTG	GCTCACTGCA	ACCTCTGCCT	CCCAGGTTCA	AGCGATTCTC	CTGCCTCAGC
1801	CTCCAGAGTA	GCTGGGATTTC	CAGACACCCA	CCACCACGTC	CAGCTAGTTT	TTGTATTTAT
1861	AATAGAGATG	GGGTTTCACC	ATTGGGCCA	GGCTGGTCTC	AAACTCGTGA	CCTCAGATGA
1921	TCCACCCACC	TCCACCTCCC	AAAGTCCTGG	GATTACAGGC	ATGAGCCACC	ACTCCCAGCC
1981	CAACCAGGAG	CTTTTTAAAA	GTAGATCCAC	TGTGTCCTGG	CCCAAATCCA	CCAGCTGCCT
2041	CAGAGTCTCA	CAGGCTAGGC	CTGTGTTTT	AAGAATGCTG	TGAGTGATTC	TGACATACAA
2101	CCCAGCTAG	GAATAACAGC	CCCACTAGGC	TGGCTGACTC	ACCTCCCTC	TCATCTTCT
2161	AGGACTCTGT	TTTCCCCATT	GCGGGGGATT	TCGGCTCATC	AAAGTACACC	AATTGACTCT
2221	CAGCATCACT	GAGCTTTTC	TTTCACATCC	AGGGTGAGTT	TAAGTCAGTG	CTTCTCTGGG
2281	TCTCACAGGA	GTGGACATTC	TAAGGCCAGC	ATCTCCTCTG	AGTAACTCAC	TCCCCGATGA
2341	TGGGAGTTG	ACTTTCCCTT	GGTTATGAGT	TACAGGATGA	AAAGTCAGGTG	CAAACACTTA
2401	TTTCTTCAAG	CCAACAAATC	CTAGCACCTC	CTCGATCTCA	GAGAAGGTCA	GCAGACATGT
2461	GTGTGCCACG	TTTCTTCATC	TCAAGAGCTG	TGTATCATAG	TGGGAAACTG	GACTTGCAAA
2521	TGGCTATGCA	GGAAGAGAAAG	GCTGTGTGAG	TGTCGGCCCC	TGGGTAGAGG	CTGTCTTGT
2581	TGAAACCGTG	GTGCCCGAC	AAAAGCCGGA	AAGCGAATCT	CCTTCTACTG	CACCTGCAGG
2641	CTCTGGGGCC	AAGCATGTT	CGGGCGAGAG	GATATTAGG	GATTCTGGG	TTTAGCTTTC
2701	TCCGTTTTC	CGTTCAGTTC	ACTCTGGCCC	TGGCTGTCTC	CAAAGGAGAG	GACTGATACC
2761	ATGGGATCAA	GTCCTTATGT	TCAAGCTCCG	GTCTGGGAAG	CTGAGTCTCC	ATCTTTTCT
2821	GAGGCCAAGG	CATTGTTCTG	ACAAC TGCCC	TTGACTCCAG	TTCCCTCAGG	ATGAGGGCCG
2881	TGGCTTTCT	TGCCCACCT	TCTGCTCTG	AATCCTTCCT	CGCAGCCTCT	AACCACACTG
2941	CTAGCCCTCA	TCTCTGGCTT	GCTGCCAATT	TCCTCTGGCA	CTATCCTCCC	TAGCTGGCTG
3001	CAAACCCACC	TGTTGTTTT	TGGGTTTTT	AGAGATGGGG	TCTCGCTCTG	TTGCAATCAT
3061	AGCTCACTGC	AGCATCGAAC	TCTTGGGCTC	GACAATCCTC	CCACCTCAAC	CTCCTAAATA
3121	GCTGAGACTA	TAGGTGCCA	CCACCACATC	TGGCTTATTT	TTTTATTTT	TTGTAAGAGA
3181	TGGAGTCTCA	CTAGATTACC	CAGGCTGCTC	TCAAACCTCT	GGCCTCAAGG	GATCCTCCCA
3241	CTTCTGCCTC	CCAAAGTGT	GGGATTACAG	GCATGAGCCC	CAGTGCCGA	TCGCCACTTG
3301	TTTCTCTTG	CTTACTC				

Score	Start	End	Qsize	Identity	Chro	Strand	Start	End	Span
1598	1720	3317	3317	100%	10	(+)	21606655	21608252	1598
1698	1	1698	3317	100%	10	(+)	93980711	93982408	1698

BLA(S)T Output: 10q23.32(+)(93,982,408)::GCTCCCAGATGCACTGTAGCA::10p12.31(+)(21,606,655)

Rearrangement_C (breakpoints of paracentric inv(10))

1	CATGGTTG	TTTGAGAAGG	AAATTGTCAA	GACTTCCTCT	CTCTCAGGCT	GGGTTGGTT
61	ACTGGAACAT	TTAGGACACT	TTGAGCAGCA	GGTAACGTAA	CACCAAAATT	AAACAATGCA
121	TAAATGCATT	AGATTGTGAG	CCTGCGAGTT	TAGAGATAAG	ACACTATGTT	CTCTGGAGGA
181	TTGGCTCAAT	TCAGTGGTT	TAACTCCACG	TTCCCTCAAC	TCTCTGGACT	CATCCTCAAG
241	GCCTAGAGCA	AGATGTCTGC	AGCCATTCCA	GGCCTCAGTT	ATACCAATGT	CCAGAGGGAG
301	AGAGGGTTTC	CCCTCCAAAAA	TTTCTCTCAA	GAGTGTAGGG	GAAGGGCCAG	GCTCGGTGGC
361	TCATGCCTGT	AATCCCAGAA	CTTGGGAGGG	CCGAGGCAGG	CGGATCACCT	GAGGTTGGGA
421	GTTCAAGACC	AGCCTGACCA	ACATGGAGAA	ACCCCCTCTC	TGCTAAAAT	ACAAAAAAA
481	AAAAAAATAG	CCGGGAGTGG	TGGTGCATGC	GTGTAATCCC	AGCTACTTGG	GAGGCTGAGG
541	TAGGAGAACAT	GCTTGAACCC	GGGAGGAGGA	GGTGCAGTG	AGCCGAGATC	GCGCCATTGT
601	ACTCCAGCCT	GGGCAACAAG	AGCGAAACTC	CATCTAAAAC	AAAAGAATGT	AGGGGAAAAA
661	ACCAATACCC	TTTCCTCATC	CATCACAAGG	GTCATGGCAG	ATACTCCTAT	AACAAGAGAC
721	AGAGTAACAA	GAGAAAAGCA	TCACAAATT	ATTAAACCA	GGTTACGTG	ACAGGGAGC
781	CTTCAAAGT	GAAGACCTGA	AGACCCAGGG	AAGACTGTGC	TTTTGTGCTG	AGTCTGATGG
841	AAGAAGTGA	{CAG}AAAAAAA	AAAAAAAAAA	AAAGGCCGGG	CGCAGTGA	CACGACTGTA
901	ATTCCAGCAG	TTTGGGAGGC	TGAGGCAGGT	GGATCACCTG	AGGTCAAGGAG	TTCAAGACCA
961	GCCTGGCCAA	CATGGTAAA	CCCTGTCTCT	AATAAAAATA	AAAAAAATT	AGCCGGGTGT
1021	GGTGGTGGGC	GCCTGTAATC	GCAGCTACTC	AGGAGGCTGA	GGCAGAATTG	CTTGAACCCA
1081	GGAGATGGAG	GTTGCAGTGT	GCCGACATGG	TCCCACTGGA	CTCCAGCCTG	GGCGACAGAG
1141	TGAGATTCCA	TCTAAAAAAA	AAAAAAAGAA	AAAGCCCCTC	GTTGAAAACA	GTGTGGAGAT
1201	TATAAAAATA	GAACCACCAT	ACACTTCAGC	AACCTTGCTA	CTGGGTATCT	ACCCCCGCAA
1261	AAAAAGAAAT	CATTTTATAT	ATAAAAAAAT	ACCTGTGCTC	ATATGTTAT	TGCAGCACTA
1321	TTCACAATAG	CAGAGTCATG	GAATCAACCT	AAGTGACCAT	CAACGGAGGG	CTGGCTAAAG
1381	AAAATGCACT	CTAAATACAC	AACAGAGGCC	GGGCGCCTGA	AAATGCACTC	TAAATACACA
1441	ACAGTGGCTC	ACGCCTGTAA	CCCAGCACTT	TGGGAGGCCG	AGGCGGATGG	ATCACCGAGGT
1501	CAGGAGATCA	AGACCACATCCT	GGTTAACACCG	GTGAAACCCC	GTCTCTACTA	AAAATACAAA

1561	AAAAATTAGC	CGGGCGTGGT	GGTGGGCACC	TGTAGTCCC	GCTACTTGGG	AGGCTGAGGC
1621	AGGACAATGG	CGTGAACCCG	GGAGGCAGAG	CTTGCAGTG	GCCAAGATCG	CGCCACTGCA
1681	CTCCAGGCTG	GGCGACAGAG	CGAGACTCCG	TCTAAAAAA	AAAAAAAAAA	AATACACAAC
1741	AGAATACTAT	TCAGGCATAA	AAAAGAAACA	ATGTCTTTG	CAGCAACATG	GATGGAAC TG
1801	GAGTCCATTA	TCTTAAGTGA	AAGAACTCAG	AAACAGAAAG	ACATTGCATG	TTCTCACTTA
1861	TAAGTGGGAG	TTGAATAATA	TGGACCCAGG	GACATAGAAT	GCAAAATAAT	AGACGCTGGA
1921	GACTTGGAGG	TGTAAGCGGG	TGGGAGGGAT	GGGAGGTTGC	TTGGTGGATA	TAAAG

Score	Start	End	Qsize	Identity	Chro	Strand	Start	End	Span
1125	851	1975	1975	100%	10	(-)	21605510	21606634	1125
853	1	853	1975	100%	10	(+)	23658350	23659202	853

BLA(S)T Output: 10p12.2(+) (23,659,20{0-2})::10p12.31(-) (21,606,63{4-2})

Next-Gen Cytogenetic Nomenclature:

Short System

46,XY,inv(10)(p13q24)dn.seq[GRCh37/hg19] inv(10)(p12.2p12.31)(p12.2q23.32)dn

Detailed System

46,XY,inv(10)(p13q24)dn.seq[GRCh37/hg19] inv(10)(qter->q23.32(93,983,897~)::p12.2q23.32(23,659,495~-93,982,408)::GCTCCCAGATGCACTGTAGCA::p12.31p12.2(21,606,655-23,659,20{0-2})::p12.31(21,606,63{4-2})->pter)dn

DGAP285

46,Y,inv(X)(p11.2q28).arr(1-22)x2,(XY)x1.seq[GRCh37/hg19] inv(X)(p11.21q28)

Prenatal History: A 22 year-old G1P0 female had a spontaneous conception and uncomplicated pregnancy until comprehensive ultrasound screening at 22.5 weeks, which revealed hydrocephalus, hypoplastic and irregularly shaped cerebellum, unilateral left multi-cystic kidney, and single umbilical artery. Amniocentesis was performed on the same day at 22.5 weeks. Fetal echocardiography at 23.1 weeks was reported to be normal. Follow-up fetal ultrasounds at 23.1 and 28 weeks continued to be significant for the previously reported abnormal findings. At 31.4 weeks the mother presented at an outside hospital for decreased fetal movements and intrauterine fetal demise was detected. The parents declined any post-mortem studies.

Sequencing Results and Interpretation of Convergent Genomic Evidence: Sequencing of the prenatal DNA sample identified the inversion breakpoints within *FAM104B* at Xp11.21 and within a non-genic region at Xq28. The breakpoints at Xq28 disrupt a TBR, which may result in genomic rewiring of the surrounding TADs and TBRs. *MTM1*, a hemizygous gene associated with X-linked centronuclear myopathy (a prenatal onset fatal disease with clinical findings including decreased fetal movements and hydrocephalus),^{19; 20} is located in a TBR upstream to the Xq28 breakpoints, and therefore dysregulation of *MTM1* might be contributory to the phenotype of DGAP285 (Figure 4B, Table 6).

Next-Gen Cytogenetic Nomenclature:

Short System

46,Y,inv(X)(p11.2q28).seq[GRCh37/hg19] inv(X)(p11.21q28)

Detailed System

46,Y,inv(X)(p11.2q28).seq[GRCh37/hg19] inv(X)(qter->q28(150,286,207~)::p11.21q28(55,174,723~-150,284,569~)::p11.21(55,174,381~)->pter)

DGAP288

46,XX,t(6;17)(q13;q21)dn.arr(1-22,X) x2.seq[GRCh37/hg19] t(6;17)(q21;q24.3)dn

Prenatal History: A 37 year-old G3P2 female had an abnormal fetal ultrasound with a cystic hygroma identified at 11.1 weeks. CVS was performed at 11.6 weeks. At 28 weeks polyhydramnios and micrognathia were detected on ultrasound examination. At 34 weeks, fetal MRI revealed findings suggesting Pierre Robin sequence including a small jaw index consistent with micrognathia and retrognathia, glossptosis, and suspicion for cleft palate without cleft lip.

Postnatal History: C-section was performed at 39 weeks and continuous positive airway pressure was applied after birth. Physical examination finding of cleft palate was consistent with Pierre Robin sequence, and additional findings included small low-set ears, a flat nasal bridge, hypotelorism, a short wide neck, and a large space between the 1st-2nd phalanges. The newborn received nasogastric feeding due to the cleft palate.

Sequencing Results and Interpretation of Convergent Genomic Evidence: Sequencing of the prenatal DNA sample identified the translocation breakpoints within non-genic regions at 6q21 and 17q24.3. An analysis of the protein-coding genes localized in the same TAD as the breakpoints revealed that the 17q24.3 breakpoints are within the same 1.88 Mb TAD as SOX9 and within its well known upstream cis-regulatory region for Pierre Robin sequence.²¹⁻²³ DGAP288 had decreased SOX9 RNA expression and an overlapping phenotype of Pierre Robin sequence (Figure 4C, 5, Table 6).

Rearrangement_A (on der(6))

1	ATAACAGAAG	CATTCTTAG	TCACCCTAAT	GATAGACAGT	GAAGCAATCT	GGTGAATGGT
61	TAGGATGTTA	GTTGGATGGG	AGGATTGAA	AAGGAGCAGA	TATAGTTGAG	TATTGAAAG
121	CAAGAATTCT	GTGTTGGTACA	TTTAAGTTG	AGAAGTCAAT	TTTATGGACG	TCCAAGGAGA
181	GATATTGCTT	AGGTAGTTAA	ATGATTGAGT	CAAACATTCA	TGGGAAAGGT	GAGAGCTAAA
241	AACATAAACT	AGGGAGTTAT	TAGCTTATAA	AGTTAACCTT	TAAAGCCATG	GGATTCAACG
301	TTTCCACCTA	GAACATATGT	GTTGTTAGAG	AAAAGTGTGA	GGCTTGAGCC	CTAGACCATG
361	ACAATACGTA	GACATCAGGA	AGACGAGAAG	GATCCAGGAA	AGGATATAGG	AAGGAGTAGC
421	CAGTGAATA	GAAGGTAAGC	AAATGAACAA	AAATGTCCTG	GAAGAAAAGT	GAAAAAAGGT
481	TTCAAGGAGG	AGAAAAGTGT	CCACTGTGTC	CAGTGAATT	GATGAATTAA	ATGAGGCAAG
541	AAATGAGAAT	TGATCATTGG	ATTGTTAAC	AGAGGTCACT	GGTGACTGAT	AAATTTCACT
601	GGAGTGATCA	AGGTGAAAGC	AAGATTGGAG	AGTGTTCACA	AGATAATGAG	ACAGGAAGAA
661	CTGGAGACAG	AAATAACTCT	TTCGAAGAGT	TTTCATCTAA	{AGG} ATTTGCC	TTCAGCCATT
721	TCTCAGTTAG	GAAAAATACA	GATTCTGGGG	GAAAGTTATT	CACAGAGAAA	GTAAAAATTG
781	CCAGTGGGTC	TTTTTTTTT	TTTCTTCCAG	AAATAAAAGG	AT	

Score	Start	End	Qsize	Identity	Chro	Strand	Start	End	Span
703	1	703	822	100%	6	(+)	112975342	112976044	703
116	701	822	822	95.9%	17	(+)	69728017	69728137	121

BLA(S)T Output: 6q21(+)(112,976,04{2-4})::17q24.3(+)(69,728,01{7-9})

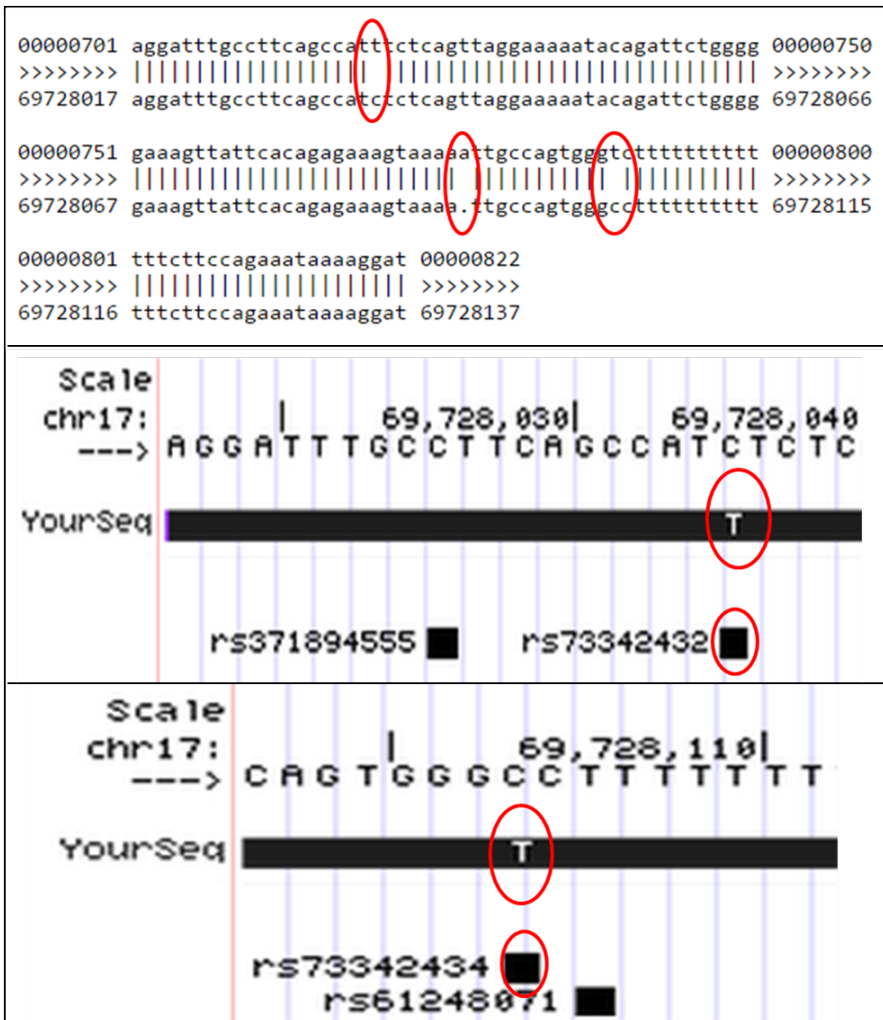


Figure S-DGAP288_1. BLA(S)T Output, Rearrangement_A on der(6): Circled mismatches represent a SNP (dbSNP build 141, rs73342432), an additional repetitive nucleotide “A”, and another SNP (dbSNP build 141, rs73342434); respectively.

Rearrangement_B (on der(17))

1	CTGGGTATT	ACAGAAAAAG	ATGTTGAGCC	TTCTTCTAGG	CAGAGACAAC	TCTTCTAGAA
61	AATATCTCAT	ACAATAAAGA	TTGATTATCA	CATTGTTTAG	TGTGTAATTC	ATGTGTTCTC
121	AAAATTTCC	TTAGAGGTAT	AGCAGTTACA	GACATACCCC	AAATACATAA	ATCTGTGCTT
181	GTACTAAGAG	AAACTTGGTG	TCAATTATTTC	ACTTCCAAA	AGGATTCACT	AGATGTCATC
241	CTCAGTGATT	TTCCTTAGAG	CGTTTCAGGT	GGGATTTGAG	TTATCAAAC	TGGTTTCATT
301	TGTGCTTCG	TGAATATACC	TATTTGGTAA	GATCTGTTT	GCCAAATTCA	GTCCAATACA
361	AATTGGTCTT	GAATCCTATT	CAAGGGAGAT	TATTTTAAA	GGACCTGAGG	GACTTCATTA
421	TAACCACAGC	TTCTTCTACC	CCGGATGCC	CATGCCCTAA	GACTCCCAAG	AGCAGCAGCT
481	TTCCAGCCAT	GTCCTGAGTT	TCTGGGGCAG	AGTAAAGCCC	TTTATTTC	TCTAAAGGGC
541	TTTAGGGAAA	TAGCTGGTAG	CTGGAAGGAA	ACATGAGATT	AAGAGAGGGT	TTATTTCTATT
601	GTTTCAAAG	TTGAGATTTA	ATGTACATAT	TATGAAATGC	ACAGATCTTA	CATGTACTTA
661	GTTCTGATAA	ATGCACATAC	CATGTGGCAT	GCACACTCTT	ATGAAGATAT	AGAGCATT
721	TCTCAGTCCA	GAACATTCCC	TTTTAGCCAT	TCTAGTCAAT	ACATATATCA	TCCTACTTTC
781	CCTTATCTAC	TCCATATGAA	GCAACTATTG	TTCTGATTTC	TCTCAACATA	GAACATTCTT
841	GCCTAGTCCA	AGAGTCGTA	TCAATGGAAT	CACAGGGTGT	GTC	

Score	Start	End	Qsize	Identity	Chro	Strand	Start	End	Span
517	1	517	883	100%	17	(+)	69727490	69728006	517
357	525	883	883	99.8%	6	(+)	112976031	112976389	359

BLA(S)T Output: 17q24.3(+)(69,728,006)::CCCTTTA::6q21(+)(112,976,031)

or

BLA(S)T Output: 17q24.3(+)(69,728,006)::6q21(112,976,045-112,976,039)::6q21(+)(112,976,031)

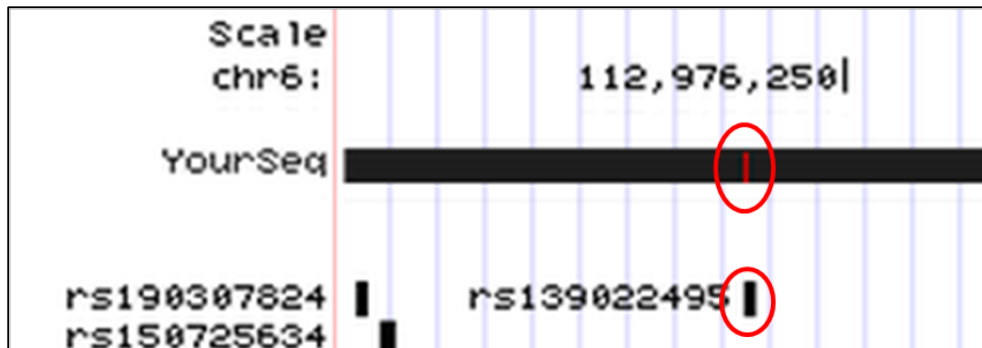


Figure S-DGAP288_2. BLA(S)T Output, Rearrangement_B on der(17): Circled mismatch represents a SNP (dbSNP build 141, rs139022495).

Next-Gen Cytogenetic Nomenclature:

Short System

46,XX,t(6;17)(q13;q21)dn.seq[GRCh37/hg19] t(6;17)(q21;q24.3)dn

Detailed System

46,XX,t(6;17)(q13;q21)dn.seq[GRCh37/hg19] t(6;17)(6pter->6q21(112,976,04{2-4})::17q24.3(69,728,01{7-9}->17qter;17pter->17q24.3(69,728,006)::CCCTTTA::6q21(112,976,031)->6qter)dn

or

46,XX,t(6;17)(q13;q21)dn.seq[GRCh37/hg19] t(6;17)(6pter->6q21(112,976,04{2-4})::17q24.3(69,728,01{7-9}->17qter;17pter->17q24.3(69,728,006)::6q21(112,976,045-112,976,039)::6q21(112,976,031)->6qter)dn

DGAP290

46,XY,t(2;7)(q33;q32)dn.arr(1-22)x2,(XY)x1.seq[GRCh37/hg19](2,7)cx,der(2)t(2;7)(q32.3;q33)inv(7)(q33q33)dn,der(7)t(2;7)dn

Prenatal History: A 38 year-old G2P2 female conceived after IVF had a high-risk pregnancy based on first trimester combined screening results. CVS was performed at 13 weeks 6 days. Ultrasound examinations at 16.4 and 18 weeks were normal. Due to a family history of congenital heart anomalies, fetal echocardiography was performed at 16.4 weeks and was interpreted to be normal. The parents decided to terminate the pregnancy at 23 weeks due to uncertainty of the clinical significance of the balanced rearrangement.

Sequencing Results and Interpretation of Convergent Genomic Evidence: Sequencing of the prenatal DNA sample identified the translocation breakpoints disrupting *HECW2* at 2q32.3 and *NUP205* at 7q33, with an additional non-genic disruption at 7q33. An analysis of the protein-coding genes localized in the same TAD as the breakpoints did not reveal any monoallelic or imprinted genes associated with an abnormal phenotype (Figure 4D, Table 6).

BLA(S)T Outputs of Sequencing Results:

Rearrangement_A (on der(2))

1	ATAATACTTC	CTAAACCCAC	AGAATTAAAG	TCTTACAGAA	ATGTATAAAT	GCACAGCATG
61	GATCATCTTT	TTAGCTAATA	TAAATGCAGT	TCATAAGAGG	AAGAAAAAAA	TTAAAATGCT
121	TTAGAAAGAA	TACTTTGAAA	TCAAGATAGA	CTATCCAGCA	AAATAAATTC	TAAAATCATG
181	CCCAACTAAA	GAAAAAGGAA	ACACGATAAA	AACACGAAAA	CAAATAAAGT	TAAAAAAA
241	AAAAAGCCTG	TAAGCTGCTT	AGTATTTCA	TACTGTTAAA	ACATGTTAGT	TGTCAAAAGT
301	CCAGGAGAGT	TATAGTTGTA	ACAAACACGG	TAAGGACATT	TAATGCAAA	TCTCTTATC
361	CTAGGAGTTC	CCAAA _{CTCGT}	GATTGTCCTG	TAGGTTAAAA	ATTCAAGGAGT	GGCTTAGCTA
421	AGTGGTCCTG	GCTCGGGTTC	GTTATGAAGT	TGCCCACCC	TAAATTCCCT	AGAGGGCCTT
481	TTATCTCACC	ATCTGGTTCT	CTAACTTCTT	CACAAAGCAT	ATTATAGTCA	CACCCTCAGG
541	TTCATCTTTA	TACTATATCT	TCCTGAGAGT	ACCCCTGAATT	TGATCTTGT	TCAAAAGCCA
601	ATTTTTTAA	ATTTTAGCAT	TGTTTGCCAT	CCAAAGAGGC	TGCAAACCTT	AAAACCCACC
661	AGGTCTTCAC	TGCTTTATAT	ATTATAATT	TTCTCTGACT	TGTTTCTCTC	CTCTTGTATT
721	TTACTA					

Score	Start	End	Qsize	Identity	Chro	Strand	Start	End	Span
369	1	373	726	99%	2	(+)	197163823	197164194	372
351	376	726	726	100%	7	(-)	135905573	135905923	351

BLA(S)T Output: 2q32.3(+)(197,164,194)::AA::7q33(-)(135,905,923)

```

000000001 ataatactcctaaacccacagaatttaagtcttacagaaatgtataaat 000000050
>>>>>> ||||||| ||||| ||||| ||||| ||||| ||||| ||||| >>>>>
197163823 ataatactcctaaacccacagaatttaagtcttacagaaatgtataaat 197163872

000000051 gcacagcatggatcatcttttagctaataatataatgcagttcataagagg 000000100
>>>>>> | ||||| ||||| ||||| ||||| ||||| ||||| >>>>>
197163873 gtacagcatggatcatcttttagctaataatataatgcagttcataagagg 197163922

000000101 aagaaaaaaaattaaaatgctttagaaagaatactttgaaatcaagataga 000000150
>>>>>> ||||||| ||||| ||||| ||||| ||||| ||||| >>>>>
197163923 aagaaaaaaaattaaaatgctttagaaagaatactttgaaatcaagataga 197163972

000000151 ctatccagcaaataattctaaaatcatgcccaactaaagaaaaaggaa 000000200
>>>>>> ||||||| ||||| ||||| ||||| ||||| ||||| >>>>>
197163973 ctatccagcaaataattctaaaatcatgcccaactaaagaaaaaggaa 197164022

000000201 acacgataaaaacacgaaaacaaaataagttaaaaaaaaaaaaagcctg 000000250
>>>>>> ||||||| ||||| ||||| ||||| ||||| ||||| >>>>>
197164023 acacgataaaaacacgaaaacaaaataagttaaaaaaaaaaaaa.gcctg 197164071

000000251 taagctgcttagtatttcatactgttaaacatgttagtgtcaaaagt 000000300
>>>>>> ||||||| ||||| ||||| ||||| ||||| >>>>>
197164072 taagctgcttagtatttcatactgttaaacatgttagtgtcaaaagt 197164121

000000301 ccaggagagttatagttgtacaacaaacacggttaaggacattaatgaaaa 000000350
>>>>>> ||||||| ||||| ||||| ||||| >>>>>
197164122 ccaggagagttatagttgtacaacaaacacggttaaggacattaatgaaaa 197164171

000000351 tctcttatccttaggagttccca 000000373
>>>>>> ||||||| ||||| ||||| >>>>>
197164172 tctcttatccttaggagttccca 197164194

```

Figure S-DGAP290_1. BLA(S)T Output, Rearrangement_A on der(2): Circled mismatch represents an additional repetitive nucleotide “A”.

Rearrangement_B (on der(7))

1	GCCAGGATT	CTTATTTCC	CAGTTGCAGT	ATCTACCATT	TTCTAACAAA	GGTAGGCCAT
61	TATTTTCCCG	TATTTATAAG	AACACATTAA	TAATTCCATG	TTAAGTGATT	TTATTATAC
121	AATATTGGG	GGAATTCTGT	TCTCATTCTG	ATACTTTGGC	TTCTTTGTTA	TTTGGGTTTC
181	TTTTGTAAT	TTCTGCTTAA	AGAAGGCTGA	TATTTTAACT	GCTAGCAAAA	ACTTATTAA
241	ATATAGCCTA	TCAAGGATGG	AATTGATTC	TCTTACAACA	AATAAAATTT	AAAGATTGTG
301	TTGAAGGGAT	TAGAAAATTA	ATGGGAATT	AAAGTTTTG	AATGAAAATT	GTTTACAAA
361	GATTTCTGAT	TTTCTCTTCC	CAGGCTGTT	ATGAGGAAAA	AAAAAAATCCT	GGTTTATT
421	TGTTTCTTGT	GTTTGTATTG	AAACCAATTC	AGATCTGAA	ATGAAAAGTT	GAAAACTAAT
481	TATGGTAGAA	AACAGTTTA	ACTTAGTTA	TTGACATGGC	TAACAATTAT	TCCAGGCTAA
541	TGCAGTCTTA	TCGAGATCT	ACTTTATTT	CTTTTGACC	AACTTTAAC	AGTTTCTGA
601	ATTCAAGACTA	TATTCAGACA	GTCTTAGCT	GTGAGTTT	TTAAAAGTT	AGCTTGTGTC
661	ATCTTTATGT	TTTAGGAAGT	TGAGGCTCAC	ACATGCCATA	AACAAATTTC	TATTACTAGT
721	AATTGTCAGC	ATCTAATTTA	CCTTTAGAG	TAATGGCGTT	AGACCTCTGA	GAATTATCTA
781	ATGGCAAAG	GTTTTCACT	CTATTTCAT	AAGTGTCTTA	TTTTAGTTC	TGGGATT
841	GACAGTGT	TCAGAACATC	TTAAGGGGCC	TAAAACAAAA	CAAAGCAAA	TAAAAACAGA
901	CTGCTGGGAC	CCACTCCAGA	CCTACTGAAC	CAGAATCTCT	AAGATCTGGG	TACCAAGAAT
961	ATGCATTTA	TTTTTAAAG	TC			

Score	Start	End	Qsize	Identity	Chro	Strand	Start	End	Span
838	1	840	982	99.9%	7	(+)	135298971	135299810	840
141	842	982	982	100%	2	(+)	197164206	197164346	141

BLA(S)T Output: 7q33(+)(135,299,810)::G::2q32.3(+)(197,164,206)

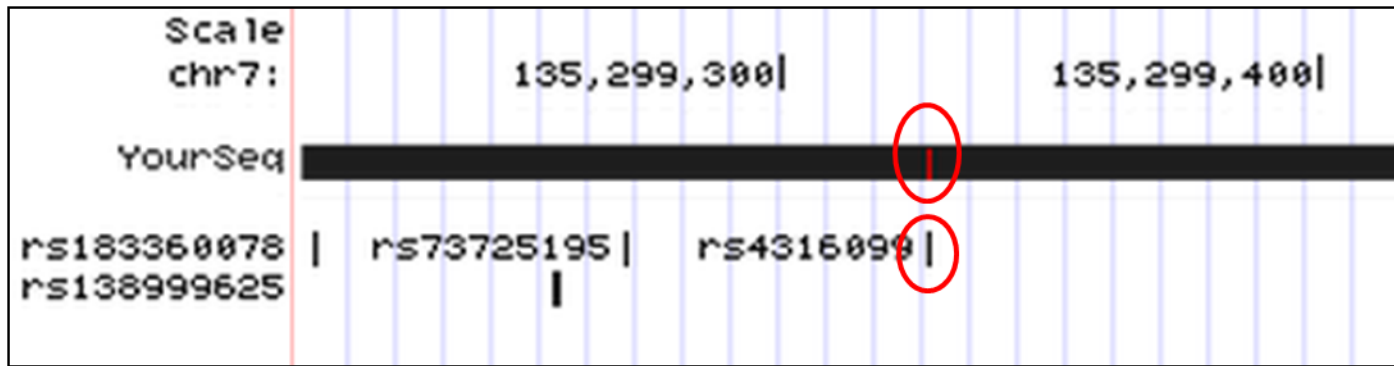


Figure S-DGAP290_2. BLA(S)T Output, Rearrangement_B on der(7): Circled mismatch represents a SNP (dbSNP build 141, rs4316099).

Rearrangement_C (on der(2))

1	CAAAACAAAT	ACATAAGAAA	AATTAAACTT	AAATTGCATG	ATTTTATAAT	ACCTCAATTA
61	ATGATGTGGT	TTAACATTTA	ATTAAGGCTG	AGAATCACTT	ATACAATAGT	TTTTATTTTT
121	ATTTATTTAT	TTTTTATTGT	AGAGACAGGG	TCTCACTCTA	TTGCCAGGC	TGTACTTGAA
181	CTCCTTGCCT	CAGTGTCCCT	CCTGTCTCAG	CCTACCTAAG	CACTGGGATT	ATAGGCGCGA
241	GCCACTGTGC	CTGGTCCTAC	AATAAGAGTT	TTTTAATCCA	ATACTATTTT	AATATGCTTG
301	ACATTGAAAC	CCTAAACTGT	GACAGTATAA	ACATAAAATT	AACCATAATAA	CAACTACTAAT
361	AATAATTTC	GGCAAAGCTA	AATGAAGTTT	TATAAAACAC	ATACCATAAT	AGGTAAGATG
421	TTAATTTTA	TTTTTAATTA	GGTGTAAAGA	GGGTTCTAA	AAGCTTCTTA	{A} GATAATAAA
481	TATTTACTGC	TGCTTTAAC	CATTAAGGTT	TGGTTAATT	TGCTGTGTAG	CAATAGATAAA
541	TAAGTTGCCA	CTGACTTTA	ATTATTGTAA	AATCAATGAG	GAGATGTCTG	GCCTCATAGA
601	AGATTTACCT	GACATGAATC	AGCCCTCTTC	CTGATTCTAA	CATATAGAAA	TGATGGAAAA
661	ACTACAAAAAA	GCTTGAATAA	AATAGTCATG	TAAC TGAGAA	AATGGAATCC	CTAGATAATA
721	AAAACATAGA	GAGAAATCAC	AGTCATTG	GAAGGGTAAA	GTGAACGTAG	TAACCTGGCC
781	CATTGAGGTT	TATGAGATAT	AGGATTGTGT	AAAGGATGAG	GCTGAAGTTT	TCATGCAGGG
841	TCAGCAGCTG	GAAACAAGTC	CAATTGTATA	AGGCCAAGAG	CCTACAAGGG	TGCACTCTCT
901	TCACAAATAT	AAAGTTGAC	TTTCCAGCCT	GGAAAAGCAA	CAAAGAAACT	TGTTAACAT
961	TCAAGACTTT	TTCATCCACT	GATTATTCTT	TGTCCCTTG	TTATGAGAGA	GTTCTTGAA
1021	AACAAAGCAA	AGCAAGTGCA				

Score	Start	End	Qsize	Identity	Chro	Strand	Start	End	Span
471	1	471	1040	100%	7	(-)	135299812	135300282	471
570	471	1040	1040	100%	7	(+)	135905924	135906493	570

BLA(S)T Output: 7q33(-)(135,299,81{2})::7q33(+)(135,905,92{4})

Next-Gen Cytogenetic Nomenclature:

Short System

46,XY,t(2;7)(q33;q32)dn.seq[GRCh37/hg19](2,7)cx,der(2)t(2;7)(q32.3;q33)inv(7)(q33q33)dn,der(7)t(2;7)dn

Detailed System

46,XY,t(2;7)(q33;q32)dn.seq[GRCh37/hg19](2,7)cx,der(2)(2pter->2q32.3(197,164,194)::AA::7q33(135,905,923-135,299,81{2})::7q33(135,905,92{4})->7qter)dn,der(7)(7pter->7q33(135,299,810)::G::2q32.3(197,164,206)->2qter)dn

DGAP295

46,XY,t(2;11)(p13.1;p15.5)dn.arr(1-22)x2,(XY)x1.seq[GRCh37/hg19](2,11)cx,der(2)inv(11)(p15.5)inv(11)(p15.5)t(2;11)(p13.3;p15.5)dn,der(11)t(2;11)dn

Prenatal History: A 21 year-old G2P1 female had positive first trimester serum screening for trisomies 13 and 18. Of note, the PAPP-A value was very low (0.1 percentile). cfDNA testing failed at both 12 and 14 weeks, due to low fetal fractions. Fetal ultrasonography was normal until 19 weeks, when an anatomical survey revealed severe growth restriction (~3 weeks delayed) and an amniocentesis was performed. Ultrasound examinations at 25 and 29 weeks showed decreased amniotic fluid volume and continued growth restriction. A fetal echocardiogram at 25 weeks was interpreted to be within normal limits. At 29 weeks, the mother was hospitalized after the fetal ultrasound revealed that the fetus continued to have significant intrauterine growth restriction (~10 weeks delayed).

Postnatal History: An emergency C-section occurred at 31 weeks, following an ultrasound examination with no observation of fetal movement. The newborn weighed 450 grams with an otherwise normal physical examination and was admitted and followed in the NICU. The newborn was discharged from the hospital after 21 weeks in stable condition.

Sequencing Results and Interpretation of Convergent Genomic Evidence: Sequencing of the prenatal DNA sample identified the translocation breakpoints disrupting *GFPT1* at 2p13.3 and multiple non-genic regions at 11p15.5 within a 70 kb distribution. Interestingly, the breakpoints at 11p15.5 are located within the same 600 kb TAD as *IGF2*, a region well known to be associated with Silver-Russell syndrome through imprinted loss of function (epimutation)²⁴, overlapping with the phenotype of DGAP295 (Figure 4E, Table 6).

Next-Gen Cytogenetic Nomenclature:

Short System

46,XY,t(2;11)(p13.1;p15.5)dn.arr(1-22)x2,(XY)x1.seq[GRCh37/hg19]
(2,11)cx,der(2)inv(11)(p15.5)inv(11)(p15.5)t(2;11)(p13.3;p15.5)dn,der(11)t(2;11)dn

Detailed System

46,XY,t(2;11)(p13.1;p15.5)dn.arr(1-22)x2,(XY)x1.seq[GRCh37/hg19] (2,11)cx,der(2)(11pter->11p15.5(1,915,057~)::11p1.55(1,936,993~1,960,727~)::11p15.5(1,936,668~1,915,843~)::11p15.5(1,961,361~1,984,895~)::2p13.3(69,588,420~)->2qter)dn,der(11)(2pter->2p13.3(69,588,264)::11p15.5(1,985,019~)->11qter)dn

Supplementary Figures

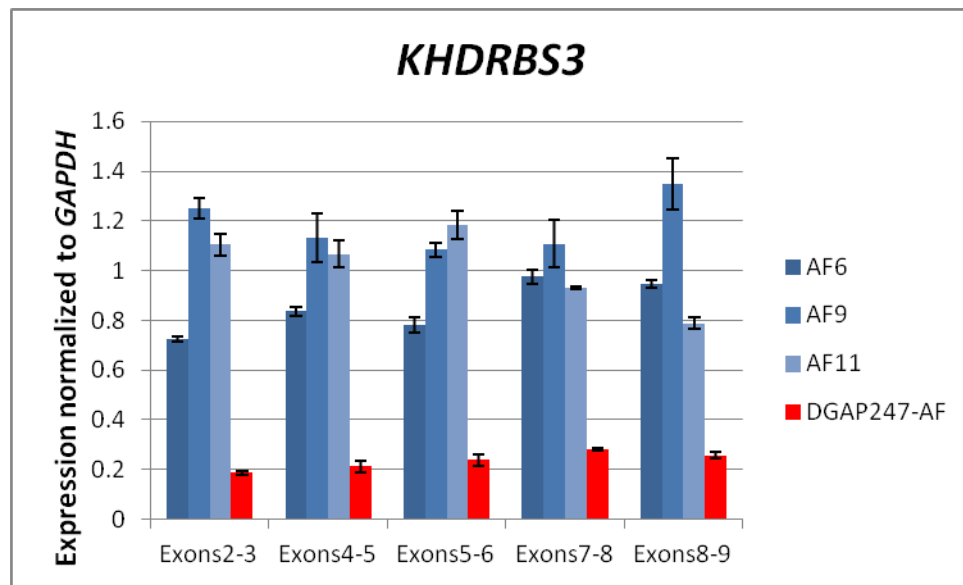


Figure S1. DGAP247 amniotic fluid *KHDRBS3* expression: Decreased expression of *KHDRBS3* in the amniotic fluid sample of DGAP247 in comparison to three amniotic fluid control samples (normalized to *GAPDH*).

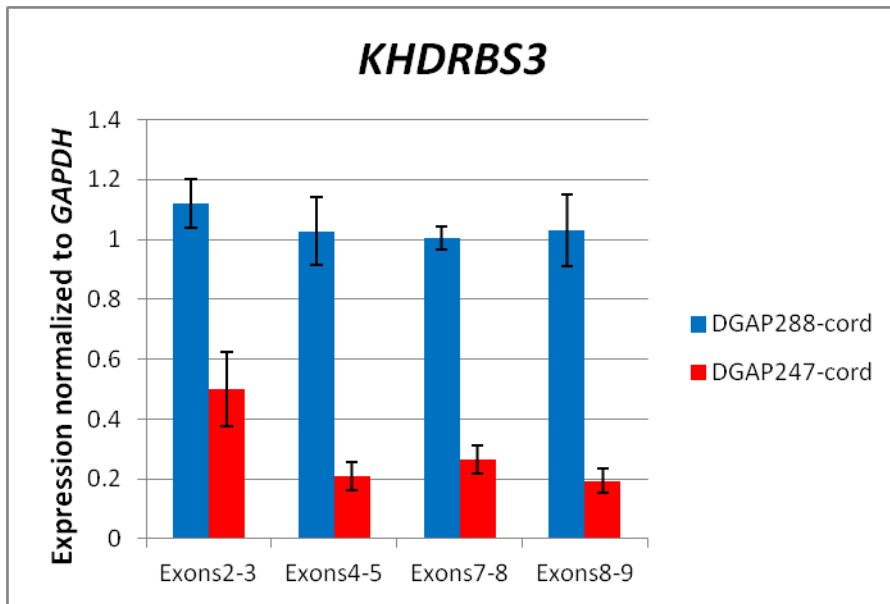


Figure S2. DGAP247 cord blood *KHDRBS3* expression: Decreased expression of *KHDRBS3* in the cord blood sample of DGAP247 in comparison to the cord blood sample of DGAP288 (normalized to *GAPDH*).

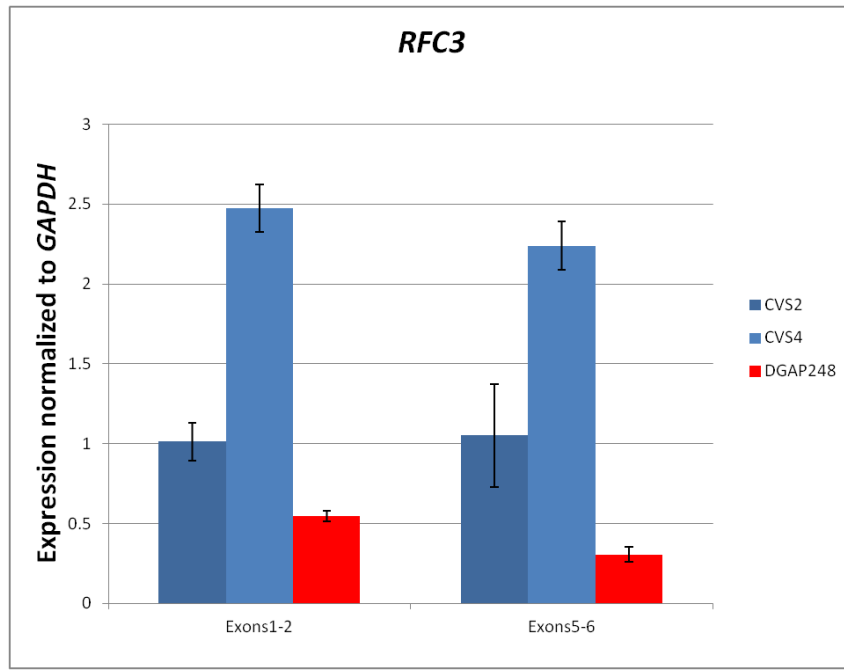


Figure S3. DGAP248 CVS *RFC3* Expression: Decreased expression of *RFC3* in the CVS of DGAP248 in comparison to two CVS control samples (normalized to *GAPDH*).

Table S1. Next-Gen Breakpoint Nucleotides of the Analyzed Cases

Case	Next-Gen Band	`Next-Gen Breakpoint Nucleotides (GRCh37/hg19)	
DGAP239	6q13	Rearrangement_A: 70,405,86{7-8}	Rearrangement_B: 70,405,86{7-9}
	8q12.2	Rearrangement_A: 61,628,67{1-2}	Rearrangement_B: 61,628,66{7-9}
DGAP247	8q11.21	Rearrangement_A: 51,889,501	Rearrangement_B: 51,889,502
	8q24.23	Rearrangement_A: 136,495,820	Rearrangement_B: 136,495,823
DGAP248	2p12	Rearrangement_A: 78,301,91{1-2}	Rearrangement_B: 78,301,90{8-5}
	13q13.2	Rearrangement_A: 34,542,73{2-1}	Rearrangement_B: 34,542,7{20-23}
DGAP258	6p25.3	Rearrangement_A: 776,81{6}	Rearrangement_B: 776,787
	6q16.1	Rearrangement_A: 93,191,54{7}	Rearrangement_B: 93,191,545
DGAP259	3p26.3	Rearrangement_D: 1,408,99{6}	Rearrangement_G: 1,408,984
	3p24.3	Rearrangement_A: 17,392,144	Rearrangement_C: 17,392,136
	5q14.3	Rearrangement_B: 88,756,2{48-56}	Rearrangement_E: 88,756,2{39-40}
	7q35	Rearrangement_B: 147,718,91{1-9}	Rearrangement_E: 147,718,90{7-8}
	7q36.3	Rearrangement_A: 155,701,797	Rearrangement_C: 155,700,873
	9p23	Rearrangement_F: 9,646,47{5}	Rearrangement_I: 9,646,471
	18p11.31	Rearrangement_D: 6,375,05{1}	Rearrangement_G: 6,559,611 Rearrangement_H: 6,375,0{52-48} and 6,559,{598-602}
	18q21.3	Rearrangement_F: 54,660,13{8}	Rearrangement_I: 54,660,136
DGAP268	10p12.31	Rearrangement_B: 21,606,655	Rearrangement_C: 21,606,63{4-2}
	10p12.2	Rearrangement_A: 23,659,495~	Rearrangement_C: 23,659,20{0-2}
	10q23.32	Rearrangement_A: 93,983,897~	Rearrangement_B: 93,982,408
DGAP285	Xp11.21	Rearrangement_A: 55,174,723~	Rearrangement_B: 55,174,381~
	Xq28	Rearrangement_A: 150,286,207~	Rearrangement_B: 150,284,569~
DGAP288	6q21	Rearrangement_A: 112,976,04{2-4}	Rearrangement_B: 112,976,031
	17q24.3	Rearrangement_A: 69,728,01{7-9}	Rearrangement_B: 69,728,006
DGAP290	2q32.3	Rearrangement_A: 197,164,194	Rearrangement_B: 197,164,206
	7q33	Rearrangement_A: 135,905,923	Rearrangement_B: 135,299,810 Rearrangement_C: 135,299,81{2} and 135,905,92{4}
DGAP295	2p13.3	Rearrangement_D: 69,588,420~	Rearrangement_E: 69,588,264~
	11p15.5	Rearrangement_A: 1,915,057~ Rearrangement_D: 1,915,843~	Rearrangement_B: 1,960,727~ Rearrangement_C: 1,961,361~ Rearrangement_A: 1,936,993~ Rearrangement_B: 1,936,668~
		Rearrangement_C: 1,984,895~	Rearrangement_E: 1,985,019~

Table S2. Analyzed topologically associated domains (TADs) and topological boundary regions (TBRs)

Case	Next-Gen Band	TAD and TBR nucleotides [hESC, GRCh37/hg19] ²⁵ (size)
DGAP239	6q13	TBR: 69,103,279-69,343,279 (240kb) TAD: 69,343,279-70,903,279 (1.56 Mb) TAD: 70,903,279-71,743,279 (840kb)
	8q12.2	TAD: 59,557,446-60,917,446 (1.36 Mb) TBR: 60,917,446-60,957,446 (40 kb) TAD: 60,957,446-61,317,446 (360kb) TBR: 61,317,446-61,557,446 (240kb) TAD: 61,557,446-62,037,446 (480kb) TAD: 62,037,446-62,517,446 (480kb) TBR: 62,517,446-62,557,446 (40kb) TAD: 62,557,446-64,037,446 (1.48 Mb) TBR: 64,037,446-64,117,446 (80kb)
DGAP247	8q11.21	TBR: 48,677,447-48,917,447 (240kb) TAD: 48,917,447-49,837,447 (920kb) TBR: 49,837,447-49,877,447 (40kb) TAD: 49,877,447-52,757,447 (2.88 Mb) TBR: 52,757,447-52,957,447 (200kb) TAD: 52,957,447-53,317,447 (360kb) TBR: 53,317,447-53,437,447 (120kb) TAD: 53,437,447-54,797,447 (1.36 Mb)
	8q24.23	TAD: 134,490,818-135,890,818 (1.4 Mb) TAD: 135,890,818-137,770,818 (1.88 Mb) TAD: 137,770,818-139,130,818 (1.36 Mb)
DGAP248	2p12	TAD: 75,866,492-76,826,492 (960kb) TBR: 76,826,492-77,146,492 (80kb) TAD: 77,146,492-79,226,492 (2.08 Mb) TAD: 79,226,492-80,146,489 (919kb) TBR: 80,146,489-80,266,489 (120kb)
	13q13.2	TAD: 32,902,000-34,342,000 (1.44 Mb) TBR: 34,342,000-34,382,000 (40kb) TAD: 34,382,000-36,542,000 (2.16 Mb) TAD: 36,542,000-37,582,000 (1.04 Mb) TBR: 37,582,000-37,622,000 (40kb)
DGAP258	6p25.3	TAD: 135,000-1,455,001 (1.32 Mb) TAD: 1,455,001-2,735,001 (1.28 Mb) TBR: 2,735,001-2,775,001 (40kb)
	6q16.1	TAD: 90,623,279-91,183,279 (560kb) TBR: 91,183,279-91,223,279 (40kb) TAD: 91,223,279-93,463,279 (2.24 Mb) TBR: 93,463,279-93,503,279 (40kb) TAD: 93,503,279-94,143,279 (640kb)
DGAP259	3p26.3	TAD: 60,000-2,145,000 (2.085 Mb) TBR: 2,145,000-2,225,000 (80kb) TAD: 2,225,000-3,225,000 (1 Mb)
	3p24.3	TAD: 15,624,996-16,304,996 (680kb) TAD: 16,304,996-16,624,996 (320kb) TAD: 16,624,996-17,304,996 (680kb) TAD: 17,304,996-17,904,996 (600kb) TAD: 17,904,996-18,464,996 (560kb) TBR: 18,464,996-18,504,996 (40kb) TAD: 18,504,996-19,064,996 (560kb)
	5q14.3	TAD: 86,684,244-88,004,244 (1.32 Mb) TAD: 88,004,244-90,124,244 (2.12 Mb)
	7q35	TAD: 145,809,067-147,969,067 (2.16 Mb) TAD: 147,969,067-148,209,067 (240kb) TAD: 148,209,067-148,649,067 (440kb) TBR: 148,649,067-148,809,067 (160kb) TAD: 148,809,067-149,129,067 (320kb)
	7q36.3	TBR: 153,729,067-155,147,248 (1.418 Mb) TAD: 155,147,248-155,587,239 (439kb) TAD: 155,587,239-157,187,239 (1.6 Mb) TAD: 157,187,239-159,128,663 (1.94 Mb)
	9p23	TAD: 7,570,000-8,330,000 (760kb) TAD: 8,330,000-9,290,000 (960kb) TAD: 9,290,000-9,970,000 (680kb) TAD: 9,970,000-11,370,000 (1.4 Mb)

Case	Next-Gen Band	TAD and TBR nucleotides [hESC, GRCh37/hg19] ²⁵ (size)
DGAP259 (continued)	18p11.31	TAD: 3,690,000-5,090,000 (1.4 Mb) TAD: 5,090,000-6,530,000 (1.44 Mb) TAD: 6,530,000-6,930,000 (400kb) TAD: 6,930,000-7,210,000 (280kb) TAD: 7,210,000-8,530,000 (1.32Mb) TBR: 8,530,000-8,610,000 (80kb)
	18q21.3	TBR: 52,649,002-52,729,002 (320kb) TAD: 52,729,002-54,329,002 (1.6 Mb) TAD: 54,329,002-55,289,002 (960kb) TAD: 55,289,002-56,169,020 (880kb)
DGAP268	10p12.31	TAD: 21,159,994-22,239,994 (1.08 Mb) TBR: 22,239,994-22,279,994 (40kb) TAD: 22,279,994-23,399,994 (1.12 Mb)
	10p12.2	TAD: 23,399,994-24,839,994 (1.44 Mb) TBR: 24,839,994-24,879,994 (40kb)
	10q23.32	TAD: 92,650,020-93,690,020 (1.04 Mb) TBR: 93,690,020-93,770,020 (80kb) TAD: 93,770,020-94,210,020 (440kb) TBR: 94,210,020-94,410,020 (200kb) TAD: 94,410,020-95,290,010 (879.99kb)
DGAP285	Xp11.2	TBR: 55,103,275-55,143,275 (40kb) TAD: 55,143,275-56,263,275 (1.12 Mb) TBR: 56,263,275-56,303,275 (40kb)
	Xq28	TBR: 148,592,095-149,929,342 (1.337 Mb) TAD: 149,929,342-150,249,342 (320kb) TBR: 150,249,342-150,289,342 (40kb) TAD: 150,289,342-150,889,344 (600kb)
DGAP288	6q21	TBR: 112,413,307-112,493,307 (80kb) TAD: 112,493,307-114,253,307 (1.76 Mb)
	17q24.3	TBR: 68,608,405-68,648,405 (40kb) TAD: 68,648,405-70,528,405 (1.88 Mb) TBR: 70,528,405-70,568,405 (40kb)
DGAP290	2q32.3	TAD: 196,211,755-196,931,755 (720kb) TAD: 196,931,755-198,251,755 (1.32 Mb) TAD: 198,251,755-198,651,755 (400kb)
	7q33	TAD: 134,309,460-134,949,460 (640kb) TAD: 134,949,460-136,829,460 (1.88 Mb) TAD: 136,829,460-137,309,460 (480kb)
DGAP295	2p13.3	TAD: 69,186,496-69,546,496 (360kb) TBR: 69,546,496-69,586,496 (40kb) TAD: 69,586,496-70,106,496 (520kb) TAD: 70,106,496-70,506,496 (400kb)
	11p15.5	TAD: 850,000-1,523,424 (673kb) TBR: 1,523,424-1,603,424 (80kb) TAD: 1,603,424-2,203,424 (600kb) TAD: 2,203,424-2,443,424 (240kb)

Table S3. Convergent Genomic Analysis of DGAP239 6q13 breakpoints

DGAP239: 6q13 breakpoints on Rearrangement_A: 70,405,86{7-8} and Rearrangement_B: 70,405,86{7-9}							
Genes	Nucleotides (GRCh37/hg19)	Description	OMIM ²⁶	OMIM Morbid ²⁶	DDG2P ²⁷	%HI ⁸	Notes
<i>ADGRB3</i>	69345259-70099403	Adhesion G Protein-Coupled Receptor B3	+	-	-	3.02	No reported phenotypic association Homologous to <i>ADGRB1</i> , an angiogenesis inhibitor that is a candidate for involvement in development of glioblastoma. ²⁸
<i>LMBRD1</i> (Disrupted)	70385694-70507003	LMBR1 Domain Containing 1	+	+	+	12.92	Biallelic loss of function (autosomal recessive) is associated with Methylmalonic Aciduria and Homocystinuria, cbIF type. ²⁹ (no phenotype overlap with DGAP239)
<i>COL19A1</i>	70576463-70919679	Collagen, Type XIX, Alpha 1	+	-	-	26.71	
<i>COL9A1</i>	70924764-71012786	Collagen, Type IX, Alpha 1	+	+	+	23.89	Some evidence for haploinsufficiency (autosomal dominant, monoallelic mode) exists for the Multiple Epiphyseal Dysplasia type 6 (MED6) phenotype. However, it has been reported that although mutations in <i>COL9A1</i> can cause MED, they are not the major causes of MED and at least one additional locus exists in such cases. ³⁰
<i>FAM135A</i>	71122644-71270877	Family With Sequence Similarity 135, Member A	-	-	-	26.1	
<i>SDHAF4</i>	71276620-71299272	Succinate Dehydrogenase Complex Assembly Factor 4	-	-	-	63.15	
<i>SMAP1</i>	71377479-71571718	Small Arfgap 1	+	-	-	34.54	
<i>B3GAT2</i>	71566382-71666741	Beta-1,3-Glucuronyltransferase 2	+	-	-	33.88	

DDG2P: Developmental Disorders Genotype-to-Phenotype Database, +: Confirmed DDG2P gene, HI: Haploinsufficiency index (in red if <10%)

Shaded rows: Protein coding genes located within the same hESC topologically associated domain (TAD)²⁵ with the breakpoints

Table S4. Convergent Genomic Analysis of DGAP239 8q12.2 breakpoints

DGAP239: 8q12.2 breakpoints on Rearrangement_A: 61,628,67{1-2} and Rearrangement_B: 61,628,66{7-9}							
Genes	Nucleotides (GRCh37/hg19)	Description	OMIM ²⁶	OMIM Morbid ²⁶	DDG2P ²⁷	%HI ⁸	Notes
NSMAF	59496063-59572403	Neutral Sphingomyelinase (N-SMase) Activation Associated Factor	+	-	-	39.33	
TOX	59717977-60031767	Thymocyte Selection-Associated High Mobility Group Box	+	-	-	2.83	Linkage-disequilibrium mapping of a pulmonary tuberculosis susceptibility locus near the 3' end of TOX ³¹
CA8	61099906-61193971	Carbonic Anhydrase VIII	+	+	+	10.02	Biallelic loss of function (autosomal recessive) associated with Cerebellar Ataxia, Mental Retardation, and Dysequilibrium Syndrome 3 ³²
RAB2A	61429416-61536186	RAB2A, Member RAS Oncogene Family	+	-	-	11.01	
CHD7 (Disrupted)	61591337-61779465	Chromodomain Helicase DNA Binding Protein 7	+	+	+	2.4	Haploinsufficiency (autosomal dominant, monoallelic) reported in association with CHARGE syndrome, with mutations in over 90% of cases meeting diagnostic criteria of CHARGE syndrome ³³ (Consistent with the clinical diagnosis of CHARGE syndrome during the postnatal period of DGAP239)
CLVS1	61969717-62414204	Clavesin 1	+	-	-	14.59	
ASPH	62413116-62627155	Aspartate Beta-Hydroxylase	+	+	P	46.75	Biallelic loss of function (autosomal recessive) associated with Traboulsi Syndrome ³⁴
NKAIN3	63161150-63912211	Na+/K+ Transporting Atpase Interacting 3	+	-	-	24.34	
GGH	63927638-63951730	Gamma-Glutamyl Hydrolase (Conjugase, Folylpolygammaglutamyl Hydrolase)	+	-	-	63.59	
TPPA	63961112-63998612	Tocopherol (Alpha) Transfer Protein	+	+	-	46.94	Biallelic loss of function (autosomal recessive) associated with Ataxia with Isolated Vitamin E Deficiency ³⁵
YTHDF3	64081112-64125346	YTH N(6)-Methyladenosine RNA Binding Protein 3	-	-	-	6.55	No reported phenotype association

DDG2P: Developmental Disorders Genotype-to-Phenotype Database, +: Confirmed DDG2P gene, P: Probable DDG2P gene, HI: Haploinsufficiency index (in red if <10%)
Shaded rows: Protein coding genes located within the same hESC topologically associated domain (TAD)²⁵ with the breakpoints

Table S5. Convergent Genomic Analysis of DGAP247 8q11.2 breakpoints.

DGAP247: 8q11.2 breakpoints on Rearrangement_A: 51,889,501 and Rearrangement_B: 51,889,502							
Genes	Nucleotides (GRCh37/hg19)	Description	OMIM ²⁶	OMIM Morbid ²⁶	DDG2P ²⁷	%HI ⁸	Notes
PRKDC	48685669-48872743	Protein Kinase, DNA-Activated, Catalytic Polypeptide	+	-	-	10.36	
MCM4	48872745-48890720	Minichromosome Maintenance Complex Component 4	+	+	-	13.9	Biallelic loss of function (autosomal recessive) associated with Natural Killer Cell and Glucocorticoid Deficiency with DNA Repair Defect ³⁶
UBE2V2	48920960-48977268	Ubiquitin-Conjugating Enzyme E2 Variant 2	+	-	-	12.96	
EFCAB1	49623348-49647870	EF-Hand Calcium Binding Domain 1	-	-	-	44.58	
SNAI2	49830249-49834299	Snail Family Zinc Finger 2	+	+	-	5.15	Haploinsufficiency (autosomal dominant, monoallelic) reported to be associated with piebaldism ³⁷ Biallelic loss of function (autosomal recessive) associated with Waardenburg Syndrome, Type 2D ³⁸
C8orf22	49966870-49988649	Chromosome 8 Open Reading Frame 22	-	-	-	81.46	
SNTG1	50822349-51706678	Syntrophin, Gamma 1	+	-	-	43.69	
PXDNL	52232138-52722005	Peroxidasin-Like	+	-	-	85.15	
PCMTD1	52730140-52811735	Protein-L-Isoaspartate (D-Aspartate) O-Methyltransferase Domain Containing 1	-	-	-	21.84	
ST18	53023399-53373519	Suppression Of Tumorigenicity 18, Zinc Finger	-	-	-	15.51	
FAM150A	53446597-53478067	Family With Sequence Similarity 150, Member A	-	-	-	80.59	
RB1CC1	53535016-53658403	RB1-Inducible Coiled-Coil 1	+	-	-	10.33	
NPBWR1	53850991-53853677	Neuropeptides B/W Receptor 1	+	-	-	47.38	
OPRK1	54138284-54164257	Opioid Receptor, Kappa 1	+	-	-	28.99	
ATP6V1H	54628117-54756118	Atpase, H+ Transporting, Lysosomal 50/57 kda, V1 Subunit H	+	-	-	20.78	
RGS20	54764368-54871863	Regulator Of G-Protein Signaling 20	+	-	-	69.9	

DDG2P: Developmental Disorders Genotype-to-Phenotype Database, +: Confirmed DDG2P gene, HI: Haploinsufficiency index (in red if <10%)

Shaded rows: Protein coding genes located within the same hESC topologically associated domain (TAD)²⁵ with the breakpoints

Table S6. Convergent Genomic Analysis of DGAP247 8q24.23 breakpoints

DGAP247: 8q24.23 breakpoints on Rearrangement_A: 136,495,820 and Rearrangement_B: 136,495,823							
Genes	Nucleotides (GRCh37/hg19)	Description	OMIM ²⁶	OMIM Morbid ²⁶	DDG2P ²⁷	%HI ⁸	Notes
<i>ST3GAL1</i>	134467091- 134584183	ST3 Beta-Galactoside Alpha- 2,3-Sialyltransferase 1	+	-	-	61.67	
<i>ZFAT</i>	135490031- 135725292	Zinc Finger And AT Hook Domain Containing	+	-	-	57.4	
<i>KHDRBS3</i> (Disrupted)	136469700- 136668965	KH Domain Containing, RNA Binding, Signal Transduction Associated 3	+	-	-	10.52	No reported phenotype association

DDG2P: Developmental Disorders Genotype-to-Phenotype Database, +: Confirmed DDG2P gene, HI: Haploinsufficiency index (in red if <10%)

Shaded row: Protein coding gene located within the same hESC topologically associated domain (TAD)²⁵ with the breakpoints

Table S7. Convergent Genomic Analysis of DGAP248 2p12 breakpoints

DGAP248: 2p12 breakpoints on Rearrangement_A: 78,301,91{1-2} and Rearrangement_B: 78,301,90{8-5}							
Genes	Nucleotides (GRCh37/hg19)	Description	OMIM ²⁶	OMIM Morbid ²⁶	DDG2P ²⁷	%HI ⁸	Notes
MRPL19	75873909-75917977	Mitochondrial Ribosomal Protein L19	+	-	-	41.5	
GCFC2	75879126-75938115	GC-Rich Sequence DNA-Binding Factor 2	+	-	-	68.95	
LRRTM4	76974845-77820445	Leucine Rich Repeat Transmembrane Neuronal 4	+	-	-	7.26	No reported phenotype association Structure and expression profile of <i>LRRTM</i> mRNAs in mice suggest a role in development and maintenance of the vertebrate nervous system ¹³
REG3G	79252812-79255631	Regenerating Islet-Derived 3 Gamma	+	-	-	90.1	
REG1B	79312156-79315145	Regenerating Islet-Derived 1 Beta	+	-	-	94.05	
REG1A	79347488-79350545	Regenerating Islet-Derived 1 Alpha	+	-	-	91.34	
REG3A	79384132-79386879	Regenerating Islet-Derived 3 Alpha	+	-	-	92.13	
CTNNA2	79412357-80875905	Catenin (Cadherin-Associated Protein), Alpha 2	+	-	-	2.24	No reported phenotype association

DDG2P: Developmental Disorders Genotype-to-Phenotype Database, +: Confirmed DDG2P gene, HI: Haploinsufficiency index (in red if <10%)

Shaded row: Protein coding gene located within the same hESC topologically associated domain (TAD)²⁵ with the breakpoints

Table S8. Convergent Genomic Analysis of DGAP248 13q13.2 breakpoints

DGAP248: 13q13.2 breakpoints on Rearrangement_A: 34,542,73{2-1} and Rearrangement_B: 34,542,7{20-23}							
Genes	Nucleotides (GRCh37/hg19)	Description	OMIM M ²⁶	OMIM Morbid ² ₆	DDG2P ²⁷	%HI ⁸	Notes
BRCA2	32889611-32973805	Breast Cancer 2, Early Onset	+	+	+	13.3	Germline mutations associated with familial Breast-Ovarian Cancer Susceptibility 2 ³⁹ , homozygous or compound heterozygous mutations involved in Fanconi anemia complementation group D1 ⁴⁰
N4BP2L2	33006554-33112970	NEDD4 Binding Protein 2-Like 2	+	-	-	75.5	
PDS5B	33160564-33352157	PDS5 Cohesin Associated Factor B	+	-	-	24.83	
KL	33590207-33640282	Klotho	+	+	-	16.22	Biallelic loss of function (autosomal recessive) associated with Hyperphosphatemic Familial Tumoral Calcinosis ⁴¹
STARD13	33677272-33924767	Star-Related Lipid Transfer (START) Domain Containing 13	+	-	-	41.15	
RFC3 (Disrupted)	34392186-34540695	Replication Factor C (Activator 1) 3, 38 kda	+	-	-	4.93	No reported phenotype association
NBEA	35516424-36247159	Neurobeachin	+	-	-	6.83	Disrupted in a patient with a <i>de novo</i> translocation and idiopathic autism, ¹⁰ a linkage study implicated its localization on chromosome 16 for autism ⁴² and haploinsufficiency causes autism-like behaviors in animal models ^{11; 12}
MAB21L1	36047926-36050832	Mab-21-Like 1 (C. Elegans)	+	-	-	10.38	
DCLK1	36345478-36705443	Doublecortin-Like Kinase 1	+	-	-	6.47	No reported phenotype association A microtubule-associated kinase that can undergo autophosphorylation ⁴³
SOHLH2	36742345-36871979	Spermatogenesis And Oogenesis Specific Basic Helix-Loop-Helix 2	+	-	-	71.56	
CCDC169	36801182-36871977	Coiled-Coil Domain Containing 169	-	-	-	79.84	
SPG20	36875775-36944317	Spastic Paraplegia 20 (Troyer Syndrome)	+	+	-	43.36	Biallelic loss of function (autosomal recessive) associated with Spastic Paraplegia 20 ⁴⁴
CCNA1	37005967-37017019	Cyclin A1	+	-	-	33.13	
SERTM1	37248049-37271976	Serine-Rich And Transmembrane Domain Containing 1	-	-	-	49.92	
RFXAP	37393361-37403241	Regulatory Factor X-Associated Protein	+	+	-	65.91	Biallelic loss of function (autosomal recessive) associated with B-cell lymphocyte syndrome, type II, complementation group D ⁴⁵
SMAD9	37418968-37494902	SMAD Family Member 9	+	+	-	11.22	Haploinsufficiency (autosomal dominant, monoallelic) reported to be associated with primary pulmonary hypertension, type 2 ⁴⁶
ALG5	37523912-37574398	ALG5, Dolichyl-Phosphate Beta-Glucosyltransferase	+	-	-	22.12	
EXOSC8	37572953-37583750	Exosome Component 8	+	-	-	6.92	Biallelic loss of function (autosomal recessive) associated with Pontocerebellar hypoplasia, type 1C ⁴⁷
SUPT20H	37583449-37633850	Suppressor Of Ty 20 Homolog (<i>S. Cerevisiae</i>)	+	-	-	18.6	

DDG2P: Developmental Disorders Genotype-to-Phenotype Database, +: Confirmed DDG2P gene, HI: Haploinsufficiency index

Shaded rows: Protein coding genes located within the same hESC topologically associated domain (TAD)²⁵ with the breakpoints

Table S9. Convergent Genomic Analysis of DGAP258 6p25.3 breakpoints

DGAP 258: 6p25.3 breakpoints on Rearrangement_A: 776,81{6} and Rearrangement_B: 776,787							
Genes	Nucleotides (GRCh37/hg19)	Description	OMIM ²⁶	OMIM Morbid ²⁶	DDG2P ²⁷	%HI ⁸	Notes
<i>FOXF2</i>	1390069-1395832	Forkhead Box F2	+	-	-	29.64	
<i>FOXC1</i>	1610681-1614127	Forkhead Box C1	+	+	+	9.01	Haploinsufficiency (autosomal dominant, monoallelic) reported to be associated with multiple ocular malformation syndromes including Peters anomaly (PAN), iridogoniodysgenesis anomaly (IGDA), Axenfeld-Rieger syndrome type 3 (RIEG3) ^{48; 49} and 6p25.3 Dandy-Walker malformation ⁵⁰
<i>GMDS</i>	1624041-2245926	GDP-Mannose 4,6-Dehydratase	+	-	-	3.84	Suggestive association with 6p25.3 Dandy-Walker malformation along with deletion of <i>FOXC1</i> ⁵⁰
<i>MYLK4</i>	2663863-2751200	myosin light chain kinase family, member 4	-	-	-	57.67	
<i>WRNIP1</i>	2765648-2787186	Werner helicase interacting protein 1	+	-	-	36.94	

DDG2P: Developmental Disorders Genotype-to-Phenotype Database, +: Confirmed DDG2P gene, HI: Haploinsufficiency index (in red if <10%)

Shaded row: Protein coding gene located within the same hESC topologically associated domain (TAD)²⁵ with the breakpoints

Table S10. Convergent Genomic Analysis of DGAP258 6q16.1 breakpoints

DGAP258: 6q16.1 breakpoints on Rearrangement_A: 93,191,54{7} and Rearrangement_B: 93,191,545							
Genes	Nucleotides (GRCh37/hg19)	Description	OMIM ²⁶	OMIM Morbid ²⁶	DDG2P ²⁷	%HI ⁸	Notes
<i>BACH2</i>	90636248-91006627	BTB and CNC Homology 1, Basic Leucine Zipper Transcription Factor 2	+	-	-	7.84	No reported phenotype association
<i>MAP3K7</i>	91223292-91296764	Mitogen-Activated Protein Kinase Kinase Kinase 7	+	-	-	2.75	No reported phenotype association
<i>EPHA7</i>	93949738-94129265	EPH Receptor A7	+	-	-	2.77	No reported phenotype association

DDG2P: Developmental Disorders Genotype-to-Phenotype Database, +: Confirmed DDG2P gene, HI: Haploinsufficiency index (in red if <10%)

Shaded row: Protein coding gene located within the same hESC topologically associated domain (TAD)²⁵ with the breakpoints

Table S11. Convergent Genomic Analysis of DGAP259 3p26.3 breakpoints

DGAP259: 3p26.3 breakpoints on Rearrangement_D: 1,408,99{6} and Rearrangement_G: 1,408,984							
Genes	Nucleotides (GRCh37/hg19)	Description	OMIM ²⁶	OMIM Morbid ²⁶	DDG2P ²⁷	%HI ⁸	Notes
<i>CNTN6</i> (Disrupted)	1134260-1445901	Contactin 6	+	-	-	39.69	No reported phenotype association A neural adhesion molecule of the contactin subgroup of the immunoglobulin superfamily ⁵¹
<i>CNTN4</i>	2140497-3099645	Contactin 4	+	-	-	6.9	A boy with t(3;10)(p26;q26)dn and characteristic features of 3p- syndrome (autosomal dominant) is reported to have a translocation breakpoint on chromosome 3 within the minimal candidate region for 3p deletion syndrome disrupting the <i>CNTN4</i> mRNA transcript at 3p26.3-p26.2 ⁵² (relevant to cerebral and renal malformation phenotype of DGAP259)
<i>IL5RA</i>	3111233-3168297	Interleukin 5 Receptor, Alpha	+	-	-	87.3	
<i>TRNT1</i>	3168600-3192563	tRNA Nucleotidyl Transferase, CCA-Adding, 1	+	-	-	70.26	
<i>CRBN</i>	3190676-3221394	Cereblon	+	+	-	31.14	

DDG2P: Developmental Disorders Genotype-to-Phenotype Database, +: Confirmed DDG2P gene, HI: Haploinsufficiency index (in red if <10%)

Shaded rows: Protein coding genes located within the same hESC topologically associated domain (TAD)²⁵ with the breakpoints

Table S12. Convergent Genomic Analysis of DGAP259 3p24.3 breakpoints

DGAP259: 3p24.3 breakpoints on Rearrangement_A: 17,392,144 and Rearrangement_C: 17,392,136							
Genes	Nucleotides (GRCh37/hg19)	Description	OMIM ²⁶	OMIM Morbid ²⁶	DDG2P ²⁷	%HI ⁸	Notes
BTD	15642848-15687329	Biotinidase	+	+	+	76.15	Biallelic loss of function (autosomal recessive) associated with biotinidase deficiency ⁵³
ANKRD28	15708743-15901278	Ankyrin Repeat Domain 28	+	-	-	19.04	
GALNT15	16216156-16273499	Polypeptide N-Acetylgalactosaminyltransferase 15	+	-	-	65.27	
DPH3	16299485-16306479	Diphthamide Biosynthesis 3	+	-	-	19.41	
OXNAD1	16306706-16391806	Oxidoreductase NAD-Binding Domain Containing 1	-	-	-	63.97	
RFTN1	16355081-16555533	Raftlin, Lipid Raft Linker 1	-	-	-	61.2	
DAZL	16628299-16711813	Deleted In Azoospermia-Like	+	-	-	15.92	
PLCL2	16844159-17132086	Phospholipase C-Like 2	+	-	-	38.08	
TBC1D5 (Disrupted)	17198654-18486309	TBC1 Domain Family, Member 5	+	-	-	5.84	No reported phenotype association
SATB1	18386879-18487080	SATB Homeobox 1 (Special AT-rich sequence-binding protein-1)	+	-	-	2.15	A global genome-organizer and matrix attachment region-binding protein mediating chromatin looping by tethering multiple genomic loci and recruiting chromatin-remodeling enzymes to regulate chromatin structure and gene expression ^{16; 17} (DGAP259 has a complex chromosome rearrangement involving five different chromosomes.) Role in cortical neurons to facilitate neuronal plasticity and regulate expression of key neuronal genes ⁵⁴ and required for medial ganglionic eminence-derived interneuron differentiation, connectivity, and survival ⁵⁵ (relevant to cerebral malformation phenotype of DGAP259)

DDG2P: Developmental Disorders Genotype-to-Phenotype Database, +: Confirmed DDG2P gene, HI: Haploinsufficiency index (in red if <10%)

Shaded row: Protein coding gene located within the same hESC topologically associated domain (TAD)²⁵ with the breakpoints

Table S13. Convergent Genomic Analysis of DGAP259 5q14.3 breakpoints

DGAP259: 5q14.3 breakpoints on Rearrangement_B: 88,756,2{48-56} and Rearrangement_E: 88,756,2{39-40}							
Genes	Nucleotides (GRCh37/hg19)	Description	OMIM ²⁶	OMIM Morbid ²⁶	DDG2P ²⁷	%HI ⁸	Notes
RASA1	86563705-86687748	RAS p21 Protein Activator (GTPase Activating Protein) 1	+	+	+	2.57	Haploinsufficiency (autosomal dominant, monoallelic) reported to be associated with Parkes Weber Syndrome and Capillary malformation-Arteriovenous malformation ⁵⁶
CCNH	86687311-86708836	Cyclin H	+	-	-	7.31	Regulation of cell cycle progression, no reported phenotype association
TMEM161B	87485450-87565293	Transmembrane Protein 161B	-	-	-	9.65	
MEF2C	88013975-88199922	Myocyte Enhancer Factor 2C	+	+	+	0.26	Haploinsufficiency (autosomal dominant, monoallelic) reported to be associated with Mental retardation, Stereotypic movements, Epilepsy and cerebral malformations (MRSME) ¹⁵ and cases with hypoplastic corpus callosum ^{57, 58} , long range regulation associated phenotype also reported in a <i>de novo</i> translocation case ²² (relevant to cerebral malformation and hypoplastic corpus callosum phenotype of DGAP259) Role in synaptic plasticity and hippocampal-dependent learning and memory ⁵⁹ (9p23 breakpoints of DGAP259 disrupt PTPRD1 with similar role)
CETN3	89688078-89705603	Centrin, EF-Hand Protein, 3	+	-	-	5.94	Present in centrosomes and lays an important role in early cleavage of frog embryos ⁶⁰
MBLAC2	89754020-89770585	Metallo-Beta-Lactamase Domain Containing 2	-	-	-	38.68	
POLR3G	89767565-89810370	Polymerase (RNA) III (DNA Directed) Polypeptide G (32kd)	-	-	-	38.97	
LYSMD3	89811428-89825401	Lysm, Putative Peptidoglycan-Binding, Domain Containing 3	-	-	-	28.58	
ADGRV1	89825161-90460038	Adhesion G Protein-Coupled Receptor V1	+	+	-	25.58	Biallelic loss of function (autosomal recessive) associated with Usher syndrome, type 2C ⁶¹

DDG2P: Developmental Disorders Genotype-to-Phenotype Database, +: Confirmed DDG2P gene, HI: Haploinsufficiency index (in red if <10%)

Shaded rows: Protein coding genes located within the same hESC topologically associated domain (TAD)²⁵ with the breakpoints

Table S14. Convergent Genomic Analysis of DGAP259 7q35 breakpoints

DGAP259: 7q35 breakpoints on Rearrangement_B: 147,718,91{1-9} and Rearrangement_E: 147,718,90{7-8}							
Genes	Nucleotides (GRCh37/hg19)	Description	OMIM ²⁶	OMIM Morbid ²⁶	DDG2P ²⁷	%HI ⁸	Notes
CNTNAP2 (Disrupted)	145813453-148118090	Contactin Associated Protein-Like 2	+	+	+	4.94	Susceptibility to Autism type 15 ⁶² , homozygous or compound heterozygous mutations causing Cortical Dysplasia-Epilepsy Syndrome ⁶³ and Pitt-Hopkins-like syndrome (PTHSL1) ⁶⁴ (relevant to cerebral malformation phenotype of DGAP259) (18q21 breakpoints of DGAP259 mapping one downstream of <i>TCF4</i> , a monoallelic gene in Pitt-Hopkins Syndrome)
C7orf33	148287657-148312952	Chromosome 7 Open Reading Frame 33	-	-	-	97.83	
CUL1	148395006-148498128	Cullin 1	+	-	-	4.3	No reported phenotype association Regulates mammalian G1/S transition by specifically targeting mammalian G1 cell cycle regulators for ubiquitin-dependent degradation ⁶⁵
EZH2	148504475-148581413	Enhancer of Zeste 2 Polycomb Repressive Complex 2 Subunit	+	+	+	3.07	Critical role during normal and perturbed development of hematopoietic and central nervous systems ⁶⁶ and a member of the Polycomb group, which maintains homeotic repression and is thought to control gene expression by regulating chromatin ¹⁸ (In addition to the cerebral malformation phenotype of DGAP259 has a complex chromosome rearrangement.)
PDIA4	148700154-148725733	Protein Disulfide Isomerase Family A, Member 4	-	-	-	70.97	
ZNF786	148766735-148787874	Zinc Finger Protein 786	-	-	-	92.01	
ZNF425	148799876-148823438	Zinc Finger Protein 425	-	-	-	92.53	
ZNF398	148823508-148880116	Zinc Finger Protein 398	-	-	-	61.58	
ZNF282	148892577-148923339	Zinc Finger Protein 282	+	-	-	64.68	
ZNF212	148936742-148952700	Zinc Finger Protein 212	+	-	-	67.39	
ZNF783	148959262-148994393	Zinc Finger Family Member 783	-	-	-	82.83	
ZNF777	149128454-149158214	Zinc Finger Protein 777	-	-	-	52.36	
ZNF746	149169885-149194908	Zinc Finger Protein 746	+	-	-	59.83	

DDG2P: Developmental Disorders Genotype-to-Phenotype Database, +: Confirmed DDG2P gene, HI: Haploinsufficiency index (in red if <10%)

Shaded row: Protein coding gene located within the same hESC topologically associated domain (TAD)²⁵ with the breakpoints

Table S15. Convergent Genomic Analysis of DGAP259 7q36.3 breakpoints

DGAP259: 7q36.3 breakpoints on Rearrangement_A: 155,701,797 and Rearrangement_C: 155,700,873							
Genes	Nucleotides (GRCh37/hg19)	Description	OMIM ²⁶	OMIM Morbid ²⁶	DDG2P ²⁷	%HI ⁸	Notes
PAXIP1	154735397-154794794	PAX Interacting (with Transcription-Activation Domain) Protein 1	+	-	-	48.56	
HTR5A	154862034-154877459	5-Hydroxytryptamine (Serotonin) Receptor 5a, G Protein-Coupled	+	-	-	59.81	
INSIG1	155089486-155101945	Insulin Induced Gene 1	+	-	-	73.03	
EN2	155250824-155257526	Engrailed Homeobox 2	+	-	-	23.56	
CNPY1	155266901-155326557	Canopy Fgf Signaling Regulator 1	+	-	-	63.67	
RBM33	155437145-155574179	Rna Binding Motif Protein 33	-	-	-	42.71	
SHH	155592680-155604967	Sonic Hedgehog	+	+	+	0.66	Haploinsufficiency (autosomal dominant, monoallelic) associated with Holoprosencephaly type 3 (HPE3), with long range regulation associated phenotype (relevant to cerebral malformation phenotype of DGAP259)
RNF32	156432975-156469824	Ring Finger Protein 32	+	-	-	75.12	
LMBR1	156461646-156685924	Limb Development Membrane Protein 1	+	+	-	24.09	
NOM1	156742417-156765876	Nucleolar Protein With Mif4g Domain 1	+	-	-	80.94	
MNX1	156786745-156803345	Motor Neuron And Pancreas Homeobox 1	+	+	+	0.84	Haploinsufficiency (autosomal dominant, monoallelic) associated with Curarino Syndrome (sacral malformation) ⁶⁹
UBE3C	156931607-157062066	Ubiquitin Protein Ligase E3c	+	-	-	59.16	
DNAJB6	157128075-157210133	Dnaj (Hsp40) Homolog, Subfamily B, Member 6	+	+	-	47.78	
PTPRN2	157331750-158380480	Protein Tyrosine Phosphatase, Receptor Type, N Polypeptide 2	+	-	-	45.29	
NCAPG2	158424003-158497520	Non-SMC Condensin II Complex, Subunit G2	+	-	-	45.05	
ESYT2	158523686-158622944	Extended Synaptotagmin-Like Protein 2	-	-	-	55.86	
WDR60	158649269-158749438	WD Repeat Domain 60	+	+	+	89.69	
VIPR2	158820866-158937649	Vasoactive Intestinal Peptide Receptor 2	+	-	-	73.84	

DDG2P: Developmental Disorders Genotype-to-Phenotype Database, +: Confirmed DDG2P gene, HI: Haploinsufficiency index (in red if <10%)

Shaded rows: Protein coding genes located within the same hESC topologically associated domain (TAD)²⁵ with the breakpoints

Table S16. Convergent Genomic Analysis of DGAP259 9p23 breakpoints

DGAP259: 9p23 breakpoints on Rearrangement_F: 9,646,47{5} and Rearrangement_I: 9,646,471							
Genes	Nucleotides (GRCh37/hg19)	Description	OMIM ²⁶	OMIM Morbid ²⁶	DDG2P ²⁷	%HI ⁸	Notes
<i>TMEM261</i>	7796490-7888380	Transmembrane Protein 261	-	-	-	87.18	
<i>PTPRD</i> (Disrupted)	8314246-10612723	Protein Tyrosine Phosphatase, Receptor Type, D	+	-	-	0.14	Homozygous microdeletion causes trigonocephaly, hearing loss, and intellectual disability, overlapping phenotypes with the autosomal dominant 9p deletion syndrome⁷⁰ (relevant cerebral malformation phenotype of DGAP259) Role in synaptic plasticity and hippocampal-dependent learning and memory ⁷¹ (5q14.3 breakpoints of DGAP259 within same TAD as MEF2C with similar role)
<i>TYRP1</i>	12685439-12710290	Tyrosinase-Related Protein 1	+	+	+	21.84	

DDG2P: Developmental Disorders Genotype-to-Phenotype Database, +: Confirmed DDG2P gene, HI: Haploinsufficiency index (in red if <10%)

Shaded row: Protein coding gene located within the same hESC topologically associated domain (TAD)²⁵ with the breakpoints

Table S17. Convergent Genomic Analysis of DGAP259 18p11.31 breakpoints

DGAP259: 18p11.31 breakpoints on Rearrangement_D: 6,375,05{1}, Rearrangement_G: 6,559,611 and Rearrangement_H: 6,375,0{52-48} and 6,559,{598-602}							
Genes	Nucleotides (GRCh37/hg19)	Description	OMIM ²⁶	OMIM Morbid ²⁶	DDG2P ²⁷	%HI ⁸	Notes
DLGAP1	3496030-4455335	Discs, Large (Drosophila) Homolog-Associated Protein 1	+	-	-	7.58	Candidate gene for schizophrenia ⁷²
C18orf42	5145284-5197502	Chromosome 18 Open Reading Frame 42	-	-	-	64.35	
ZBTB14	5289018-5297052	Zinc Finger And Btb Domain Containing 14	+	-	-	28.98	
EPB41L3	5392383-5630699	Erythrocyte Membrane Protein Band 4.1-Like 3	+	-	-	35.28	
TMEM200C	5882071-5895954	Transmembrane Protein 200c	-	-	-	77.42	
L3MBTL4 (Disrupted)	5954705-6415236	L(3)Mbt-Like 4 (Drosophila)	-	-	-	59.07	No reported phenotype association
ARHGAP28	6729717-6915715	Rho Gtpase Activating Protein 28	+	-	-	60.37	
LAMA1	6941743-7117813	Laminin, Alpha 1	+	-	+	60.73	Biallelic loss of function (autosomal recessive) associated with Poretti-Boltshauser syndrome (cerebellar dysplasia) ⁷³
LRRC30	7231123-7232045	Leucine Rich Repeat Containing 30	-	-	-	59.77	
PTPRM	7566780-8406859	Protein Tyrosine Phosphatase, Receptor Type, M	+	-	-	7.19	No reported phenotype association (Loss of PTPRM associated with pathogenic development of colorectal adenoma-carcinoma sequence) ⁷⁴
RAB12	8609443-8639379	RAB12, member RAS oncogene family	-	-	-	37.44	

DDG2P: Developmental Disorders Genotype-to-Phenotype Database, +: Confirmed DDG2P gene, HI: Haploinsufficiency index (in red if <10%)

Shaded rows: Protein coding genes located within the same hESC topologically associated domain (TAD)²⁵ with the breakpoints (blue: 5' breakpoints, red: 3' breakpoints)

Table S18. Convergent Genomic Analysis of DGAP259 18q21.3 breakpoints

DGAP259: 18q21.3 breakpoints on Rearrangement_F: 54,660,13{8} and Rearrangement_I: 54,660,136							
Genes	Nucleotides (GRCh37/hg19)	Description	OMIM ² 6	OMIM Morbid ² 6	DDG2P ²⁷	%HI ⁸	Notes
CCDC68	52568740-52626739	Coiled-Coil Domain Containing 68	-	-	-	59.77	
TCF4	52889562-53332018	Transcription Factor 4	+	+	+	0.38	Haploinsufficiency (autosomal dominant, monoallelic associated with Pitt-Hopkins Syndrome (severe epileptic encephalopathy with mental retardation) ⁷⁵ (relevant to cerebellar malformation phenotype of DGAP259) (7q35 breakpoints of DGAP259 disrupt CNTNAP2, a gene related with Pitt-Hopkins like Syndrome) ⁶⁴
TXNL1	54264439-54318831	Thioredoxin-Like 1	+	-	-	5.48	No reported phenotype association
WDR7 (Disrupted)	54318574-54698828	Wd Repeat Domain 7	+	-	-	14.85	No reported phenotype association Localized to synaptic vesicles in rat and mouse brain ⁷⁶
BOD1L2	54814293-54817531	Biorientation of Chromosomes In Cell Division 1-Like 2	-	-	-	87.92	
ST8SIA3	55018044-55038962	ST8 Alpha-N-Acetyl-Neuraminate Alpha-2,8-Sialyltransferase 3	+	-	-	11.2	
ONECUT2	55102917-55158529	One Cut Homeobox 2	+	-	-	12.99	
FECH	55215515-55254004	Ferrochelatase	+		-	28.28	
NARS	55267888-55289445	Asparaginyl-tRNA Synthetase	+	-	-	21.6	
ATP8B1	55313658-55470333	ATPase, Aminophospholipid Transporter, Class I, Type 8B, Member 1	+	+	+	41.4	Biallelic loss of function (autosomal recessive) is associated with ATP8B1-related intrahepatic cholestasis ⁷⁷
NEDD4L	55711599-56068772	Neural Precursor Cell Expressed, Developmentally Down-Regulated 4-Like, E3 Ubiquitin Protein Ligase	+	-	-	8.66	Regulator of renal sodium channels and involved in induction of mesoendodermal fates in mouse embryonic stem cells ⁷⁸ (renal agenesis and multicystic kidney in DGAP259)
ALPK2	56148479-56296189	Alpha-Kinase 2	-	-	-	88.74	

DDG2P: Developmental Disorders Genotype-to-Phenotype Database, +: Confirmed DDG2P gene, HI: Haploinsufficiency index (in red if <10%)

Shaded rows: Protein coding genes located within the same hESC topologically associated domain (TAD)²⁵ with the breakpoints

Table S19. Convergent Genomic Analysis of DGAP268 10p12.31 breakpoints

DGAP268: 10p12.31 breakpoints on Rearrangement_B: 21,606,655 and Rearrangement_C: 21,606,63{4-2}							
Genes	Nucleotides (GRCh37/hg19)	Description	OMIM ²⁶	OMIM Morbid ²⁶	DDG2P ²⁷	%HI ⁸	Notes
<i>NEBL</i>	21068902-21463116	Nebulette	+	-	-	21.79	
<i>C10orf113</i>	21414692-21435488	Chromosome 10 Open Reading Frame 113	-	-	-	86.51	
<i>CASC10</i>	21781587-21786191	Cancer Susceptibility Candidate 10	-	-	-	83.87	
<i>SKIDA1</i>	21802407-21814611	SKI/DACH Domain Containing 1	-	-	-	18.69	
<i>MLLT10</i>	21823094-22032559	Myeloid/Lymphoid Or Mixed-Lineage Leukemia (Trithorax Homolog, Drosophila); Translocated To, 10	+	-	-	9.19	No reported phenotype association Fused with <i>AF10</i> in rare but recurrent chromosome rearrangement of acute monoblastic leukemia (inv ins(10;11)(p12;q23q12)) ⁷⁹
<i>DNAJC1</i>	22045466-22292698	Dnaj (Hsp40) Homolog, Subfamily C, Member 1	+	-	-	38.97	
<i>EBLN1</i>	22497743-22498950	Endogenous Bornavirus-Like Nucleoprotein 1	+	-	-	90.27	
<i>COMM3</i>	22604903-22609235	COMM Domain Containing 3	-	-	-	18.42	
<i>BMI1</i>	22610140-22620413	BMI1 Proto-Oncogene, Polycomb Ring Finger	+	-	-	1.63	No reported phenotype association, strongly expressed in proliferating cerebellar precursor cells in mice and humans ⁸⁰ Important paralog of <i>PCGF5</i> (located in the vicinity of 10q23.32 breakpoints of DGAP268)
<i>SPAG6</i>	22634399-22743153	Sperm Associated Antigen 6	+	-	-	43.84	
<i>PIP4K2A</i>	22823778-23003484	Phosphatidylinositol-5-Phosphate 4-Kinase, Type II, Alpha	+	-	-	20.5	
<i>ARMC3</i>	23216953-23326518	Armadillo Repeat Containing 3	+	-	-	66.75	

DDG2P: Developmental Disorders Genotype-to-Phenotype Database, +: Confirmed DDG2P gene, HI: Haploinsufficiency index (in red if <10%)

Shaded rows: Protein coding genes located within the same hESC topologically associated domain (TAD)²⁵ with the breakpoints

Table S20. Convergent Genomic Analysis of DGAP268 10p12.2 breakpoints

DGAP268: 10p12.2 breakpoints on Rearrangement_A: 23,659,495~ and Rearrangement_C: 23,659,20{0-2}							
Genes	Nucleotides (GRCh37/hg19)	Description	OMIM ²⁶	OMIM Morbid ²⁶	DDG2P ²⁷	%HI ⁸	Notes
MSRB2	23384435-23410942	Methionine Sulfoxide Reductase B2	+	-	-	79.51	
PTF1A	23481256-23483181	Pancreas Specific Transcription Factor, 1a	+	+	+	27.41	Biallelic loss of function (autosomal recessive) associated with Pancreatic and Cerebellar Agenesis ⁸¹
C10orf67	23556124-23633774	Chromosome 10 Open Reading Frame 67	-	-	-	90.14	
OTUD1	23728198-23731308	OTU Deubiquitinase 1	+	-	-	75.7	
KIAA1217	23983675-24836772	Kiaa1217	-	-	-	41.11	
ARHGAP21	24872538-25012597	Rho Gtpase Activating Protein 21	+	-	-	56.74	

DDG2P: Developmental Disorders Genotype-to-Phenotype Database, +: Confirmed DDG2P gene, HI: Haploinsufficiency index (in red if <10%)

Shaded rows: Protein coding genes located within the same hESC topologically associated domain (TAD)²⁵ with the breakpoints

Table S21. Convergent Genomic Analysis of DGAP268 10q23.32 breakpoints

DGAP268: 10q23.32 breakpoints on Rearrangement_A: 93,983,897~ and Rearrangement_B: 93,982,408							
Genes	Nucleotides (GRCh37/hg19)	Description	OMIM ²⁶	OMIM Morbid ²⁶	DDG2P ²⁷	%HI ⁸	Notes
<i>RPP30</i>	92631473-92668312	Ribonuclease P/MRP 30 kda Subunit	+	-	-	26.31	
<i>ANKRD1</i>	92671853-92681033	Ankyrin Repeat Domain 1 (Cardiac Muscle)	+	+	-	22.32	
<i>PCGF5</i>	92979908-93044088	Polycomb Group Ring Finger 5	-	-	-	8.55	No reported phenotype association Important paralog of <i>BMI1</i> (located in the vicinity of 10p12.31 breakpoints of DGAP268)
<i>HECTD2</i>	93170096-93274586	HECT Domain Containing E3 Ubiquitin Protein Ligase 2	-	-	-	16.83	
<i>PPP1R3C</i>	93388199-93392811	Protein Phosphatase 1, Regulatory Subunit 3C	+	-	-	39.43	
<i>TNKS2</i>	93558069-93625033	Tankyrase, TRF1-Interacting Ankyrin-Related ADP-Ribose Polymerase 2	+	-	-	11.01	
<i>FGFBP3</i>	93666346-93669240	Fibroblast Growth Factor Binding Protein 3	-	-	-	84.27	
<i>BTAF1</i>	93683526-93790082	BTAF1 RNA Polymerase II, B-TFIID Transcription Factor-Associated, 170 kda	+	-	-	5	No reported phenotype association
<i>CPEB3</i> (Disrupted)	93806449-94050844	Cytoplasmic Polyadenylation Element Binding Protein 3	+	-	-	12.96	No reported phenotype association
<i>MARCH5</i>	94050920-94113721	Membrane-Associated Ring Finger (C3HC4) 5	+	-	-	7.01	No reported phenotype association
<i>IDE</i>	94211441-94333833	Insulin-Degrading Enzyme	+	-	-	1.37	No reported phenotype association
<i>KIF11</i>	94353043-94415150	Kinesin Family Member 11	+	+	+	9.02	Haploinsufficiency (autosomal dominant, monoallelic) associated with microcephaly with or without chorioretinopathy, lymphedema, or mental retardation ⁸²
<i>HHEX</i>	94447945-94455403	Hematopoietically Expressed Homeobox	+	-	-	7.77	No reported phenotype association
<i>EXOC6</i>	94590935-94819250	Exocyst Complex Component 6	+	-	-	7.76	No reported phenotype association
<i>CYP26C1</i>	94821021-94828454	Cytochrome P450, Family 26, Subfamily C, Polypeptide 1	+	+	-	38.94	Biallelic loss of function (autosomal recessive) associated with Focal facial dermal dysplasia, type IV ⁸³
<i>CYP26A1</i>	94833232-94837647	Cytochrome P450, Family 26, Subfamily A, Polypeptide 1	+	-	-	9.92	No reported phenotype association
<i>MYOF</i>	95066186-95242074	Myoferlin	+	-	-	23.07	
<i>CEP55</i>	95256389-95288849	Centrosomal Protein 55 kda	+	-	-	30.24	

DDG2P: Developmental Disorders Genotype-to-Phenotype Database, +: Confirmed DDG2P gene, HI: Haploinsufficiency index (in red if <10%)
Shaded rows: Protein coding genes located within the same hESC topologically associated domain (TAD)²⁵ with the breakpoints

Table S22. Convergent Genomic Analysis of DGAP285 Xp11.21 breakpoints

DGAP285: Xp11.21 breakpoints on Rearrangement_A: 55,174,723~ and Rearrangement_B: 55,174,381~							
Genes	Nucleotides (GRCh37/hg19)	Description	OMIM ²⁶	OMIM Morbid ²⁶	DDG2P ²⁷	%HI ⁸	Notes
PAGE2B	55101496-55105342	P Antigen Family, Member 2B	-	-	-	96.76	
PAGE2	55115441-55119275	P Antigen Family, Member 2 (Prostate Associated)	+	-	-	96.53	
FAM104B (Disrupted)	55169535-55187743	Family With Sequence Similarity 104, Member B	-	-	-	93.08	No reported phenotype association
MTRNR2L10	55207824-55208944	MT-RNR2-Like 10	-	-	-	89.08	
PAGE5	55246788-55250541	P Antigen Family, Member 5 (Prostate Associated)	-	-	-	96.87	
PAGE3	55284848-55291279	P Antigen Family, Member 3 (Prostate Associated)	+	-	-	96.96	
MAGEH1	55478538-55479998	Melanoma Antigen Family H1	+	-	-	77.09	
USP51	55511049-55515635	Ubiquitin Specific Peptidase 51	-	-	-	73.85	
FOXR2	55649833-55652621	Forkhead Box R2	+	-	-	90.12	
RRAGB	55744172-55785207	Ras-Related GTP Binding B	+	-	-	34.1	
KLF8	56258854-56314322	Kruppel-Like Factor 8	+	-	-	60.52	

DDG2P: Developmental Disorders Genotype-to-Phenotype Database, +: Confirmed DDG2P gene, HI: Haploinsufficiency index (in red if <10%)

Shaded rows: Protein coding genes located within the same hESC topologically associated domain (TAD)²⁵ with the breakpoints

Table S23. Convergent Genomic Analysis of DGAP285 Xq28 breakpoints

DGAP285: Xq28 breakpoints on Rearrangement_A: 150,286,207~ and Rearrangement_B: 150,284,569~							
Genes	Nucleotides (GRCh37/hg19)	Description	OMIM ²⁶	OMIM Morbid ²⁶	DDG2P ²⁷	%HI ⁸	Notes
<i>IDS</i>	148558521-148615470	Iduronate 2-Sulfatase	+	+	+	14.02	Hemizygous loss of function (X-linked recessive) associated with Mucopolysaccharidosis II ⁸⁴
<i>CXorf40A</i>	148621900-148632055	Chromosome X Open Reading Frame 40A	+	-	-	86.75	No reported phenotype association
<i>MAGEA9B</i>	148663308-148669116	Melanoma Antigen Family A9B	+	-	-	99.76	No reported phenotype association
<i>MAGEA9</i>	148663309-148669116	Melanoma Antigen Family A9	+	-	-	96.82	No reported phenotype association
<i>TMEM185A</i>	148678216-148713568	Transmembrane Protein 185A	+	-	-	38.34	No reported phenotype association
<i>MAGEA11</i>	148769894-148798926	Melanoma Antigen Family A11	+	-	-	95.69	No reported phenotype association
<i>HSFX2</i>	148855725-148858528	Heat Shock Transcription Factor Family, X Linked 2	-	-	-	99.69	
<i>HSFX1</i>	148855726-148858525	Heat Shock Transcription Factor Family, X Linked 1	-	-	-	99.26	
<i>MAGEA8</i>	149009941-149014609	Melanoma Antigen Family A8	+	-	-	96	No reported phenotype association
<i>CXorf40B</i>	149097745-149107029	Chromosome X Open Reading Frame 40B	-	-	-	86.08	
<i>MAMLD1</i>	149529689-149682448	Mastermind-Like Domain Containing 1	+	+	P	71.77	Hemizygous loss of function (X-linked recessive) associated with X-linked hypospadias, type II ⁸⁵
<i>MTM1</i>	149737069-149841795	Myotubularin 1	+	+	+	12.54	Hemizygous loss of function (X-linked recessive) associated with X-linked myotubular myopathy ⁸⁶ (overlapping phenotype with DGAP285)
<i>MTMR1</i>	149861435-149933576	Myotubularin Related Protein 1	+	-	-	31.42	
<i>CD99L2</i>	149934810-150067289	CD99 Molecule-Like 2	+	-	-	82.42	No reported phenotype association
<i>HMGB3</i>	150148982-150159248	High Mobility Group Box 3	+	+	-	36.49	Hemizygous loss of function (X-linked recessive) associated with syndromic microphthalmia, 13 ⁸⁷
<i>GPR50</i>	150345125-150349937	G Protein-Coupled Receptor 50	+	-	-	81.88	No reported phenotype association
<i>VMA21</i>	150564987-150577836	VMA21 Vacuolar H+-Atpase Homolog (<i>S. Cerevisiae</i>)	+	+	-	51.64	Hemizygous loss of function (X-linked recessive) associated with X-linked myopathy with excessive autophagy ⁸⁸
<i>PASD1</i>	150732094-150845211	PAS Domain Containing 1	-	-	-	99.84	
<i>PRRG3</i>	150863596-150874396	Proline Rich Gla (G-Carboxyglutamic Acid) 3 (Transmembrane)	+	-	-	58.49	No reported phenotype association
<i>FATE1</i>	150884507-150891666	Fetal And Adult Testis Expressed 1	+	-	-	95.68	No reported phenotype association

DDG2P: Developmental Disorders Genotype-to-Phenotype Database, +: Confirmed DDG2P gene, P: Probable DDG2P gene, HI: Haploinsufficiency index (in red if <10%)

Shaded rows: Protein coding genes located within the neighboring hESC topologically associated domains (TAD)²⁵ and the topological boundary regions (TBR) around the breakpoints

Table S24. Convergent Genomic Analysis of DGAP288 6q21 breakpoints

DGAP288: 6q21 breakpoints on Rearrangement_A: 112,976,04{2-4}and Rearrangement_B: 112,976,031							
Genes	Nucleotides (GRCh37/hg19)	Description	OMIM ²⁶	OMIM Morbid ²⁶	DDG2P ²⁷	%HI ⁸	Notes
<i>WISP3</i>	112375275- 112392171	WNT1 Inducible Signaling Pathway Protein 3	+	+	-	48.76	Biallelic loss of function (autosomal recessive) associated with progressive pseudorheumatoid arthropathy of childhood ⁸⁹
<i>TUBE1</i>	112391980- 112408732	Tubulin, Epsilon 1	+	-	-	14.86	
<i>FAM229B</i>	112408802- 112423993	Family With Sequence Similarity 229, Member B	-	-	-	19.09	
<i>LAMA4</i>	112429963- 112576141	Laminin, Alpha 4	+	-	-	35.21	
<i>RFPL4B</i>	112668532- 112672498	Ret Finger Protein-Like 4B	-	-	-	99.43	
<i>MARCKS</i>	114178541- 114184648	Myristoylated Alanine-Rich Protein Kinase C Substrate	+	-	-	64.72	

DDG2P: Developmental Disorders Genotype-to-Phenotype Database, +: Confirmed DDG2P gene, HI: Haploinsufficiency index (in red if <10%)

Shaded rows: Protein coding genes located within the same hESC topologically associated domain (TAD)²⁵ with the breakpoints

Table S25. Convergent Genomic Analysis of DGAP288 17q24.3 breakpoints

DGAP288: 17q24.3 breakpoints on Rearrangement_A: 69,728,01{7-9} and Rearrangement_B: 69,728,006							
Gene	Nucleotides (GRCh37/hg19)	Description	OMIM ²⁶	OMIM Morbid ²⁶	DDG2P ²⁷	%HI ⁸	Notes
SOX9	70117161- 70122561	SRY (sex determining region Y)-box 9	+	+	+	0.56	Haploinsufficiency (autosomal dominant, monoallelic) associated with Campomelic dysplasia ⁹⁰ Haploinsufficient (autosomal dominant, monoallelic) long-range cis-regulation associated with Pierre-Robin Sequence ²² (overlapping phenotype with DGAP288)

DDG2P: Developmental Disorders Genotype-to-Phenotype Database, +: Confirmed DDG2P gene, HI: Haploinsufficiency index (in red if <10%)

Shaded row: SOX9 is the only protein coding gene located within the same hESC topologically associated domain (TAD)²⁵ with the breakpoints

Table S26. Convergent Genomic Analysis of DGAP290 2q32.3 breakpoints

DGAP290: 2q32.3 breakpoints on Rearrangement_A: 197,164,194 and Rearrangement_B: 197,164,206							
Genes	Nucleotides (GRCh37/hg19)	Description	OMIM ²⁶	OMIM Morbid ²⁶	DDG2P ²⁷	%HI ⁸	Notes
<i>SLC39A10</i>	196440701-196602426	Solute Carrier Family 39 (Zinc Transporter), Member 10	+	-	-	36.25	
<i>DNAH7</i>	196602427-196933536	Dynein, Axonemal, Heavy Chain 7	+	-	-	48.83	
<i>STK17B</i>	196998290-197041227	Serine/Threonine Kinase 17b	+	-	-	37.72	
<i>HECW2</i> (Disrupted)	197059094-197458416	HECT, C2 And WW Domain Containing E3 Ubiquitin Protein Ligase 2	-	-	-	18.5	No reported phenotype association
<i>CCDC150</i>	197504278-197628214	Coiled-Coil Domain Containing 150	-	-	-	62.11	
<i>GTF3C3</i>	197627756-197664449	General Transcription Factor IIIC, Polypeptide 3, 102 kda	+	-	-	30.03	
<i>C2orf66</i>	197669726-197675000	Chromosome 2 Open Reading Frame 66	-	-	-	77.88	
<i>PGAP1</i>	197697728-197792520	Post-GPI Attachment To Proteins 1	+	+	-	32.33	Biallelic loss of function (autosomal recessive) associated with mental retardation, type 4 ⁹¹
<i>ANKRD44</i>	197831741-198175897	Ankyrin Repeat Domain 44	-	-	-	28.93	
<i>SF3B1</i>	198254508-198299815	Splicing Factor 3b, Subunit 1, 155 kda	+	-	-	4.28	No reported phenotype association
<i>COQ10B</i>	198318147-198340032	Coenzyme Q10B	-	-	-	38.85	
<i>HSPD1</i>	198351305-198381461	Heat Shock 60 kda Protein 1 (Chaperonin)	+	+	+	2.85	Haploinsufficiency (autosomal dominant, monoallelic) associated with spastic paraparesis, type 13 ⁹²
<i>HSPE1</i>	198364718-198368181	Heat Shock 10 kda Protein 1	+	-	-	9.58	
<i>MOB4</i>	198380295-198418423	MOB Family Member 4, Phocean	+	-	-	4.45	
<i>RFTN2</i>	198432948-198540769	Raftlin Family Member 2	-	-	-	66.28	
<i>MARS2</i>	198570087-198573113	Methionyl-TRNA Synthetase 2, Mitochondrial	+	+	-	47.49	Biallelic loss of function (autosomal recessive) associated with Spastic ataxia, type 3 ⁹³
<i>BOLL</i>	198591603-198651486	Boule-Like RNA-Binding Protein	+	-	-	18.25	

DDG2P: Developmental Disorders Genotype-to-Phenotype Database, +: Confirmed DDG2P gene, HI: Haploinsufficiency index (in red if <10%)

Shaded rows: Protein coding genes located within the same hESC topologically associated domain (TAD)²⁵ with the breakpoints

Table S27. Convergent Genomic Analysis of DGAP290 7q33 breakpoints

DGAP290: 7q33 breakpoints on Rearrangement_A: 135,905,923, Rearrangement_B: 135,299,810, and Rearrangement_C: 135,299,81{2} and 135,905,92{4}							
Genes	Nucleotides (GRCh37/hg19)	Description	OMIM ²⁶	OMIM Morbid ²⁶	DDG2P ²⁷	%HI ⁸	Notes
<i>BPGM</i>	134331560-134364565	2,3-Bisphosphoglycerate Mutase	+	+	-	22.09	Biallelic loss of function (autosomal recessive) associated with erythrocytosis due to bisphosphoglycerate mutase deficiency ⁹⁴
<i>CALD1</i>	134429003-134655479	Caldesmon 1	+	-	-	20.29	
<i>AGBL3</i>	134671259-134832715	ATP/GTP Binding Protein-Like 3	-	-	-	64.12	
<i>C7orf49</i>	134777115-134855547	Chromosome 7 Open Reading Frame 49	-	-	-	80.37	
<i>TMEM140</i>	134832824-134850967	Transmembrane Protein 140	-	-	-	83.19	
<i>WDR91</i>	134868590-134896316	WD Repeat Domain 91	-	-	-	46.24	
<i>STRA8</i>	134916731-134943244	Stimulated By Retinoic Acid 8	+	-	-	56.99	
<i>CNOT4</i>	135046547-135194875	CCR4-NOT Transcription Complex, Subunit 4	+	-	-	6.19	No reported phenotype association
<i>NUP205</i> (Disrupted)	135242667-135333505	Nucleoporin 205 kda	+	-	-	11.41	No reported phenotype association
<i>C7orf73</i>	135347244-135378166	Chromosome 7 Open Reading Frame 73	-	-	-	24.72	
<i>SLC13A4</i>	135365985-135414006	Solute Carrier Family 13 (Sodium/Sulfate Symporter), Member 4	+	-	-	40.17	
<i>FAM180A</i>	135413096-135433594	Family With Sequence Similarity 180, Member A	-	-	-	63.78	
<i>MTPN</i>	135611509-135662101	Myotrophin	+	-	-	15.72	
<i>LUZP6</i>	135612022-135612198	Leucine Zipper Protein 6	+	-	-	86.19	
<i>CHRM2</i>	136553416-136705002	Cholinergic Receptor, Muscarinic 2	+	+	-	11.59	A SNP variation may predispose to alcohol dependence, drug dependence, and affective disorders ⁹⁵
<i>PTN</i>	136912088-137028611	Pleiotrophin	+	-	-	5.33	No reported phenotype association
<i>DGKI</i>	137065783-137531838	Diacylglycerol Kinase, Iota	+	-	-	12.1	

DDG2P: Developmental Disorders Genotype-to-Phenotype Database, +: Confirmed DDG2P gene, HI: Haploinsufficiency index (in red if <10%)

Shaded rows: Protein coding genes located within the same hESC topologically associated domain (TAD)²⁵ with the breakpoints

Table S28. Convergent Genomic Analysis of DGAP295 2p13.3 breakpoints

DGAP295: 2p13.3 breakpoints on Rearrangement_D: 69,588,420~ and Rearrangement_E: 69,588,264~							
Genes	Nucleotides (GRCh37/hg19)	Description	OMIM ²⁶	OMIM Morbid ²⁶	DDG2P ²⁷	%HI ⁸	Notes
<i>GFPT1</i> (Disrupted)	69546905-69614382	Glutamine--Fructose-6-Phosphate Transaminase 1	+	+	-	22.36	Biallelic loss of function (autosomal recessive) associated with congenital myasthenia, type 12 ⁹⁶
<i>NFU1</i>	69622882-69664760	NFU1 Iron-Sulfur Cluster Scaffold	+	+	+	7.52	Biallelic loss of function (autosomal recessive) associated with multiple mitochondrial dysfunctions syndrome, type 1 ⁹⁷
<i>AAK1</i>	69688532-69901481	AP2 Associated Kinase 1	+	-	-	27.81	
<i>ANXA4</i>	69871557-70053596	Annexin A4	+	-	-	36.41	
<i>GMCL1</i>	70056774-70108528	Germ Cell-Less, Spermatogenesis Associated 1	-	-	-	27.55	
<i>SNRNP27</i>	70120692-70132707	Small Nuclear Ribonucleoprotein 27 kda (U4/U6.U5)	-	-	-	21.9	
<i>MXD1</i>	70124820-70170077	MAX Dimerization Protein 1	+	-	-	19.62	
<i>ASPRV1</i>	70187226-70189397	Aspartic Peptidase, Retroviral-Like 1	+	-	-	44.23	
<i>PCBP1</i>	70314585-70316332	Poly(Rc) Binding Protein 1	+	-	-	22.38	
<i>C2orf42</i>	70377012-70475747	Chromosome 2 Open Reading Frame 42	-	-	-	28.59	
<i>TIA1</i>	70436576-70475792	TIA1 Cytotoxic Granule-Associated RNA Binding Protein	+	+	-	3.8	Haploinsufficiency (autosomal dominant, monoallelic mode) associated with Welander distal myopathy ⁹⁸
<i>PCYOX1</i>	70484518-70508323	Prenylcysteine Oxidase 1	+	-	-	55.49	

DDG2P: Developmental Disorders Genotype-to-Phenotype Database, +: Confirmed DDG2P gene, HI: Haploinsufficiency index (in red if <10%)

Shaded rows: Protein coding genes located within the same hESC topologically associated domain (TAD)²⁵ with the breakpoints

Table S29. Convergent Genomic Analysis of DGAP295 11p15.5 breakpoints

DGAP295: 11p15.5 Breakpoints on Rearrangement_A (1,915,057~ and 1,936,993~), Rearrangement_B (1,960,727~ and 1,936,668~), Rearrangement_C (1,915,843~ and 1,961,361~), Rearrangement_D (1,984,895~), and Rearrangement_E (1,985,019~)							
Gene	Nucleotides (GRCh37/hg19)	Description	OMIM ²⁶	OMIM Morbid ²⁶	DDG2P ²⁷	%Hi ⁸	Notes
<i>TSPAN4</i>	842808-867116	Tetraspanin 4	+	-	-	71.26	
<i>CHID1</i>	867357-915058	Chitinase Domain Containing 1	+	-	-	70.14	
<i>AP2A2</i>	924894-1012239	Adaptor-Related Protein Complex 2, Alpha 2 Subunit	+	-	-	72.44	
<i>MUC6</i>	1012821-1036706	Mucin 6, Oligomeric Mucus/Gel-Forming	+	-	-	92.04	
<i>MUC2</i>	1074875-1104419	Mucin 2, Oligomeric Mucus/Gel-Forming	+	-	-	78.34	
<i>MUC5AC</i>	1151580-1222364	Mucin 5AC, Oligomeric Mucus/Gel-Forming	+	-	-	82.42	
<i>MUC5B</i>	1244296-1283406	Mucin 5B, Oligomeric Mucus/Gel-Forming	+	+	-	94.15	
<i>TOLLIP</i>	1295601-1330884	Toll Interacting Protein	+	-	-	45.23	
<i>BRSK2</i>	1411129-1483919	BR Serine/Threonine Kinase 2	+	-	-	60.26	
<i>MOB2</i>	1490687-1522477	MOB Kinase Activator 2	+	-	-	62.66	
<i>DUSP8</i>	1575274-1593150	Dual Specificity Phosphatase 8	+	-	-	69.59	
<i>KRTAP5-1</i>	1605572-1606513	Keratin Associated Protein 5-1	+	-	-	82.35	
<i>KRTAP5-2</i>	1618409-1619524	Keratin Associated Protein 5-2	-	-	-	76.65	
<i>KRTAP5-3</i>	1628795-1629693	Keratin Associated Protein 5-3	-	-	-	84.7	
<i>KRTAP5-4</i>	1642188-1643368	Keratin Associated Protein 5-4	-	-	-	84.14	
<i>KRTAP5-5</i>	1651033-1652160	Keratin Associated Protein 5-5	-	-	-	76.4	
<i>KRTAP5-6</i>	1718425-1718985	Keratin Associated Protein 5-6	-	-	-	68.6	
<i>IFITM10</i>	1753640-1771821	Interferon Induced Transmembrane Protein 10	-	-	-	80.26	
<i>CTSD</i>	1773982-1785222	Cathepsin D	+	+	+	51.46	
<i>SYT8</i>	1848709-1858751	Synaptotagmin VIII	+	-	-	92.25	
<i>TNNI2</i>	1860219-1862910	Troponin I Type 2 (Skeletal, Fast)	+	+	-	67.71	
<i>LSP1</i>	1874200-1913497	Lymphocyte-Specific Protein 1	+	-	-	87.89	
<i>PRR33</i>	1910375-	Proline Rich 33	-	-	-	93.45	

	1912084						
TNNT3	1940792-1959936	Troponin T Type 3 (Skeletal, Fast)	+	+	-	54.88	
MRPL23	1968508-2005752	Mitochondrial Ribosomal Protein L23	+	-	-	79.39	
IGF2	2150342-2170833	Insulin-Like Growth Factor 2	+	+	+	79.01	Imprinted loss of function (epimutation) is associated with Silver-Russel Syndrome ²⁴ (overlapping phenotype with DGAP295)
INS	2181009-2182571	Insulin	+	+	-	80.96	
TH	2185159-2193107	Tyrosine Hydroxylase	+	+	+	6.58	
ASCL2	2289725-2292182	Achaete-Scute Family Bhlh Transcription Factor 2	+	-	-	71.06	
C11orf21	2316875-2324279	Chromosome 11 Open Reading Frame 21	+	-	-	98.55	
TSPAN32	2323227-2339430	Tetraspanin 32	+	-	-	90.86	
CD81	2397407-2418649	CD81 Molecule	+	+	-	64.93	
TSSC4	2421718-2425106	Tumor Suppressing Subtransferable Candidate 4	+	-	-	88.63	
TRPM5	2425745-2444275	Transient Receptor Potential Cation Channel, Subfamily M, Member 5	+	-	-	76.97	

DDG2P: Developmental Disorders Genotype-to-Phenotype Database, +: Confirmed DDG2P gene, HI: Haploinsufficiency index (in red if <10%)

Shaded rows: Protein coding genes located within the same hESC topologically associated domain (TAD)²⁵ with the breakpoints

REFERENCES

1. Talkowski, M.E., Ordulu, Z., Pillalamarri, V., Benson, C.B., Blumenthal, I., Connolly, S., Hanscom, C., Hussain, N., Pereira, S., Picker, J., et al. (2012). Clinical diagnosis by whole-genome sequencing of a prenatal sample. *N Engl J Med* 367, 2226-2232.
2. Pagon, R.A., Graham, J.M., Jr., Zonana, J., and Yong, S.L. (1981). Coloboma, congenital heart disease, and choanal atresia with multiple anomalies: CHARGE association. *J Pediatr* 99, 223-227.
3. Blake, K.D., Davenport, S.L., Hall, B.D., Hefner, M.A., Pagon, R.A., Williams, M.S., Lin, A.E., and Graham, J.M., Jr. (1998). CHARGE association: an update and review for the primary pediatrician. *Clin Pediatr (Phila)* 37, 159-173.
4. Verloes, A. (2005). Updated diagnostic criteria for CHARGE syndrome: a proposal. *Am J Med Genet A* 133A, 306-308.
5. Brown, G.C. (1982). Optic nerve hypoplasia and colobomatous defects. *J Pediatr Ophthalmol Strabismus* 19, 90-93.
6. Maumenee, I.H., and Mitchell, T.N. (1990). Colobomatous malformations of the eye. *Trans Am Ophthalmol Soc* 88, 123-132; discussion 133-125.
7. Suzuki, Y., Kawase, E., Nishina, S., and Azuma, N. (2006). Two patients with different features of congenital optic disc anomalies in the two eyes. *Graefes Arch Clin Exp Ophthalmol* 244, 259-261.
8. Huang, N., Lee, I., Marcotte, E.M., and Hurles, M.E. (2010). Characterising and predicting haploinsufficiency in the human genome. *PLoS Genet* 6, e1001154.
9. Bowman, G.D., O'Donnell, M., and Kuriyan, J. (2004). Structural analysis of a eukaryotic sliding DNA clamp-clamp loader complex. *Nature* 429, 724-730.
10. Castermans, D., Wilquet, V., Parthoens, E., Huysmans, C., Steyaert, J., Swinnen, L., Fryns, J.P., Van de Ven, W., and Devriendt, K. (2003). The neurobeachin gene is disrupted by a translocation in a patient with idiopathic autism. *J Med Genet* 40, 352-356.
11. Wise, A., Tenezaca, L., Fernandez, R.W., Schatoff, E., Flores, J., Ueda, A., Zhong, X., Wu, C.F., Simon, A.F., and Venkatesh, T. (2015). Drosophila mutants of the autism candidate gene neurobeachin (rugose) exhibit neurodevelopmental disorders, aberrant synaptic properties, altered locomotion, impaired adult social behavior and activity patterns. *J Neurogenet*, 1-34.
12. Nuytens, K., Gantois, I., Stijnen, P., Iscru, E., Laeremans, A., Serneels, L., Van Eylen, L., Liebhaber, S.A., Devriendt, K., Balschun, D., et al. (2013). Haploinsufficiency of the autism candidate gene Neurobeachin induces autism-like behaviors and affects cellular and molecular processes of synaptic plasticity in mice. *Neurobiol Dis* 51, 144-151.
13. Lauren, J., Airaksinen, M.S., Saarma, M., and Timmusk, T. (2003). A novel gene family encoding leucine-rich repeat transmembrane proteins differentially expressed in the nervous system. *Genomics* 81, 411-421.
14. Fernandez, B.A., Siegel-Bartelt, J., Herbrick, J.A., Teshima, I., and Scherer, S.W. (2005). Holoprosencephaly and cleidocranial dysplasia in a patient due to two position-effect mutations: case report and review of the literature. *Clin Genet* 68, 349-359.
15. Le Meur, N., Holder-Espinasse, M., Jaillard, S., Goldenberg, A., Joriot, S., Amati-Bonneau, P., Guichet, A., Barth, M., Charollais, A., Journel, H., et al. (2010). MEF2C haploinsufficiency caused by either microdeletion of the 5q14.3 region or mutation is responsible for severe mental retardation with stereotypic movements, epilepsy and/or cerebral malformations. *J Med Genet* 47, 22-29.
16. Alvarez, J.D., Yasui, D.H., Niida, H., Joh, T., Loh, D.Y., and Kohwi-Shigematsu, T. (2000). The MAR-binding protein SATB1 orchestrates temporal and spatial expression of multiple genes during T-cell development. *Genes Dev* 14, 521-535.
17. Kohwi-Shigematsu, T., Kohwi, Y., Takahashi, K., Richards, H.W., Ayers, S.D., Han, H.J., and Cai, S. (2012). SATB1-mediated functional packaging of chromatin into loops. *Methods* 58, 243-254.
18. Chen, H., Rossier, C., and Antonarakis, S.E. (1996). Cloning of a human homolog of the Drosophila enhancer of zeste gene (EZH2) that maps to chromosome 21q22.2. *Genomics* 38, 30-37.
19. Jungbluth, H., Wallgren-Pettersson, C., and Laporte, J. (2008). Centronuclear (myotubular) myopathy. *Orphanet J Rare Dis* 3, 26.
20. Joseph, M., Pai, G.S., Holden, K.R., and Herman, G. (1995). X-linked myotubular myopathy: clinical observations in ten additional cases. *Am J Med Genet* 59, 168-173.
21. Gordon, C.T., Tan, T.Y., Benko, S., Fitzpatrick, D., Lyonnet, S., and Farlie, P.G. (2009). Long-range regulation at the SOX9 locus in development and disease. *J Med Genet* 46, 649-656.

22. Benko, S., Fantes, J.A., Amiel, J., Kleinjan, D.J., Thomas, S., Ramsay, J., Jamshidi, N., Essafi, A., Heaney, S., Gordon, C.T., et al. (2009). Highly conserved non-coding elements on either side of SOX9 associated with Pierre Robin sequence. *Nat Genet* 41, 359-364.
23. Amarillo, I.E., Dipple, K.M., and Quintero-Rivera, F. (2013). Familial microdeletion of 17q24.3 upstream of SOX9 is associated with isolated Pierre Robin sequence due to position effect. *Am J Med Genet A* 161A, 1167-1172.
24. Gicquel, C., Rossignol, S., Cabrol, S., Houang, M., Steunou, V., Barbu, V., Danton, F., Thibaud, N., Le Merrer, M., Burglen, L., et al. (2005). Epimutation of the telomeric imprinting center region on chromosome 11p15 in Silver-Russell syndrome. *Nat Genet* 37, 1003-1007.
25. Dixon, J.R., Selvaraj, S., Yue, F., Kim, A., Li, Y., Shen, Y., Hu, M., Liu, J.S., and Ren, B. (2012). Topological domains in mammalian genomes identified by analysis of chromatin interactions. *Nature* 485, 376-380.
26. Amberger, J.S., Bocchini, C.A., Schiettecatte, F., Scott, A.F., and Hamosh, A. (2015). OMIM.org: Online Mendelian Inheritance in Man (OMIM(R)), an online catalog of human genes and genetic disorders. *Nucleic Acids Res* 43, D789-798.
27. Bragin, E., Chatzimichali, E.A., Wright, C.F., Hurles, M.E., Firth, H.V., Bevan, A.P., and Swaminathan, G.J. (2014). DECIPHER: database for the interpretation of phenotype-linked plausibly pathogenic sequence and copy-number variation. *Nucleic Acids Res* 42, D993-D1000.
28. Shiratsuchi, T., Nishimori, H., Ichise, H., Nakamura, Y., and Tokino, T. (1997). Cloning and characterization of BAI2 and BAI3, novel genes homologous to brain-specific angiogenesis inhibitor 1 (BAI1). *Cytogenet Cell Genet* 79, 103-108.
29. Rutsch, F., Gailus, S., Miousse, I.R., Suormala, T., Sagne, C., Toliat, M.R., Nurnberg, G., Wittkampf, T., Buers, I., Sharifi, A., et al. (2009). Identification of a putative lysosomal cobalamin exporter altered in the cblF defect of vitamin B12 metabolism. *Nat Genet* 41, 234-239.
30. Czarny-Ratajczak, M., Lohiniva, J., Rogala, P., Kozlowski, K., Perala, M., Carter, L., Spector, T.D., Kolodziej, L., Seppanen, U., Glazar, R., et al. (2001). A mutation in COL9A1 causes multiple epiphyseal dysplasia: further evidence for locus heterogeneity. *Am J Hum Genet* 69, 969-980.
31. Grant, A.V., El Baghdadi, J., Sabri, A., El Azbaoui, S., Alaoui-Tahiri, K., Abderrahmani Rhorfi, I., Gharbaoui, Y., Abid, A., Benkirane, M., Raharimanga, V., et al. (2013). Age-dependent association between pulmonary tuberculosis and common TOX variants in the 8q12-13 linkage region. *Am J Hum Genet* 92, 407-414.
32. Najmabadi, H., Hu, H., Garshasbi, M., Zemojtel, T., Abedini, S.S., Chen, W., Hosseini, M., Behjati, F., Haas, S., Jamali, P., et al. (2011). Deep sequencing reveals 50 novel genes for recessive cognitive disorders. *Nature* 478, 57-63.
33. Janssen, N., Bergman, J.E., Swertz, M.A., Tranebjaerg, L., Lodahl, M., Schoots, J., Hofstra, R.M., van Ravenswaaij-Arts, C.M., and Hoefsloot, L.H. (2012). Mutation update on the CHD7 gene involved in CHARGE syndrome. *Hum Mutat* 33, 1149-1160.
34. Haddad, R., Uwaydat, S., Dakroub, R., and Traboulsi, E.I. (2001). Confirmation of the autosomal recessive syndrome of ectopia lentis and distinctive craniofacial appearance. *Am J Med Genet* 99, 185-189.
35. Ouahchi, K., Arita, M., Kayden, H., Hentati, F., Ben Hamida, M., Sokol, R., Arai, H., Inoue, K., Mandel, J.L., and Koenig, M. (1995). Ataxia with isolated vitamin E deficiency is caused by mutations in the alpha-tocopherol transfer protein. *Nat Genet* 9, 141-145.
36. Gineau, L., Cognet, C., Kara, N., Lach, F.P., Dunne, J., Veturi, U., Picard, C., Trouillet, C., Eidenschenk, C., Aoufouchi, S., et al. (2012). Partial MCM4 deficiency in patients with growth retardation, adrenal insufficiency, and natural killer cell deficiency. *J Clin Invest* 122, 821-832.
37. Sanchez-Martin, M., Perez-Losada, J., Rodriguez-Garcia, A., Gonzalez-Sanchez, B., Korf, B.R., Kuster, W., Moss, C., Spritz, R.A., and Sanchez-Garcia, I. (2003). Deletion of the SLUG (SNAI2) gene results in human piebaldism. *Am J Med Genet A* 122A, 125-132.
38. Sanchez-Martin, M., Rodriguez-Garcia, A., Perez-Losada, J., Sagrera, A., Read, A.P., and Sanchez-Garcia, I. (2002). SLUG (SNAI2) deletions in patients with Waardenburg disease. *Hum Mol Genet* 11, 3231-3236.
39. Wooster, R., Bignell, G., Lancaster, J., Swift, S., Seal, S., Mangion, J., Collins, N., Gregory, S., Gumbs, C., and Micklem, G. (1995). Identification of the breast cancer susceptibility gene BRCA2. *Nature* 378, 789-792.
40. Alter, B.P., Rosenberg, P.S., and Brody, L.C. (2007). Clinical and molecular features associated with biallelic mutations in FANCD1/BRCA2. *J Med Genet* 44, 1-9.

41. Ichikawa, S., Imel, E.A., Kreiter, M.L., Yu, X., Mackenzie, D.S., Sorenson, A.H., Goetz, R., Mohammadi, M., White, K.E., and Econo, M.J. (2007). A homozygous missense mutation in human KLOTHO causes severe tumoral calcinosis. *J Clin Invest* 117, 2684-2691.
42. Collaborative Linkage Study of, A. (2001). An autosomal genomic screen for autism. *Am J Med Genet* 105, 609-615.
43. Lin, P.T., Gleeson, J.G., Corbo, J.C., Flanagan, L., and Walsh, C.A. (2000). DCAMKL1 encodes a protein kinase with homology to doublecortin that regulates microtubule polymerization. *J Neurosci* 20, 9152-9161.
44. Patel, H., Cross, H., Proukakis, C., Hershberger, R., Bork, P., Ciccarelli, F.D., Patton, M.A., McKusick, V.A., and Crosby, A.H. (2002). SPG20 is mutated in Troyer syndrome, an hereditary spastic paraparesis. *Nat Genet* 31, 347-348.
45. Villard, J., Lisowska-Grospierre, B., van den Elsen, P., Fischer, A., Reith, W., and Mach, B. (1997). Mutation of RFXAP, a regulator of MHC class II genes, in primary MHC class II deficiency. *N Engl J Med* 337, 748-753.
46. Shintani, M., Yagi, H., Nakayama, T., Saji, T., and Matsuoka, R. (2009). A new nonsense mutation of SMAD8 associated with pulmonary arterial hypertension. *J Med Genet* 46, 331-337.
47. Boczonadi, V., Muller, J.S., Pyle, A., Munkley, J., Dor, T., Quartararo, J., Ferrero, I., Karcagi, V., Giunta, M., Polvikoski, T., et al. (2014). EXOSC8 mutations alter mRNA metabolism and cause hypomyelination with spinal muscular atrophy and cerebellar hypoplasia. *Nat Commun* 5, 4287.
48. Berry, F.B., Lines, M.A., Oas, J.M., Footz, T., Underhill, D.A., Gage, P.J., and Walter, M.A. (2006). Functional interactions between FOXC1 and PITX2 underlie the sensitivity to FOXC1 gene dose in Axenfeld-Rieger syndrome and anterior segment dysgenesis. *Hum Mol Genet* 15, 905-919.
49. Nishimura, D.Y., Searby, C.C., Alward, W.L., Walton, D., Craig, J.E., Mackey, D.A., Kawase, K., Kanis, A.B., Patil, S.R., Stone, E.M., et al. (2001). A spectrum of FOXC1 mutations suggests gene dosage as a mechanism for developmental defects of the anterior chamber of the eye. *Am J Hum Genet* 68, 364-372.
50. Aldinger, K.A., Lehmann, O.J., Hudgins, L., Chizhikov, V.V., Bassuk, A.G., Ades, L.C., Krantz, I.D., Dobyns, W.B., and Millen, K.J. (2009). FOXC1 is required for normal cerebellar development and is a major contributor to chromosome 6p25.3 Dandy-Walker malformation. *Nat Genet* 41, 1037-1042.
51. Lee, S., Takeda, Y., Kawano, H., Hosoya, H., Nomoto, M., Fujimoto, D., Takahashi, N., and Watanabe, K. (2000). Expression and regulation of a gene encoding neural recognition molecule NB-3 of the contactin/F3 subgroup in mouse brain. *Gene* 245, 253-266.
52. Fernandez, T., Morgan, T., Davis, N., Klin, A., Morris, A., Farhi, A., Lifton, R.P., and State, M.W. (2004). Disruption of contactin 4 (CNTN4) results in developmental delay and other features of 3p deletion syndrome. *Am J Hum Genet* 74, 1286-1293.
53. Pomponio, R.J., Coskun, T., Demirkol, M., Tokatli, A., Ozalp, I., Huner, G., Baykal, T., and Wolf, B. (2000). Novel mutations cause biotinidase deficiency in Turkish children. *J Inher Metab Dis* 23, 120-128.
54. Balamotis, M.A., Tamberg, N., Woo, Y.J., Li, J., Davy, B., Kohwi-Shigematsu, T., and Kohwi, Y. (2012). Satb1 ablation alters temporal expression of immediate early genes and reduces dendritic spine density during postnatal brain development. *Mol Cell Biol* 32, 333-347.
55. Close, J., Xu, H., De Marco Garcia, N., Batista-Brito, R., Rossignol, E., Rudy, B., and Fishell, G. (2012). Satb1 is an activity-modulated transcription factor required for the terminal differentiation and connectivity of medial ganglionic eminence-derived cortical interneurons. *J Neurosci* 32, 17690-17705.
56. Eerola, I., Boon, L.M., Mulliken, J.B., Burrows, P.E., Dompert, A., Watanabe, S., Vanwijck, R., and Vikkula, M. (2003). Capillary malformation-arteriovenous malformation, a new clinical and genetic disorder caused by RASA1 mutations. *Am J Hum Genet* 73, 1240-1249.
57. Saitsu, H., Igarashi, N., Kato, M., Okada, I., Kosho, T., Shimokawa, O., Sasaki, Y., Nishiyama, K., Tsurusaki, Y., Doi, H., et al. (2011). De novo 5q14.3 translocation 121.5-kb upstream of MEF2C in a patient with severe intellectual disability and early-onset epileptic encephalopathy. *Am J Med Genet A* 155A, 2879-2884.
58. Nowakowska, B.A., Obersztyn, E., Szymanska, K., Bekiesinska-Figatowska, M., Xia, Z., Ricks, C.B., Bocian, E., Stockton, D.W., Szczaluba, K., Nawara, M., et al. (2010). Severe mental retardation, seizures, and hypotonia due to deletions of MEF2C. *Am J Med Genet B Neuropsychiatr Genet* 153B, 1042-1051.
59. Barbosa, A.C., Kim, M.S., Ertunc, M., Adachi, M., Nelson, E.D., McAnally, J., Richardson, J.A., Kavalali, E.T., Monteggia, L.M., Bassel-Duby, R., et al. (2008). MEF2C, a transcription factor that facilitates learning and memory by negative regulation of synapse numbers and function. *Proc Natl Acad Sci U S A* 105, 9391-9396.

60. Middendorp, S., Paoletti, A., Schiebel, E., and Bornens, M. (1997). Identification of a new mammalian centrin gene, more closely related to *Saccharomyces cerevisiae* CDC31 gene. *Proc Natl Acad Sci U S A* 94, 9141-9146.
61. Abadie, C., Blanchet, C., Baux, D., Larrieu, L., Besnard, T., Ravel, P., Biboulet, R., Hamel, C., Malcolm, S., Mondain, M., et al. (2012). Audiological findings in 100 USH2 patients. *Clin Genet* 82, 433-438.
62. Arking, D.E., Cutler, D.J., Brune, C.W., Teslovich, T.M., West, K., Ikeda, M., Rea, A., Guy, M., Lin, S., Cook, E.H., et al. (2008). A common genetic variant in the neurexin superfamily member CNTNAP2 increases familial risk of autism. *Am J Hum Genet* 82, 160-164.
63. Strauss, K.A., Puffenberger, E.G., Huentelman, M.J., Gottlieb, S., Dobrin, S.E., Parod, J.M., Stephan, D.A., and Morton, D.H. (2006). Recessive symptomatic focal epilepsy and mutant contactin-associated protein-like 2. *N Engl J Med* 354, 1370-1377.
64. Zweier, C., de Jong, E.K., Zweier, M., Orrico, A., Ousager, L.B., Collins, A.L., Bijlsma, E.K., Oortveld, M.A., Ekici, A.B., Reis, A., et al. (2009). CNTNAP2 and NRXN1 are mutated in autosomal-recessive Pitt-Hopkins-like mental retardation and determine the level of a common synaptic protein in *Drosophila*. *Am J Hum Genet* 85, 655-666.
65. Yu, Z.K., Gervais, J.L., and Zhang, H. (1998). Human CUL-1 associates with the SKP1/SKP2 complex and regulates p21(CIP1/WAF1) and cyclin D proteins. *Proc Natl Acad Sci U S A* 95, 11324-11329.
66. Di Meglio, T., Kratochwil, C.F., Vilain, N., Loche, A., Vitobello, A., Yonehara, K., Hrycaj, S.M., Roska, B., Peters, A.H., Eichmann, A., et al. (2013). Ezh2 orchestrates topographic migration and connectivity of mouse precerebellar neurons. *Science* 339, 204-207.
67. Belloni, E., Muenke, M., Roessler, E., Traverso, G., Siegel-Bartelt, J., Frumkin, A., Mitchell, H.F., Donis-Keller, H., Helms, C., Hing, A.V., et al. (1996). Identification of Sonic hedgehog as a candidate gene responsible for holoprosencephaly. *Nat Genet* 14, 353-356.
68. Anderson, E., Devenney, P.S., Hill, R.E., and Lettice, L.A. (2014). Mapping the Shh long-range regulatory domain. *Development* 141, 3934-3943.
69. Ross, A.J., Ruiz-Perez, V., Wang, Y., Hagan, D.M., Scherer, S., Lynch, S.A., Lindsay, S., Custard, E., Belloni, E., Wilson, D.I., et al. (1998). A homeobox gene, HLXB9, is the major locus for dominantly inherited sacral agenesis. *Nat Genet* 20, 358-361.
70. Chouair, N., Mignon-Ravix, C., Cacciagli, P., Abou Ghoch, J., Fawaz, A., Megarbane, A., Villard, L., and Chouery, E. (2015). Evidence that homozygous PTPRD gene microdeletion causes trigonocephaly, hearing loss, and intellectual disability. *Mol Cytogenet* 8, 39.
71. Uetani, N., Kato, K., Ogura, H., Mizuno, K., Kawano, K., Mikoshiba, K., Yakura, H., Asano, M., and Iwakura, Y. (2000). Impaired learning with enhanced hippocampal long-term potentiation in PTPdelta-deficient mice. *EMBO J* 19, 2775-2785.
72. Li, J.M., Lu, C.L., Cheng, M.C., Luu, S.U., Hsu, S.H., and Chen, C.H. (2013). Genetic analysis of the DLGAP1 gene as a candidate gene for schizophrenia. *Psychiatry Res* 205, 13-17.
73. Aldinger, K.A., Mosca, S.J., Tetreault, M., Dempsey, J.C., Ishak, G.E., Hartley, T., Phelps, I.G., Lamont, R.E., O'Day, D.R., Basel, D., et al. (2014). Mutations in LAMA1 cause cerebellar dysplasia and cysts with and without retinal dystrophy. *Am J Hum Genet* 95, 227-234.
74. Sudhir, P.R., Lin, S.T., Chia-Wen, C., Yang, S.H., Li, A.F., Lai, R.H., Wang, M.J., Chen, Y.T., Chen, C.F., Jou, Y.S., et al. (2015). Loss of PTprm associates with the pathogenic development of colorectal adenoma-carcinoma sequence. *Sci Rep* 5, 9633.
75. Zweier, C., Peippo, M.M., Hoyer, J., Sousa, S., Bottani, A., Clayton-Smith, J., Reardon, W., Saraiva, J., Cabral, A., Gohring, I., et al. (2007). Haploinsufficiency of TCF4 causes syndromal mental retardation with intermittent hyperventilation (Pitt-Hopkins syndrome). *Am J Hum Genet* 80, 994-1001.
76. Kawabe, H., Sakisaka, T., Yasumi, M., Shingai, T., Izumi, G., Nagano, F., Deguchi-Tawarada, M., Takeuchi, M., Nakanishi, H., and Takai, Y. (2003). A novel rabconnectin-3-binding protein that directly binds a GDP/GTP exchange protein for Rab3A small G protein implicated in Ca(2+)-dependent exocytosis of neurotransmitter. *Genes Cells* 8, 537-546.
77. Bull, L.N., van Eijk, M.J., Pawlikowska, L., DeYoung, J.A., Juifn, J.A., Liao, M., Klomp, L.W., Lomri, N., Berger, R., Scharschmidt, B.F., et al. (1998). A gene encoding a P-type ATPase mutated in two forms of hereditary cholestasis. *Nat Genet* 18, 219-224.

78. Gao, S., Alarcon, C., Sapkota, G., Rahman, S., Chen, P.Y., Goerner, N., Macias, M.J., Erdjument-Bromage, H., Tempst, P., and Massague, J. (2009). Ubiquitin ligase Nedd4L targets activated Smad2/3 to limit TGF-beta signaling. *Mol Cell* 36, 457-468.
79. Tanabe, S., Bohlander, S.K., Vignon, C.V., Espinosa, R., 3rd, Zhao, N., Strissel, P.L., Zeleznik-Le, N.J., and Rowley, J.D. (1996). AF10 is split by MLL and HEAB, a human homolog to a putative *Caenorhabditis elegans* ATP/GTP-binding protein in an invins(10;11)(p12;q23q12). *Blood* 88, 3535-3545.
80. Leung, C., Lingbeek, M., Shakhova, O., Liu, J., Tanger, E., Saremaslani, P., Van Lohuizen, M., and Marino, S. (2004). Bmi1 is essential for cerebellar development and is overexpressed in human medulloblastomas. *Nature* 428, 337-341.
81. Sellick, G.S., Barker, K.T., Stolte-Dijkstra, I., Fleischmann, C., Coleman, R.J., Garrett, C., Gloyn, A.L., Edghill, E.L., Hattersley, A.T., Wellauer, P.K., et al. (2004). Mutations in PTF1A cause pancreatic and cerebellar agenesis. *Nat Genet* 36, 1301-1305.
82. Ostergaard, P., Simpson, M.A., Mendola, A., Vasudevan, P., Connell, F.C., van Impel, A., Moore, A.T., Loeys, B.L., Ghalamkarpoor, A., Onoufriadis, A., et al. (2012). Mutations in KIF11 cause autosomal-dominant microcephaly variably associated with congenital lymphedema and chorioretinopathy. *Am J Hum Genet* 90, 356-362.
83. Slavotinek, A.M., Mehrotra, P., Nazarenko, I., Tang, P.L., Lao, R., Cameron, D., Li, B., Chu, C., Chou, C., Marqueling, A.L., et al. (2013). Focal facial dermal dysplasia, type IV, is caused by mutations in CYP26C1. *Hum Mol Genet* 22, 696-703.
84. Young, I.D., and Harper, P.S. (1982). Incidence of Hunter's syndrome. *Hum Genet* 60, 391-392.
85. Fukami, M., Wada, Y., Miyabayashi, K., Nishino, I., Hasegawa, T., Nordenskjold, A., Camerino, G., Kretz, C., Buj-Bello, A., Laporte, J., et al. (2006). CXorf6 is a causative gene for hypospadias. *Nat Genet* 38, 1369-1371.
86. Buj-Bello, A., Biancalana, V., Moutou, C., Laporte, J., and Mandel, J.L. (1999). Identification of novel mutations in the MTM1 gene causing severe and mild forms of X-linked myotubular myopathy. *Hum Mutat* 14, 320-325.
87. Scott, A.F., Mohr, D.W., Kasch, L.M., Barton, J.A., Pittiglio, R., Ingersoll, R., Craig, B., Marosy, B.A., Doheny, K.F., Bromley, W.C., et al. (2014). Identification of an HMGB3 frameshift mutation in a family with an X-linked colobomatous microphthalmia syndrome using whole-genome and X-exome sequencing. *JAMA Ophthalmol* 132, 1215-1220.
88. Ramachandran, N., Munteanu, I., Wang, P., Aubourg, P., Rilstone, J.J., Israeliyan, N., Naranian, T., Paroutis, P., Guo, R., Ren, Z.P., et al. (2009). VMA21 deficiency causes an autophagic myopathy by compromising V-ATPase activity and lysosomal acidification. *Cell* 137, 235-246.
89. Hurvitz, J.R., Suwairi, W.M., Van Hul, W., El-Shanti, H., Superti-Furga, A., Roudier, J., Holderbaum, D., Pauli, R.M., Herd, J.K., Van Hul, E.V., et al. (1999). Mutations in the CCN gene family member WISP3 cause progressive pseudorheumatoid dysplasia. *Nat Genet* 23, 94-98.
90. Kwok, C., Weller, P.A., Guioli, S., Foster, J.W., Mansour, S., Zuffardi, O., Punnett, H.H., Dominguez-Steglich, M.A., Brook, J.D., Young, I.D., et al. (1995). Mutations in SOX9, the gene responsible for Campomelic dysplasia and autosomal sex reversal. *Am J Hum Genet* 57, 1028-1036.
91. Murakami, Y., Tawamie, H., Maeda, Y., Buttner, C., Buchert, R., Radwan, F., Schaffer, S., Sticht, H., Aigner, M., Reis, A., et al. (2014). Null mutation in PGAP1 impairing Gpi-anchor maturation in patients with intellectual disability and encephalopathy. *PLoS Genet* 10, e1004320.
92. Hansen, J.J., Durr, A., Cournu-Rebeix, I., Georgopoulos, C., Ang, D., Nielsen, M.N., Davoine, C.S., Brice, A., Fontaine, B., Gregersen, N., et al. (2002). Hereditary spastic paraparesis SPG13 is associated with a mutation in the gene encoding the mitochondrial chaperonin Hsp60. *Am J Hum Genet* 70, 1328-1332.
93. Thiffault, I., Rioux, M.F., Tetreault, M., Jarry, J., Loiselle, L., Poirier, J., Gros-Louis, F., Mathieu, J., Vanasse, M., Rouleau, G.A., et al. (2006). A new autosomal recessive spastic ataxia associated with frequent white matter changes maps to 2q33-34. *Brain* 129, 2332-2340.
94. Lemarchandel, V., Joulin, V., Valentin, C., Rosa, R., Galacteros, F., Rosa, J., and Cohen-Solal, M. (1992). Compound heterozygosity in a complete erythrocyte bisphosphoglycerate mutase deficiency. *Blood* 80, 2643-2649.
95. Luo, X., Kranzler, H.R., Zuo, L., Wang, S., Blumberg, H.P., and Gelernter, J. (2005). CHRM2 gene predisposes to alcohol dependence, drug dependence and affective disorders: results from an extended case-control structured association study. *Hum Mol Genet* 14, 2421-2434.

96. Senderek, J., Muller, J.S., Dusl, M., Strom, T.M., Guergueltcheva, V., Diepolder, I., Laval, S.H., Maxwell, S., Cossins, J., Krause, S., et al. (2011). Hexosamine biosynthetic pathway mutations cause neuromuscular transmission defect. *Am J Hum Genet* 88, 162-172.
97. Navarro-Sastre, A., Tort, F., Stehling, O., Uzarska, M.A., Arranz, J.A., Del Toro, M., Labayru, M.T., Landa, J., Font, A., Garcia-Villoria, J., et al. (2011). A fatal mitochondrial disease is associated with defective NFU1 function in the maturation of a subset of mitochondrial Fe-S proteins. *Am J Hum Genet* 89, 656-667.
98. Hackman, P., Sarparanta, J., Lehtinen, S., Vihola, A., Evila, A., Jonson, P.H., Luque, H., Kere, J., Screen, M., Chinnery, P.F., et al. (2013). Welander distal myopathy is caused by a mutation in the RNA-binding protein TIA1. *Ann Neurol* 73, 500-509.